TISSUE ENGINEERING APPROACH FOR ANNULUS FIBROSUS REGENERATION

SEE YONG-SHUN, EUGENE

NATIONAL UNIVERSITY OF SINGAPORE

2010

TISSUE ENGINEERING APPROACH FOR ANNULUS FIBROSUS REGENERATION

SEE YONG-SHUN, EUGENE

B.Eng.(Hons.), NUS

A THESIS SUBMITTED

FOR THE DEGREE OF DOCTOR OF PHILOSOPHY IN BIOENGINEERING

DIVISION OF BIOENGINEERING

NATIONAL UNIVERSITY OF SINGAPORE

2010

TABLE OF CONTENTS

ACKNOWLEDGEMENTS

This work would not have been possible without the careful guidance from my supervisors, Associate Prof Toh Siew Lok and Prof James Goh. I wish to thank them both for the support and mentoring throughout the course of my doctoral studies. I would like to express my heartfelt appreciation to the staff from the Division of Bioengineering, namely Annie, Millie, Dorothy, Ernest, Matthew, Yen Ping and Jenelle, who have on numerous occasions gone out of their way to help me. The NUSTEP colleagues, Elaine, Hock Hee, Wendy, Wan Ping, Eriza, Shah, Julee, Haifeng, Hongbin, Eugene Wong, Chen Hua and Serene, I appreciate all the help you have rendered over the years! Hock Wei from the Biomechanics Teaching Lab for the use of the Instron for mechanical testing, it was really important to my project. Not forgetting the FYP and overseas attachment students, Zeming, Ziyong, Andrew and Leo, your contributions to this thesis is much appreciated!

Finally, my wife, Shiyun, you have been my pillar of support through the ups and downs of my doctoral studies; and to my newborn, Edwin, you have brought so much more joy and laughter to the family.

LIST OF TABLES

LIST OF FIGURES

	Collagen type I deposition does not increase after MMC treatment
4.1.1b	Figure showing a significant decrease of cell-sheet viability between cultures supplemented with L-Asc and DexS (last 2 days) when compared to cultures with only L-Asc throughout
4.1.2a	(a) Alamar Blue analysis of sample wells shows no significant difference in cell numbers between sonicated and unsonicated samples of both BMSCs and fibroblasts at confluence; (b) Sonication does not affect collagen structure in both rabbit derived BMSCs and fibroblasts. Silver stained SDS-PAGE of peptic collagen extracts from the cell layer at 100% confluence. No difference observed in intensity and location of bands between sonicated and un-sonicated samples. MW STD, molecular weight ladder; BMSCs, bone marrow stromal cells; S, sonicated samples; (c) Graph showing the collagen quantified with and without sonication for both BMSCs and fibroblasts. Cells were grown till confluence for this study. The results obtained are not statistically different *, $p>0.05$
4.1.2b	(a) Alamar Blue analysis of sample wells shows no significant difference in cell numbers between sonicated and unsonicated samples of both BMSCs and fibroblasts at 2 weeks post confluence. *, $p>0.05$; (b) Sonication releases collagen that is trapped within cell layer fragments even after peptic digestion in both rabbit derived BMSCs and fibroblasts. Silver stained SDS-PAGE of peptic collagen extracts from the cell layer 2 weeks after 100% confluence. An obvious difference can be observed in intensity between sonicated and un-sonicated samples. Collagen fibrils are completely released by sonication. MW STD, molecular weight ladder; BMSCs, bone marrow stromal cells; S, sonicated samples; (c) Graph showing the increase in collagen quantified by sonication with both BMSCs and fibroblasts. Cells were grown till 2 weeks post confluence for this study. The results obtained are statistically different. *, $p<0.05$.
4.1.3a	Results of collagen type I deposition at weekly time points
4.1.3b	Confocal microscopy results for cell-sheet thickness at weekly time points
4.1.3c	Phase contrast (a, b) and SEM (c, d) images of 2 week old cell-sheets

	showing very dense mesh-like structures. (a) scale bars = 1mm; (b) scale bars = 200μm; (c) scale bars = 10μm; (d) scale bars = 5μm.
4.2.1a	Oil Red-O with hematoxylin counterstain of CI and CSI cultures compared to their NI cultures. CI and CSI cultures had large cytoplasmic lipid droplets (b, d) but the non-induced controls did not have any positive stain (a, c). Scale bars = 100μm.
4.2.1b	Real Time RT-PCR of adipogenic genes (PPARγ2, aP2 and leptin) results compared between CI and CSI with their respective NI cultures (a, b) followed by a comparision of the gene expression between CI and CSI cultures (c). The level of expression of each target gene was normalized to GAPDH and calculated using the 2^{Δ}Ct formula with reference to the respective control groups, which are set to 1. For (a, b), PPARγ2 and aP2 was significantly upregulated while leptin was significantly downregulated. *$p<0.05$
4.2.2a	Safranin-O with fast green counter stain of CI and CSI micromass pellets (a, d). Immunohistochemical staining of Col I (b, e) and Col II (c, f) showed that both induced micromass pellet cultures had strong Col II staining and very weak Col I staining. Scale bars = 500μm.
4.2.2b	Real Time RT-PCR of chondrogenic genes (Sox9, Aggrecan, Col I and Col II) results compared between CI and CSI with their respective NI cultures (a, b). A comparison of gene expression was done between CI and CSI cultures (c). The level of expression of each target gene was normalized to GAPDH and calculated using the 2^{Δ}Ct formula with reference to the respective control groups, which are set to 1. Ethidium bromine gel of Col II products (d) showed close to no expression of Col II products for NI cultures. All 4 genes in induced micromass pellets were significantly upregulated. *$p<0.05$.
4.2.3a	Alizarin Red staining of CI and CSI cultures compared to their NI cultures. Both NI cultures did not have any stain (a, c) and the positive staining of CSI cultures (d) is visibly much more than in CI cultures (b). Scale bars = 500μm.

4.2.3b	Real Time RT-PCR of osteogenic genes (Runx2, Col I, ON and OPN) results compared between CI and CSI with their respective NI cultures (a, b), followed by a comparision of the gene expression between CI and CSI cultures (c). The level of expression of each target gene was normalized to GAPDH and calculated using the 2^{Δ}Ct formula with reference to the respective control groups, which are set to 1. In all graphs, all 4 genes tested were significantly upregulated. *$p<0.05$
4.3.1b	No significant difference of Young's Modulus at 25% axial compression within each Silicone NP batch before and after sterilization.
4.3.1c	Experiment done to show that the Young's Modulus of the silicone discs from batch B (top) and batch D (bottom) do not change significantly after cyclic loading
4.3.1d	Hoop strain of batches A to F. Batch B and D require 23% axial compression while batch C, E and F require 24% axial compression to attain a similar hoop strain profile to batch A. *$p>0.05$ when tested against batch A.
4.3.2a	Cells within the simulated IVD-like construct remain viable after 4 weeks of static culture
4.3.2b	H&E, Alcian blue and Safranin-O staining of simulated IVD-like assembly after 4 weeks of static culture. Scale bars = 500μm (a,b,c) and 200μm (d,e,f)
4.3.2c	Collagen Type I (left) and collagen type II (right) immunohistochemical staining of simulated IVD-like assembly in static culture for 4 weeks showed that there was stronger staining for collagen type II. Scale bars = 500μm.
4.3.2d	SDS-PAGE to determine ECM composition of 2 week old cell-sheets and 4 week static culture of simulated IVD-like assembly. 4 week static cultures showed a decrease in collagen type I expression.
4.4.1a	Cells of both the static and dynamic cultures remain viable and metabolically active over 4 weeks. However, the metabolic rate of the cells within the dynamic cultures begins to decrease after the 2nd week.

4.4.1b	SDS-PAGE collagen type I and type II between 4 weeks static culture and 2 weeks/4 weeks dynamic culture. Collagen type I deposition decreased over the 4 week dynamic culture period. Collagen type II was detected in both 4 week static and 4 week dynamic culture.
4.4.1c	H&E, Alcian blue and Safranin-O staining of simulated IVD-like assembly after 2 weeks and 4 weeks of dynamic culture. Scale bars = 500μm (a,b,c) and 200μm (d,e,f)
4.4.1d	Immunohistochemical staining of the simulated IVD-like assembly after 2 weeks (top) and 4 weeks (bottom) of dynamic culture. (a,d): IgG control; (b,e): Col I; (c,f): Col II. Scale bars = 200μm (a,b,c) and 100μm (d,e,f).
4.4.1e	Real Time RT-PCR results of common IVD genes (Sox9, Col I, Col II, Aggr, Bi, Dec) compared between 2 week and 4 week dynamic cultures against 4 week static cultures. The level of expression of each target gene was normalized to GAPDH and calculated using the 2^{Δ}Ct formula with reference to the control group, which are set to 1. At week 2, only Col II was upregulated, but at week 4, all the genes but biglycan were upregulated and Col II was further upregulated. *$p<0.05$

LIST OF ABBREVIATIONS AND SYMBOLS

BMSC	Bone Marrow Derived Mesenchymal Stem Cell
TCPS	Tissue Culture Polystyrene
SDS-PAGE	Sodium Dodecyl Sulfate Polyacrylamide Gel Electrophoresis
RT-PCR	Reverse Transcriptase Polymerase Chain Reaction
IVD	Intervertebral Disc
MMP	Matrix Metalloproteinase
TIMP	Tissue Inhibitors of Metalloproteinase
CILP	Cartilage Intermediate Layer Protein
IL-1	Interleukin-1
IFN	Interferon
TNF-α	Tumor Necrosis Factor-Alpha
ECM	Extracellular Matrix
PBS	Phosphate Buffered Saline
BSA	Bovine Serum Albumin
DAPI	4',6-diamidino-2-phenylindole
FBS	Fetal Bovine Serum

Abstract

The aim of this study was to develop a tissue engineering approach in regenerating the annulus fibrosus (AF) as part of an overall strategy to produce a tissue-engineered intervertebral disc replacement. The approach was to use bone marrow derived stem cells (BMSC) to form cell-sheets and incorporating them onto silk scaffolds to simulate the native lamellae of the AF. The *in vitro* experimental model used to study the efficacy of such a system was made up of the tissue engineering AF construct wrapped around a silicone disc to form a simulated IVD-like assembly. The AF construct was cultured within a custom-designed bioreactor that provided a mechanical stimulation to mimic the physiological condition. The results showed that BMSC cell-sheets retain their multipotentiality and were a suitable cell source for the simulated AF. The use of the bioreactor on the experimental model was shown to further enhance the efficacy in regenerating the inner AF.

CHAPTER 1

INTRODUCTION

1. INTRODUCTION

Lower Back Pain

Lower back pain causes discomfort in many individuals. If left untreated and allowed to deteriorate, discomfort might lead to disability. It is particularly predominant in 20-50 year olds and get progressively more serious in older people (Biering-Sørensen 1982). It has been reported as the most costly healthcare problem amounting to $50 billion in the United States alone (Frymoyer, & Cats-Baril 1991). Lower back pain is linked with the degeneration of the inter-vertebral disc (O'Neill et al 2002,Waddell 1996,Schwarzer et al 1995), also known as degenerative disc disease (DDD). Changes in the matrix composition (Miller et al 1988,Lyons et al 1981) and deterioration of biomechanical properties (Guiot, & Fessler 2000,Lipson, & Muir 1981), abnormal mechanical loading (Hutton et al 1998), genetic predisposition, reduced cell activity or any combination of the three may induce DDD (Lotz, & Chin 2000,Natarajan et al 1994).

IVD Structure

An IVD is found in between 2 vertebrae. It is a biologically complex structure that is separated into 3 tissue types; AF, NP and end-plates (O'Halloran, & Pandit 2007).

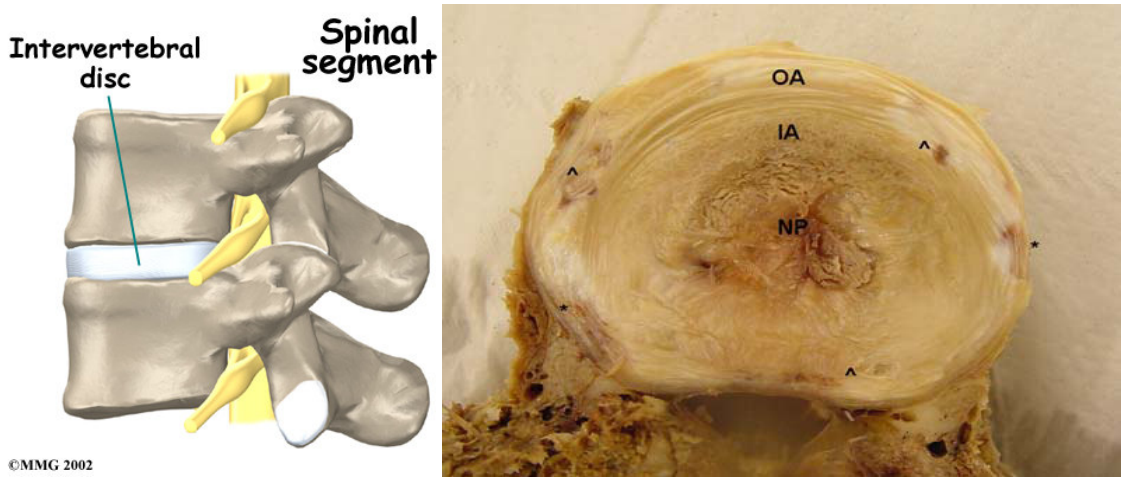

Fig 1a: Schematic drawing of the IVD between 2 vertebrae (left) and saggital section specimen of the IVD. NP nucleus pulposus, IA inner annulus fibrosus, OA outer annulus fibrosus (right)

The AF is made up of a series of highly oriented concentric layers rich in collagen surrounding the NP (Roberts et al 1989). The outer AF is made up of mainly collagen type I and to a much lesser extent, collagen type II. The amount of collagen type I fibres decrease and collagen type II fibres increase gradually near the NP (Bruehlmann et al 2002). Within these concentric layers, the collagen fibres lie parallel to each other at approximately 60^{o} angle to the spine axis. The fibres lie in opposite directions between successive layers (Hickey, & Hukins 1980). The outer region of the AF attaches to the posterior longitudinal ligaments and insert into the vertebrae body via Sharpey's fibres. The inner AF merges with the NP and the collagen fibres continue into the end-plate (Cassinelli et al 2001).

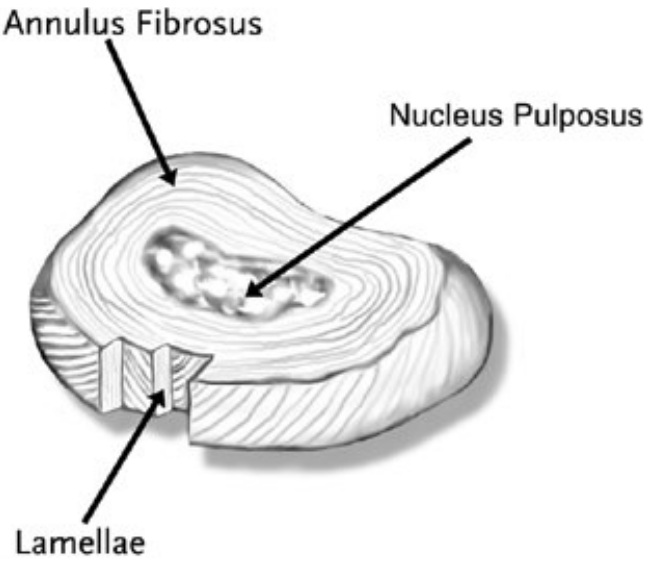

Fig 1b: Figure showing the alternating arrangements of the fibres between successive AF lamellae

The NP comprises of a more random arrangement of mostly collagen type II fibres that is dispersed within a proteoglycan-rich gelatinous matrix (Goupille et al 1998). The NP has a very high affinity for water due to the highly negative sulphated charge. The hydrostatic pressure exerted by the NP in an outward radial direction keeping the AF from collapsing inwards and allows it to accommodate compression loads.

End-plates lie between the vertebral bodies and the IVD. The central zone of the end-plate is made up of hyaline cartilage found over the perforated bony end-plate and loosely cemented to the underlying bone by a thin layer of calcium (Moore 2000), while the peripheral regions near the vertebral rim comprises an osseous component. The hyaline cartilage allows diffusion of molecules in and out of the disc while the osseous region is relatively impermeable. The end-plates is critical for the nutrition of the IVD as diffusion occurs through the central permeable region of the hyaline cartilage via vascular

buds that provide the bridge between the bone marrow of the vertebral body and the end-plate (O'Halloran, & Pandit 2007).

Together, these structures transmit weight and absorb compressive forces between adjacent vertebra and contribute significantly to the flexibility and stability needed to absorb mechanical loading.

In the normal IVD, chondrocyte-like cells synthesize collagen type II, proteoglycans and other proteins that form the matrix of the NP and the end-plates. Fibroblast-like cells secrete collagen type I and type II to form the AF. The matrix components are continually degraded by enzymes like MMPs (Goupille et al 1998), and are replaced by newly-synthesized matrix. Growth factors such as bFGF, TGF (Thompson et al 1991) and IGF (Osada et al 1996) also stimulate the chondrocyte-like and fibroblast-like cells to secrete more matrix. These growth factors are bound by CLIP and are released when the matrix is degraded (Seki et al 2005) to promote more matrix formation. TIMPs are also present to suppress MMP activation (Kang et al 1997).

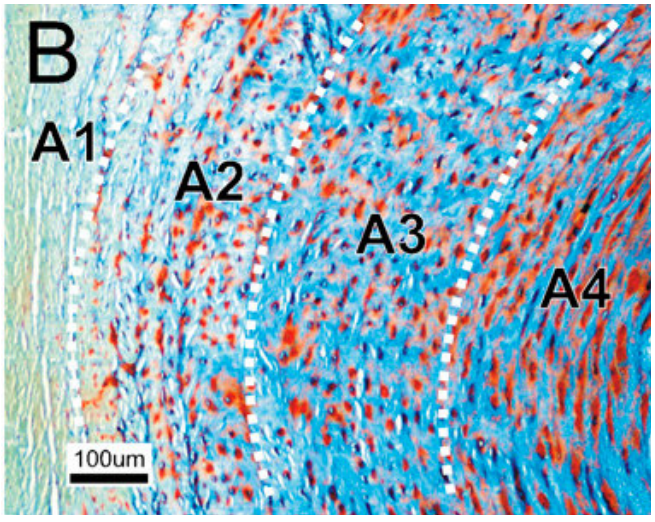

Fig 1c: Histological staining of a healthy AF. Blue staining: Alcian Blue; Orange staining: Safranin-O. Image taken from Leung *et al.* 2009

Pathophysiology of Intervertebral Disc Degeneration

Disc degeneration will occur when the matrix is not normal. This can occur when the matrix components synthesized are abnormal or if the balances between catabolic and anabolic factors shift in favour of degredation. When injury occurs to the IVD, macrophages enter the disc as a response. The machophages produce cytokines such as IL-1, IFN and TNF-α, which inhibits the synthesis of matrix proteins and increases the production of MMPs (Kobayashi et al 2005). Macrophages also secrete superoxide (O_2^-), which can degrade hyaluronic acid and proteoglycans, causing them to deaggregate, and can inhibit chondrocyte proliferation and synthesis. TNF-α and IL-1 also stimulates inducible nitric oxide synthetase to produce nitric oxide (Kang et al 1997) which has a variety of mechanisms that degrade the matrix. These are the main molecular pathways that are upregulated when IVD degeneration occurs. A number of factors have been postulated to be the cause of IVD degeneration

Aging of the IVD would results in the senescence of the cells causing them to lose the ability to proliferate and therefore result in a loss of cell numbers as the disc is unable to replace those lost to necrosis or apoptosis (Gruber et al 2007). Cells that have undergone senescence also are unable to keep up the rate of proteoglycan synthesis (Johnstone, & Bayliss 1995). The disc has a reduced ability to retain water, absorb pressure and becomes more fibrous (Haefeli et al 2006) due to the collagen content increasing and changing from type II to type I (Buckwalter 1995). This causes the NP to progressively become more solid, dry and granular (Haefeli et al 2006) and cracks will appear in the fibrous NP. The lamellae in the AF will thicken causing cracks and fissures to develop within it (Buckwalter 1995).

Nutrition would be another contributing factor to IVD degeneration, as the disc is the largest avascular tissue in they body. The nearest blood supply is found within the cartilage end-plates of the vertebral body, which would be 7-8mm from the centre of the disc (Urban et al 2004). The blood supply within the end-plates consists of a continuous capillary bed that is densest in the region of the NP and reduces significantly as it goes from the inner AF to the outer AF (Crock, & Goldwasser 1984). While the AF of an infant was supplied by blood vessels penetrating it, but these disappear by late childhood leaving only a few small capillaries (Hassler 1969). Calcification of the cartilaginous end-plates directly affects the ability of nutrients like glucose and oxygen to be transported from the blood to the cells of the IVD (Roberts et al 1996), and also the removal of wastes from the IVD. The state of low oxygen levels and lowered pH due to lactic acid build up will have adverse effects on the rate of matrix synthesis by the IVD cells (Ishihara, & Urban 1999). It has also been shown that low pH levels do not affect the ability of MMPs to be produced by the IVD cells (Razaq et al 2003), therefore a loss of nutrient transport would cause a very rapid breakdown of the IVD.

Mechanical forces like excessive torsion and compression also have deleterious effect on the IVD. Torsion occurring within the spine generates tension in the collagen fibres on one side of the annulus while the collagen fibres on the opposite side are slack (Krismer et al 1996). AF tears occur when the fibres are damaged. The tears start from the outer AF and extend inwards to the inner AF. Compressive loads within the physiological range are the stimulus for matrix turnover (Handa et al 1997). However, excessive compressive forces can lead to matrix degeneration in the IVD by the

1 downregulation genes for all anabolic proteins and the upregulation of catabolic genes
2 (Neidlinger-Wilke et al 2006).

Lane Grading System

There are many different systems of grading IVD degeneration that can be found. A Medline search found 42 such grading systems that describe cervical, lumbar disc or facet joint degeneration. Only 4 grading systems from these 42 had the Kappa or ICC interobserver reliability at > 0.60 (Kettler, & Wilke 2006). The 4 are listed below

1. Thompson et al. : Macroscopy of the Lumbar Disc (Thompson et al 1990)
2. Boos et al. : Histology of the Lumbar Disc (Boos et al 2002)
3. Lane et al. : Plain Radiography of the Lumbar Disc
4. Pfirrmann et al. : Magnetic Resonance Imaging of the Lumbar Disc (Pfirrmann et al 2001)

The grading system by Thompson et al. and Boos et al. is based on macroscopy and histology respectively, therefore is not applicable in the clinical diagnostic setting. The grading system by Lane et al. and Pfirrmann et al. is suitable as radiography and magnetic resonance imaging are applied. The diagnostic method described by Lane et al. is more sensitive in detecting end-plate calcification of the IVD. Therefore we've choosen the Lane Grading System to describe different grades of IVD degeneration.

State of the Art for Lower Back Pain Relief

In most cases, degeneration of the IVD can be treated successfully non-operatively with medication and physical therapy. However, when all non-operative treatments are exhausted, an operative treatment will be offered to patients. Currently, arthrodesis is the standard treatment for degenerative disc disease for patients who failed all best efforts of conservative care. However, the most notable and overwhelming problem with arthrodesis surgery is, persistant axial back pain. That is, there is a persistent disassociation between a radiographically successful fusion and successful relief of a patient's pain with return to normal function. Although today's modern surgical techniques easily can achieve 95% radiographic fusion rates, clinical success of pain relief lags behind in the 60% to 80% range (West et al 1991). A recent 2004 retrospective study reported rates of 16.5% at five years and 36.1% at ten years (Ghiselli et al 2004). Even if spinal fusion has been successful in relieving backache, recognition of an increased risk of adjacent level disease after fusion is a concern (Gertzbein, & Hollopeter 2002,Etebar, & Cahill 1999). Despite surgical success with disc arthroplasty, the problems associated with it have caused surgeons to look for alternatives to fusion.

Another method used to alleviate degenerative disc disease is disc athroplasty. Total disc replacements (eg. the Charité Artificial Disc, the ProDisc lumbar prosthesis, Maverick lumbar prosthesis and the FlexiCore lumbar) use a system of metal-metal or plastic-metal to relief pain by the removal of the diseased disc, restoration of disc height, and the restoration and maintenance of motion. The disadvantages of this method are that the site of injury is large.

There are also nucleus pulposus replacements (eg. The Prosthetic Disc Nucleus device, Newcleus, Aquarelle, Neudisc). These disc replacements allow the redistribution of the loads to the remaining native structures; AF and end-plates, and provide a less invasive surgical procedure. However, there have been reports of implant extrusion (Shim et al 2003) and end-plate deformities arising from The Prosthetic Disc Nucleus device.

None of the treatments listed so far are aimed at dealing with the inherent loss of function of the native IVD. This has prompted to study of feasible methods of a biological regenerative approach on treating the degenerating discs. Thus, more emphasis is being placed on tissue engineering approaches using cell-tissue based constructs that can function clinically in tissue regeneration and replacement.

Tissue Engineering

Tissue engineering is based on the application of concepts in engineering and life sciences to develop biological substitutes that restore or improve tissue function. It is founded on 3 main components; cells, signals and scaffolds, which can be used independently or in any combination.

Scaffold-based tissue engineering uses three-dimensional biodegradable scaffolds as a short term substitute for the extracellular matrix (ECM), that the seeded cells would generate their native tissue architecture and replace the role of the scaffold as it degrades (Langer, & Vacanti 1993). Conventional methods of seeding cells involve culturing of cells on TCPS until sufficient cells are obtained, followed by enzymatic digestion to detach the cells from the culture plate and finally seeding the single cell suspension onto the biodegradable scaffold (Altman et al 2002). This would involve the disruption of ECM expressed during cell culture and cell-to-cell adhesion proteins produced by the cells. The disadvantages of this method are that many cells are lost during the process of seeding onto the scaffolds, as a large portion of the cells do not actually adhere to the scaffold but seep through the pores of the scaffold (Li et al 2001,Kim et al 1998). However, those cells that manage to adhere onto the scaffolds have to re-synthesize their own ECM when they adhere to the new surface. In addition, trypsinization has been shown to change the morphology and biochemical composition of the cells that leads to a loss of cellular activity (Fujioka et al 2003).

Cell-Sheet Tissue Engineering

Currently, there is on-going research on the development of a novel tissue engineering methodology to construct three-dimensional functional tissues by layering two-dimensional cell-sheets without any biodegradable scaffold (Shimizu et al 2003,Michel et al 1999). This method which utilizes thermosensitive polymer coated TCPS to harvest the cell-sheets, is aimed at solving some problems faced by conventional cell seeding technique. Cell-sheets can be easily handled and transplanted out of the tissue culture environment without the use of trypsin, onto the scaffolds and other tissue engineering constructs (Kikuchi et al 1998). There have been studies done on the benefits of the use of these thermosensitive plates and it is reported that thermal liftoff of the cell-sheet is less damaging to the ECM proteins (Canavan et al 2005) as compared to conventional cell-sheet detachment protocols. However this process is currently performed mostly on terminally differentiated cells (Matsuda et al 2007).

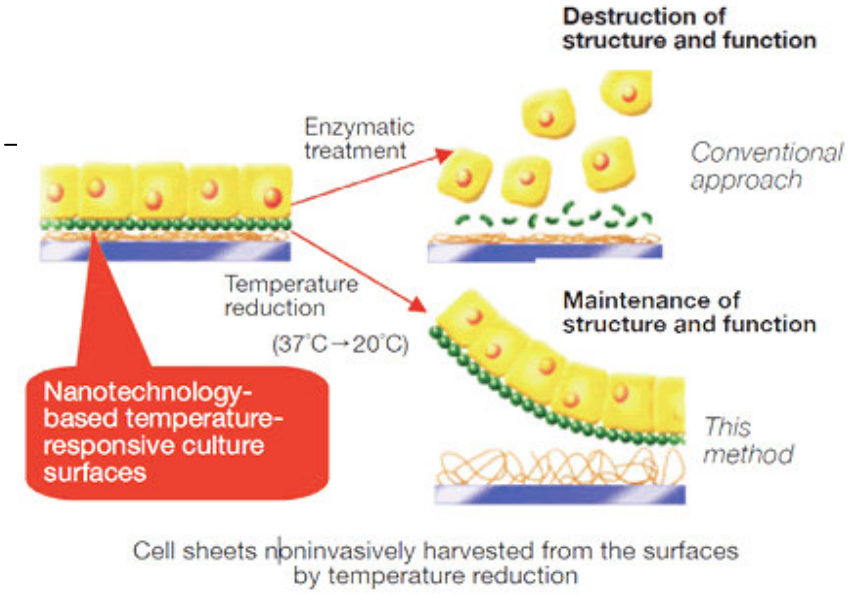

Fig 1d: Diagram representing thermosensitive polymer based cell-sheet detachment vs conventional enzymatic disruption of cell adhesion and cell-cell proteins. Image taken from www.jst.go.jp/EN/seika/01/seika15.html

These differentiated cells have limited lifespan, poor proliferation potential and require long period of culture time to obtain a cell-sheet with ECM that can be handled and manipulated without breaking apart. Therefore, growing BMSC cell-sheets that possess multilineage differentiation capability would be beneficial for various tissue engineering applications. Although studies have already shown that BMSC cell-sheets are able to, improve cardiac function after an infarction (Wang et al 2008), enhance bone formation (Nakamura et al 2010,Ouyang et al 2006) and engineer nasal alar cartilage (Zhang et al 2009), however the retention of the multilineage potential of the BMSC cell-sheets used in the studies have not been validated.

Tissue Engineering Approaches to IVD Regeneration

. In IVD tissue engineering, the aim is to induce regeneration of the tissue *in situ* by biological manipulation or to develop a functional tissue construct *in vitro* that is able to be implanted into the body which will be able to restore normal physiological function. Since the mechanical properties of the IVD are closely related to the ECM components, tissue engineering methods are mostly focused on regenerating the ECM components of the IVD to restore its function.

The state of degeneration of the IVD would determine the treatment strategy used (An et al 2003). In a situation where the AF still has the mechanical properties to withstand bulging pressures, a strategy targeted at regenerating only the NP would be appropriate. The tension within the AF attributed to the bulging of the NP would induce regeneration of the AF fibres. In cases where the AF has degenerated beyond its own ability for self repair, an implant of a tissue engineered *in vitro* construct consisting of a functional NP and AF would be more suitable. Most studies targeted at regenerating a functional IVD involve using AF cells, NP cells or BMSCs seeded onto various scaffolds and cultured *in vitro* to access cell viability and various ECM component deposition. There are also a few studies that apply a mechanical stimulus to stimulate the appropriate ECM production.

Cell Source for IVD Tissue Engineering

By conventional tissue engineering strategies, using autologous IVD cells would be an attractive source to produce a functional IVD construct. However, obtaining sufficient numbers of NP or AF cells provides a great challenge, this is due to the low cell viability (Boos et al 2002), low cell numbers and low proliferative capability (Roberts et al 2006,Le Maitre et al 2007,Gruber et al 2009) of these cells during cultivation. Moreover, obtaining these cells would involve taking a biopsy of a healthy IVD from which to extract the cells, which would mean puncturing the AF and NP thereby damaging structure and mechanical function. This method resembles protocols used to induce IVD degeneration in animal experiments (Alini et al 2008). Thus alternative cell sources are needed.

Notochordal cells are present in the embryonic human NP (Hunter et al 2003). These cells are involved in regulating the biosynthetic activity of the NP cells, however, their numbers diminish rapidly soon after birth and by the first decade, they have all disappeared. It has been reported that their disappearance coincides with the early onset of IVD degeneration (Aguiar et al 1999). It has been shown in animal models that these cells cultured together with mature NP cells increase their proteoglycan production (Aguiar et al 1999), and would be promising if it could be translated to the human model. Unfortunately, there is no human source for these cells available (Hunter et al 2003).

Autologous adult mesenchymal cells can be obtained in larger amounts from the bone marrow (BMSCs) or from adipose tissue. These cells have been shown to possess self-renewing capacity and can differentiate into osteocytes, chondrocytes, adipocytes, tenocytes, and nerve or muscle cells (Dezawa 2008,Lin et al 2008,Wang et al 2005,Banfi

et al 2000,Pittenger et al 1999). These cells also possess the capability to produce abundant amounts of ECM (Ge et al 2005,Van Eijk et al 2004). There have been no reports on any specific markers for AF and NP cells, but it has been reported that mesenchymal stem cells adopted a gene expression profile that resembled native IVD tissue (Steck et al 2005). There has also been studies that have showed that coculturing human NP cells and human BMSCs caused the BMSCs to differentiate to NP-like phenotype cells (Richardson et al 2006). A study done by Sakai et al. found that rabbit BMSCs embedded in Atelocollagen gel was effective in slowing down disc degeneration in rabbits (Sakai et al 2003) and Risbud et al. reported that hypoxia and transforming growth factor β initiated differentiation of rat BMSCs along the chondrogenic lineage, possibly acquiring the phenotype and characteristics of NP-like cells (Risbud et al 2004). Thus, these cells may represent an attractive source from which to obtain IVD-like cells.

Signals for IVD Tissue Engineering

Studies have shown that introducing exogenous growth factors into the NP region have been shown to increase cell population (Walsh et al 2004) and restore (Imai et al 2007) or even increase disc height (An et al 2005). However, the main limitation of using exogenous growth factors is that half lives of these proteins (Wallach et al 2003). Therefore, gene therapy, which is to transfer genes to recipient cells so that they synthesize RNA and protein they encode to induce a sustained secretion of endogenous growth factors, is becoming more prominent (Nishida et al 2008). Gene delivery systems can be divided into *in vitro* and *in vivo* treatments. The *in vitro* treatment requires harvesting of the IVD cells and transduction of the gene before re-implanting them into a degenerate IVD and the *in vivo* method involves transduction of the cells *in situ* (Cassinelli et al 2001). The latter would alleviate the problem of harvesting and culturing and re-implanting the cells. Originally, gene therapy was performed using viral vectors, but recent advanced has enabled a non-virus-mediated gene therapy (Nishida et al 2006) to be used for the disc. Thus, gene therapy would be a viable option to consider in IVD tissue engineering.

There have been a number of reports using mechanical stimulus to try to achieve increased IVD cell proliferation, increased mRNA expression and matrix deposition of the related proteins (Iwashina et al 2006,Miyamoto et al 2005,Wenger et al 2005). It is hypothesized that stress fibres within the cells detect the mechanical stimulus and adapt accordingly. The NP cells within the IVD are compressed while the AF cells undergo a concentric tensile and radial compression stress due to the radial bulging of the NP. However, most work involving mechanical stimulus uses hydrostatic (Reza, & Nicoll

1 2008) and hydrodynamic (Gokorsch et al 2004) pressure on IVD cells. These methods of
2 application of mechanical stimulus do not accurately represent the physiological
3 conditions experienced within the body.

Scaffolds for IVD Tissue Engineering

In tissue engineering, scaffolds serve the purpose to mimic the ECM in the body. It is also used to provide a conducive cell adhesion environment, temporary mechanical support for the cells or to provide biochemical signals if required to promote tissue ingrowth. For the case of IVD tissue engineering, different scaffolds will have to be used in order to achieve the appropriate mechanical properties required of the NP and the AF.

There have been many reports using freeze dried atellocollagen (Sato et al 2003), collagen (Rong et al 2002,Sun et al 2001), polyglycolic acid (Mizuno et al 2004), agarose, alginate, fibrin gels (Gruber et al 1997) or silk (Chang et al 2007) as scaffolds for the NP and AF. Most reports use assessment methods like increased DNA, increased proteoglycan synthesis and gene expression to determine the suitability of the scaffold for IVD tissue engineering. For scaffolds used to study NP regeneration, despite the reports of increased DNA and ECM deposition, there was little mention on these scaffolds having the viscoelastic properties of the native NP. Studies on scaffolds for the AF report mostly collagen type II and aggrecan production instead of collagen type I, which is the more common ECM found in the native outer AF. The larger quantity of collagen type II deposited might suggest that the scaffolds would be more suitable for engineering the inner AF.

CHAPTER 2

RATIONALE

2. RATIONALE

Based on the current literature, arthrodesis is the current gold standard to relief pain from patients suffering from DDD, but it does not aim to regenerate the damaged tissue. Recently, much work has been done in an attempt to find suitable tissue engineered replacements to regenerate the IVD. There have been promising reports on NP replacements, however one of the limitations have been the lack of effective strategies to regenerate the AF.

2.1 Hypothesis

The AF consists of many distinct lamellae of dense ECM capable of withstanding the bulging pressure of the NP. BMSC cell-sheets seeded onto silk scaffolds have the potential to mimic the native lamellae structure of the AF and subjected to mechanical stimulation in a bioreactor, the assembly can successfully regenerate the appropriate ECM.

2.2 Objectives

The main aim of this project was to use BMSC cell-sheets seeded onto a combined freeze dried/knitted silk scaffolds, wrapped around a cylindrical silicone that simulates the NP and subjected to compression in a bioreactor to potentially develop a new technique to tissue engineer the AF.

The specific objectives of this project are to be carried out in 4 phases:

Phase I – Characterization of BMSC Cell-Sheet Growth Profile

(a) The goal is to determine BMSC cell-sheet viability, DNA content, collagen content and thickness over 3 weeks of hyperconfluent culture

- The information derived from the cell-sheet growth profile would allow the establishment of a standardized protocol for BMSC cell-sheet culture.

Phase II – Characterization of BMSC Cell-Sheet Multilineage Potential

(a) The goal is to determine the retention of differentiation capability into adipogenic, chondrogenic and osteogenic lineages of the BMSC cell-sheet after 2 weeks post confluent culture.

- The information obtained from the experiment would determine the viability of BMSC cell-sheet technology as a cell source for tissue engineering of more complex tissues that would involve more than 1 cell type.

Phase III - Fabrication and Verification of Simulated IVD-like Assembly Viability

(a) The goal is to determine a protocol for fabricating a simulated NP using silicone

- The protocol would allow us to attempt to control the material properties of a viscoelastic material that would be used to simulate the NP for the IVD-like assembly.

(b) The goal is to fabricate the IVD construct using BMSC cell-sheets and knitted/freeze dried combined silk scaffold to simulate the lamellae of the AF wrapped around the cylindrical silicone NP obtained from (a).

- The results would let us determine if the cell-sheet within the construct would remain viable through long term culture.

Phase IV – Fabrication of Compression Bioreactor to provide Mechanical Stimulus to IVD Assembly

(a) The goal is to design and fabricate a bioreactor unit that is capable of applying physiological loading to the IVD-like assembly

- The bioreactor would allow a compressive force to be applied to the silicone NP. The simulated NP would then bulge radially and press onto the BMSC cell-sheets and silk scaffolds wrapped around it, thus stretching the assembly circumferentially. This would allow us to study the effects on the BMSC cell-sheet and determine the feasibility of the assembly to be used for AF tissue engineering in the future.

All the above mentioned objectives would lead the way to determine whether hyperconfluent cultures would affect the multipotency of BMSC cell-sheets and its feasibility to be used as a cell source together with silk scaffolds and a silicone simulated NP, to create an IVD construct as a novel method of AF tissue engineering.

2.3 Overview

As described in Section 2.2, the listed objectives of this project were carried out in 4 phases, shown diagrammatically in Figure 2.1

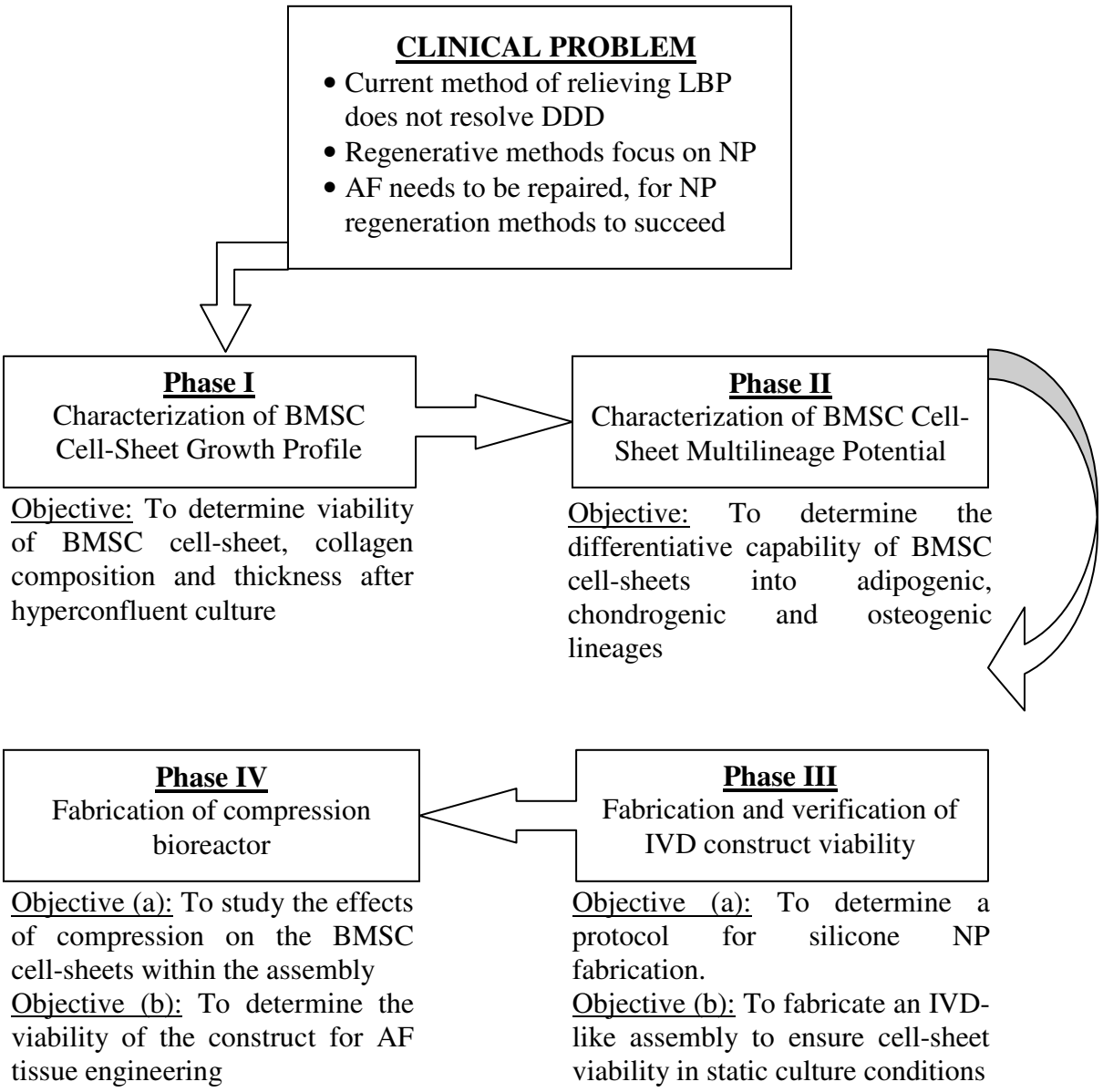

Fig 2.1: Flowchart illustrating the outline and flow of research

CHAPTER 3

METHODOLOGY

3.1 Phase I – Fabrication and Characterization of BMSC Cell-Sheet

3.1.1 Bone Marrow Isolation from New Zealand White Rabbits

Rabbit BMSCs were isolated from bone marrow aspirates which were obtained from New Zealand White Rabbits (approximately 8 weeks old). The BMSCs were then isolated from the red blood cells and plasma by differential migration during centrifugation using Ficoll-Paque PLUS (GE Healthcare). 3ml of Ficoll-Paque PLUS was added to a 15ml centrifuge tube and 4ml of blood was carefully layered on top to ensure the 2 layers do not mix. The tube is then centrifuged at 400xg for 40 minutes at 18^{o}C. The BMSCs are found in the lymphocyte layer between the plasma and Ficoll-Paque PLUS. The lymphocyte layer is removed and placed in a clean centrifuge tube and diluted with 3 volumes of 1xPBS. The tube is then centrifuged at 100xg for 10 minutes at 18^{o}C causing the cells to pellet. The supernatant was removed and discarded and 8ml of 1xPBS was used to resuspend the cells. The tube is again centrifuged at 100xg for 10 minutes at 18^{o}C. The supernatant was removed and the cells resuspended in 1ml of low glucose culture medium Dulbecco's modified Eagle's medium (LG-DMEM; Gibco, Invitrogen, CA), supplemented with 15% v/v fetal bovine serum (HyClone, Logan, UT), penicillin and streptomycin and plated on TCPS to allow the BMSCs to adhere and maintained at 37^{o}C in an incubator with 5% humidified CO_2.

3.1.2 BMSC Culture

a. Expansion of BMSCs

When primary BMSCs became near confluent, they were detached using trypsin (0.25%) /1mM ethylenediamine-tetraacetic acid (EDTA) and re-plated with a ratio of 1:3

in low glucose culture medium Dulbecco's modified Eagle's medium (LG-DMEM; Gibco, Invitrogen, CA), supplemented with 15% v/v fetal bovine serum (HyClone, Logan, UT), penicillin and streptomycin. The cultures were replenished with fresh medium at 37^{o}C every 3-4 days.

b. Freezing of excess BMSCs

Excess BMSCs were detached and counted. The BMSCs were split into aliquots of 1x10^{6} cells. Cell freezing medium was made with dimethyl sulfoxide (DMSO), fetal bovine serum and blank LG-DMEM in the ratio 1:2:7. The freezing medium was cooled to 4^{o}C prior to introducing the cells. Each aliquot of BMSCs was resuspended in 1ml of freezing medium and immediately placed into a freezing container filled with isopropanol, and placed into a -80^{o}C freezer. After 2 hours, the BMSCs were transferred into liquid nitrogen for long term storage.

3.1.3 Seeding of BMSCs onto 6-well TCPS

BMSCs were seeded at a density of 3 x 10^{5} cells/well in wells of a non-treated 6-well culture plate (NUNC, Denmark). The cells were cultured *in-vitro* in a 5% CO2 incubator at 37^{o}C till the cells reached 100% confluence (Day 0).

3.1.4 Fabrication Methods of BMSC Cell-Sheet

a. L-Ascorbic Acid supplement

At Day 0, the confluent cells were supplemented with 50µg/ml L- Ascorbic Acid (L-Asc) (Wako, Japan) in LG-DMEM. . The cultures were replenished with fresh L-Asc

supplemented medium at 37°C every 3-4 days and cultured till the desired time point. L-Asc was added to improve collagen production (Hata, & Senoo 1989) so as to obtain a more stable cell-sheet.

b. L-Ascorbic Acid with Dextran Sulphate supplements

Dextran sulphate (DexS) is an inert, negatively charged macromolecule. It has been shown that crowding using these macromolecules (also known as macromolecular crowding, MMC) improves the rate of conversion of procollagen to insoluble collagen in terminally differentiated cell lines (Lareu et al 2007).

Various experiments were done using DexS as a macromolecular crowder. The aim of the experiments was to determine if supplementing media with dextran sulphate would improve the efficiency of collagen type I deposition, thereby creating a more robust cell-sheet layer. DexS (500kDa; pK Chemicals A/S, Koge, Denmark), when supplemented to the L-Asc media, was always done after confluence, and at a concentration of 100μg/ml for 2 days.

3.1.5 Investigation on the Suitability of DexS to Aid BMSC Cell-Sheet Formation

a. SDS-PAGE Collagen Type I Quantification

The 1st experiment was done to determine if the concept of MMC works with BMSCs. Once the cells had reached confluence, half the wells were supplemented with L-Asc only, and the remaining was supplemented with both L-Asc and DexS. The cultures were maintained for 2 days before they were sacrificed for SDS-PAGE collagen type I quantification.

The 2nd experiment was done to determine if MMC can work on BMSCs in long term culture. The experiment was done up to 9 days post confluence with different culture conditions to determine the effects of MMC on BMSCs. The different culture conditions are illustrated below in Figure 3.1.5a.

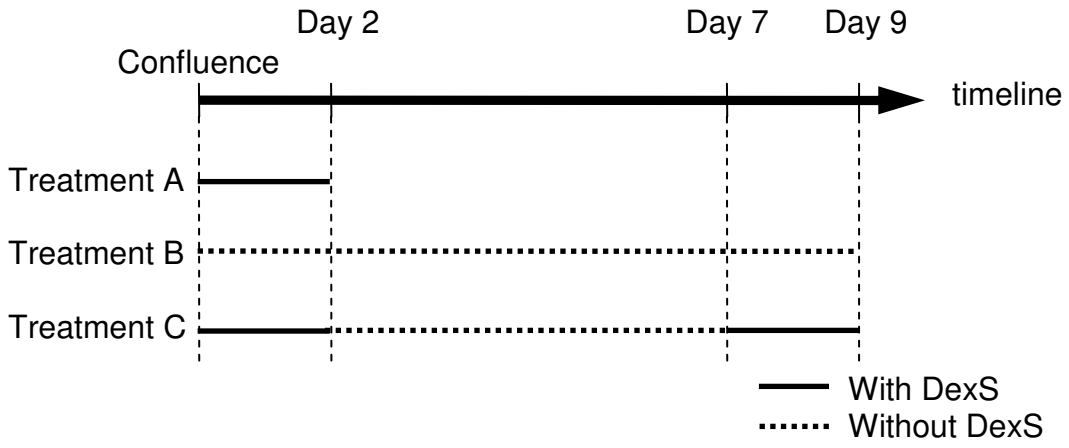

Fig 3.1.5a: Illustration of experimental timeline with and without DexS

The hyperconfluent cell-sheets were washed twice with 1xPBS after the Alamar Blue assay and digested with porcine gastric mucosa pepsin (2500 U/mg; Roche Diagnostics Asia Pacific, Singapore) in a final concentration of 0.25mg/mL. Samples were incubated at room temperature (RT) for 1h with gentle shaking followed by sonication of the solution until all cell fragments have broken up followed by 1hr incubation at RT. After the incubation step, the samples were neutralized with 0.1 N NaOH. The samples were analyzed by SDS-PAGE under non-reducing conditions (See et al 2008). A SDS gel made up of 3% stacking and 5% resolving components were used (Appendix A2). The gel was run at 50V for 30 minutes and 120V for 60 minutes. Collagen bands were stained using SilverQuest kit (Invitrogen, Carlsbad, CA) according to the manufacturer's protocol (Appendix A3). Densitometric analysis of wet gels was

performed on the GS-800 Calibrated Densitometer (Bio-Rad Laboratories, Hercules, CA) with the Quantity One v4.5.2 image analysis software (Bio-Rad Laboratories, Hercules, CA).

b. Alamar Blue Cell-Sheet Viability Assessment between DexS and non DexS treated Cell-Sheets

The experiment was done to determine if MMC had any effects on the viability of the BMSCs as compared to the non-MMC treated cells. The viability of the cells present within the hyperconfluent cell-sheets was determined using the Alamar Blue colorimetric assay (Invitrogen, CA). The cells were incubated in medium supplemented with 20% (v/v) Alamar Blue dye for 1 h. One hundred microliters of medium from each sample was read at 570/600nm in a microplate reader (Sunnyvale, CA). Medium supplemented with 20% Alamar Blue dye was used as a negative control and the percentage of Alamar Blue dye reduction was calculated according to the formula stated in Appendix A1. A percentage reduction of Alamar Blue dye would indicate that the cells assayed are viable.

3.1.6 Technique to Accurately Quantify Collagen Content in Hyperconfluent Culture

a. Cell Seeding and Culture

Both fibroblasts and BMSCs were seeded at a density of 2.5 x 10^5 cells/well in wells of a non-treated 6-well culture plate (NUNC, Denmark). The cells were grown in vitro in a 5% CO2 incubator at 37^{o}C for another 2 weeks (Day 14) after the wells reached 100% confluence (Day 0), with the medium being replaced every 3-4 days. A total of 6

wells (3 will be sonicated) for each cell type (BMSCs and fibroblasts) at each timepoint (Day 0 and Day 14) will have their relative cell numbers analyzed before sacrificing for collagen quantification.

b. Alamar Blue Analysis of Cell Numbers

The number of cells present within the hyperconfluent cell layers was determined using the Alamar Blue (Invitrogen, CA) colorimetric assay. Briefly, the cells were incubated in medium supplemented with 20% (v/v) alamar blue dye for 1 h. One hundred microliters of medium from each sample was read at 570/600nm in a in a microplate reader (Sunnyvale, CA). Medium supplemented with 20% Alamar Blue dye was used as a negative control and the percentage of Alamar Blue reduction was calculated according to the formula stated in Appendix A1. The cells were subsequently processed to analyse their collagen content after the Alamar Blue assay.

c. Sonication to Aid Cell Layer Pepsin Digestion for Collagen Quantification using SDS-PAGE

The hyperconfluent cell layers were washed twice with 1xPBS after the Alamar Blue assay and digested with porcine gastric mucosa pepsin (2500 U/mg; Roche Diagnostics Asia Pacific, Singapore) in a final concentration of 0.25mg/mL. Samples were incubated at room temperature (RT) for 1h with gentle shaking followed by sonication of the solution until all cell fragments have broken up followed by 1hr incubation at RT. For samples that were not sonicated, they were incubated for 2h at RT. After the incubation step, the samples were neutralized with 0.1 N NaOH. The samples

were analyzed by SDS-PAGE under non-reducing conditions described in (Raghunath et al 1994,Lareu et al 2007). Briefly, a 10% homemade SDS gel made up of 3% stacking and 5% resolving components is used (Appendix A2). Collagen bands are stained using SilverQuest kit (Invitrogen) according to the manufacturer's protocol (Appendix A3). Densitometric analysis of wet gels was performed on the GS-800 Calibrated Densitometer (Bio-Rad) with the Quantity One v4.5.2 image analysis software (Bio-Rad).

3.1.7 Investigation of BMSC Cell-Sheet Growth Post-Confluence

a. Alamar Blue Cell-Sheet Viability Assessment

The viability of the cells present within the hyperconfluent cell-sheets was determined using the Alamar Blue colorimetric assay (Invitrogen, CA). The cells were incubated in medium supplemented with 20% (v/v) Alamar Blue dye for 1 h. One hundred microliters of medium from each sample was read at 570/600nm in a microplate reader (Sunnyvale, CA). Medium supplemented with 20% Alamar Blue dye was used as a negative control and the percentage of Alamar Blue dye reduction was calculated according to the formula stated in Appendix A1. A percentage reduction of Alamar Blue dye would indicate that the cells assayed are viable.

b. SDS-PAGE Collagen Type I Quantification

The BMSC cell-sheets were cultured till 3 weeks post confluence, and at each weekly time point, the cell-sheets were sacrificed for collagen type I and DNA quantification.

The hyperconfluent cell-sheets were washed twice with 1xPBS after the Alamar Blue assay and digested with porcine gastric mucosa pepsin (2500 U/mg; Roche Diagnostics Asia Pacific, Singapore) in a final concentration of 0.25mg/mL. Samples were incubated at room temperature (RT) for 1h with gentle shaking followed by sonication of the solution until all cell fragments have broken up followed by 1hr incubation at RT. After the incubation step, the samples were neutralized with 0.1 N NaOH. The samples were analyzed by SDS-PAGE under non-reducing conditions (See et al 2008). A SDS gel made up of 3% stacking and 5% resolving components were used (Appendix A2). The gel was run at 50V for 30 minutes and 120V for 60 minutes. Collagen bands were stained using SilverQuest kit (Invitrogen, Carlsbad, CA) according to the manufacturer's protocol (Appendix A3). Densitometric analysis of wet gels was performed on the GS-800 Calibrated Densitometer (Bio-Rad Laboratories, Hercules, CA) with the Quantity One v4.5.2 image analysis software (Bio-Rad Laboratories, Hercules, CA).

c. Immunofluorescence for Cell-Sheet Thickness Assessment using Confocal Microscopy

Cell-sheets were fixed in -20^{o}C methanol for 10 minutes and washed with 1xPBS. A 3% BSA (w/v), dissolved in 1xPBS was added to block the sample for 30 minutes at 25^{o}C. The BSA was removed and a mouse anti collagen type I antibody (1:4000, SigmaAldrich, San Louis, MO) was incubated on the sample for 90 minutes at 25^{o}C. The samples was washed in 0.05% Tween 20 (v/v) in 1xPBS for 20 minutes and incubated with goat anti mouse Alexa Fluor 594 (1:400, Invitrogen, Carlsbad, CA) and DAPI (1:800, Invitrogen, Carlsbad, CA) for 30 minutes at 25^{o}C. The samples was washed in

0.05% Tween 20 (v/v) in 1xPBS for 20 minutes before confocal microscopy (Olympus FluoView Confocal Laser Scanning Microscopes, FV500*)*. To determine the thickness of the cell-sheet, the z-direction slicing mode was used and average of 9 points around the well was taken.

d. DNA Quantification

DNA content measured spectrophotometrically using the Hoechst 33258 method (Toh et al 2005). The fluorescence measurement of Hoechst 33258 dye was performed using a fluorescence plate reader (FLUOstar Optima, BMG Labtechnologies, Offenburg, Germany). Calf thymus DNA was used for construction of the standard curve for DNA quantification.

e. SEM Analysis

Some 2-week old cell-sheets were coated with gold using a Sputter Coater (BAL-TEC Inc) and their morphology was observed by scanning electron microscopy (SEM, JEOL JSM-5600LV, Japan) operated at a voltage of 10kV.

3.1.8 Statistical Analysis

All data is expressed as mean ± standard deviation (SD). All statistical analysis was performed by pair-wise comparison of experimental categories using two-tailed, unpaired student t-test. A p-value <0.05 was considered significant. Statistical analysis was performed using Graph Pad Software (San Diego, CA).

3.2 Phase II – Characterization of BMSC Cell-Sheet Multipotentiality and Comparison between Conventional BMSC Differentiation Protocols

3.2.1 BMSC Cell-Sheet Culture

BMSCs were seeded at a density of 3 x 10^5 cells/well in wells of a non-treated 6-well culture plate (NUNC, Denmark) for osteogenic and adipogenic differentiation cultures. For chondrogenic differentiation, 7 x 10^4 BMSCs were seeded/well in wells of a non-treated 24-well culture plate (NUNC, Denmark). The cells were cultured *in-vitro* in a 5% CO2 incubator at 37^{o}C till the cells reached 100% confluence (Day 0). Following that, the confluent cells were supplemented with 50µg/ml L- Ascorbic Acid (L-Asc) (Wako, Japan) in LG-DMEM for 2 weeks before the cell-sheets were differentiated into chondrogenic, adipogenic and osteogenic lineages.

3.2.2 Media Preparation and Culture Conditions for Differetiation of BMSC Cell-Sheets

a. Adipogenic Differentiation Medium and Culture

LG-DMEM was removed from the 14 day BMSC cell-sheet culture wells and replaced with adipogenic induction media made up of 15% FBS high glucose DMEM (HG-DMEM) supplemented with 0.5 mM isobutyl-methylxanthine (Aldrich, Milwaukee, WI), 10 µM bovine insulin, 1 µM dexamathasone, and 200 µM indomethacin (Sigma-Aldrich, St Louis, MO). The adipogenic differentiation was stimulated using 3 cycles of induction media for 4 days and maintenance media for 3 days. Maintenance media only consisted of 15% FBS in HG-DMEM. Control group wells were also cultured in maintenance media throughout. An experiment was also carried out at the start of the

induction cycle, when the culture reached hyperconfluence. This would provide a comparison between the CSI and CI cultures. The cultures were incubated at 37^{o}C in 5% CO_2 over a period of 3 weeks. The culture medium was changed every 3-4 days.

b. Chondrogenic Differentiation Medium and Culture

The 14-day BMSC cell-sheets were induced to roll up into a pellet by agitation of the sides of the cell-sheet. The cell-sheet pellets was transferred into 15ml polypropylene falcon tubes and supplemented with chondrogenic induction media as described in (Wu et al 2007). High glucose DMEM supplemented with 15% FBS, 10^{-7}M dexamethasone, 50 µg/ml L-Ascorbic acid, 4mM proline, (all from Sigma-Aldrich, St Louis, MO), 1% ITS+ premix (BD Bioscience Inc. Franklin Lakes, NJ), and 1mM sodium pyruvate was used as the chondrogenic induction media. Chondogenic differentiation was induced in the presence of 10 ng/ml Transforming Growth Factor β3 (TGF-β3) (RayBiotech Inc. Norcross, Georgia) while controls were not supplemented with TGF-β3. The differentiation capability of the cell-sheet pellets was compared to those using the well established conventional protocols for chondrogenic differentiation (Indrawattana et al 2004). This would provide a comparison between the cell-sheets induced (CSI) cultures and conventional induced (CI) cultures and also their respective non-induced (NI) control cultures. The pellets were incubated at 37^{o}C in 5% CO_2 over a period of 3 weeks. Medium was changed every 3-4 days.

c. Osteogenic Differentiation Medium and Culture

LG-DMEM was removed from the 14-day BMSC cell-sheet culture wells and replaced with osteogenic differentiation media. The osteogenic differentiation media was made up of 15% FBS HG-DMEM supplemented with 10^{-8}M dexamathasone, 50μM L-Ascorbic acid and 10mM β-glycerolphosphate (Sigma-Aldrich, St Louis, MO) and 25ng/ml Bone Morphogenic Protein 2 (BMP2) (RayBiotech Inc. Norcross, Georgia). Control group wells were cultured with only 15% FBS in HG-DMEM. In addition, an experiment was done using a seeding density of 3 x 10^4 cells/well and induction media was introduced the following day. This would provide a comparison between the CSI and CI cultures. The cultures were incubated at 37^{o}C in 5% CO_2 over a period of 4 weeks. Medium was changed every 3-4 days.

3.2.3 Histological Assessment of Differentiation

a. Histochemical staining of Adipocytes

Oil Red O staining technique was used to evaluate adipogenesis. Neutral lipid droplets found within adipocytes were stained with Oil Red O (Sigma-Aldrich, St Louis, MO). A stock solution was made with 0.5% w/v dye in Isopropanol (IPA). The working solution was used to stain the lipid droplets. The working solution was made with 6ml of stock diluted and 4ml ddH_2O. The cell-sheets were washed with 1xPBS twice and fixed with 70% ethanol for 20 sec. The cell-sheets were then stained with the working solution for 15 min. Excess dye was washed off with 70% ethanol followed by ddH_2O. The cells were then counterstained with hematoxylin for 30 sec and washed. The bright red lipid droplets were imaged using a brightfield microscope.

b. Histological and Immunohistochemical assessment of pellet cultures

The pellets were washed in 1xPBS, fixed in 10% neutral buffered formalin overnight and then embedded in paraffin. 5 μm thick sections were cut and collected on silane-coated slides for histological and immunohistochemical analysis. The Safranin O/fast green staining technique was performed as follows: after deparaffinization and rehydration, the samples were stained for 3 min with iron hemotoxylin, washed for 3 min with ddH_2O, stained for 3 min with fast green. They were washed in acetic acid for 5 sec and stained for 3 min with Safranin O. The slides were dehydrated before application of a coverslip.

Immunohistochemistry study was carried out as follows: after deparaffinization and rehydration, endogenous peroxidase in the samples was first blocked with hydrogen peroxide for 15 min before pepsin treatment for 20 min. Monoclonal antibodies of collagen type I (Sigma-Aldrich, St Louis, MO) of dilution factor 1:500, collagen type II (Chemicon Inc., Temecuela, CA) of dilution factor 1:500; and control mouse IgG isotype (Zymed Laboratories Inc. San Francisco, CA) of dilution factor 1:2500 were applied for an hour followed by incubation with biotinylated goat anti-mouse (Lab Vision Corporation, Fremont, CA) for 30 min. Streptavidin peroxidase was added for 45 min and 3,30-diaminobenzidine was used as a chromogenic agent and counterstaining was done with hematoxylin. Between each step, the slides were washed with 1xPBS. The slides were dehydrated before application of a coverslip.

c. Histochemical staining of Osteocytes

Alizarin red S staining was used to evaluate osteogenesis. Briefly, Alizarin red S (ARS) (Sigma-Aldrich, St Louis, MO) stains calcium deposits to confirm osteogenesis. The cell-sheet was washed with 1xPBS and fixed in 10% Formalin for 30 min. The cells were washed thoroughly and stained with 40mM ARS for 5 min. Excess dye was washed off thoroughly with ddH_2O and incubated with 1xPBS for 5 min. The orange-red calcium deposits were imaged using a brightfield microscope.

3.2.4 RNA Extraction and Real-Time PCR Analysis of Differentiation

Total RNA was extracted using Trizol® reagent (Invitrogen, Grand Island, NY) and purified using the RNeasy Mini Kit (Qiagen, Valencia, CA). RNA concentration was determined using NanoDrop (NanoDrop Technologies, Wilmington, DE) and complementary DNA synthesis was carried out using 100 ng of total RNA according to the manufacturer's protocol for SuperScript II reverse transcriptase with oligo(dT) primers. Real-Time PCR was done using 2µl of cDNA, 10µl of SYBR Green Master Mix (Qiagen, Valencia, CA) and the optimized concentration of primers, topped up to 20µl with nuclease free water. All reactions were performed on the real-time Mx3000P (Stratagene, CA, USA). The thermal cycling program for all PCRs was the following: 95ºC for 15 min, followed by 40 cycles of amplifications, consisted of denaturation step at 94ºC for 15 sec, an annealing step at 55ºC for 30 sec and an extension step at 72ºC for 30 sec. The genes analysed were Sox9, collagen type II (Col II) and aggrecan for chondrogenesis, Peroxisome Proliferator-Activated Receptor (PPARγ2), adipocyte binding protein 2 (aP2) and leptin for adipogenesis and Runt related transcription factor 2

(Runx2), collagen type I (Col I), osteopontin (OPN) and osteonectin (ON) for osteogenesis. Primer sequence for GAPDH and Collagen Type I (Col I) were previously described (Fan et al 2008). Remaining primers were designed using the Oligo 6.0 program and are listed in Table 3.2.4. The level of expression of the target gene, normalized to GAPDH, was then calculated using the 2^{Δ}Ct formula (Livak, & Schmittgen 2001) with reference to the respective control groups which are set to 1.

Gene	Primer Sequence	Product Size	Accession no
Sox9	F: 5' CTT CAT GAA GAT GAC CGA CGA G 3' R: 5' CTC TTC GCT CTC CTT CTT GAG G 3'	181bp	AY598935
Collagen Type II	F: 5' AAG AGC GGT GAC TAC TGG ATA G 3' R: 5' TGC TGT CTC CAT AGC TGA AGT 3'	214bp	D83228
Aggrecan	F: 5' GTG AAA GGT GTT GTG TTC CAC T 3' R: 5' TGG GGT ACC TGA CAG TCT GAT 3'	190bp	L38480
aP2	F: 5' TTG ATG AAG TCA CCG CAG AT 3' R: 5' CAT TCC ACC ACC AGT TTA TCA C 3'	142bp	AF136241
PPARγ2	F: 5' CCT GGC AAA GCA CTT GTA TGA 3' R: 5' AAC GGT GAT TTG TCT GTC GTC T 3'	102bp	AY166780
Runx2	F: 5' CCT TCC ACT CTC AGT AAG AAG A 3' R: 5' TAA GTA AAG GTG GCT GGA TAG T 3'	143bp	AY598934
Osteopontin	F: 5' GCT CAG CAC CTG AAT GTA CC 3' R: 5' CTT CGG CTC GAT GGC TAG C 3'	249bp	D16544
Osteonectin	F: 5' GAA GTT GAG GAA ACC GAA GA 3' R: 5' GGC AGG AGG AGT CGA AG 3'	199bp	AF247647

Table 3.2.4: Custom-Made Primer Sequences for Assessment of Differentiation

3.2.5 Statistical Analysis

All data is expressed as mean ± standard deviation (SD). All statistical analysis was performed by pair-wise comparison of experimental categories using two-tailed, unpaired student t-test. A *p*-value <0.05 was considered significant. Statistical analysis was performed using Graph Pad Software (San Diego, CA).

3.3 Phase III – Fabrication and Verification of Simulated IVD-like Construct Viability

3.3.1 Fabrication of Silicone Nucleus Pulposus

The silicone NP disc with a diameter of 12mm and a height of 9mm was fabricated using a stainless steel mold (Fig 3.3.1). The silicone mixture of 20:1 (v/v) silicone:elastomer (Dow Corning Corporation, Midland, MI) was well mixed and left for 60mins at 25^{o}C at 6 torr. The mixture was then poured into the mold and left for 60mins at 25^{o}C at 6 torr. After the remaining bubbles have escaped, the mold was transferred to cure for 18 hours at 100^{o}C.

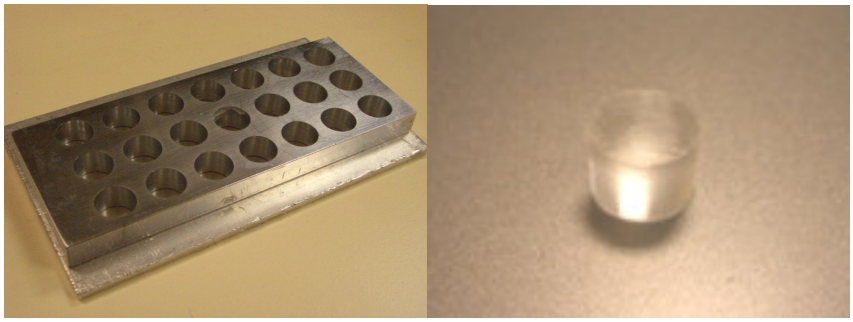

Figure 3.3.1: Stainless steel mold (left) and silicone NP (right)

3.3.2 Characterization of Silicone Nucleus Pulposus

Mechanical testing on the silicone discs was done using the Instron 3345 machine (Figure 4.3.2). A 100 N load cell was used performed at a rate of 1.125 mm/sec. A preload of 0.05 N was set before experiments were conducted. The mechanical tests were separated into many stages.

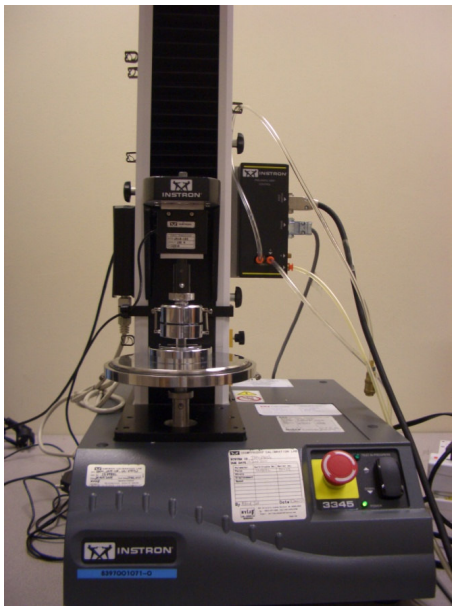

Fig 3.3.2: Instron 3345 machine used to compress and characterize the silicone NP substitute

a. Calculation of Young's Modulus

After 2 conditioning cycles of compression on the silicone NP, the data of the 3rd cycle was recorded by the Instron 3345 machine. A graph of stress vs strain was plotted from the data recorded by the Instron 3345 machine (Fig 3.3.2a). A best fit curve was obtained using a cubic equation. By substituting a strain value into the differential of the best fit cubic equation, we were able to obtain the Young's Modulus of the silicone NP at that particular strain. To standardize the mechanical testing data for characterization of the silicone NP disc, the Young's Modulus was obtained at the point of 25% compressive strain.

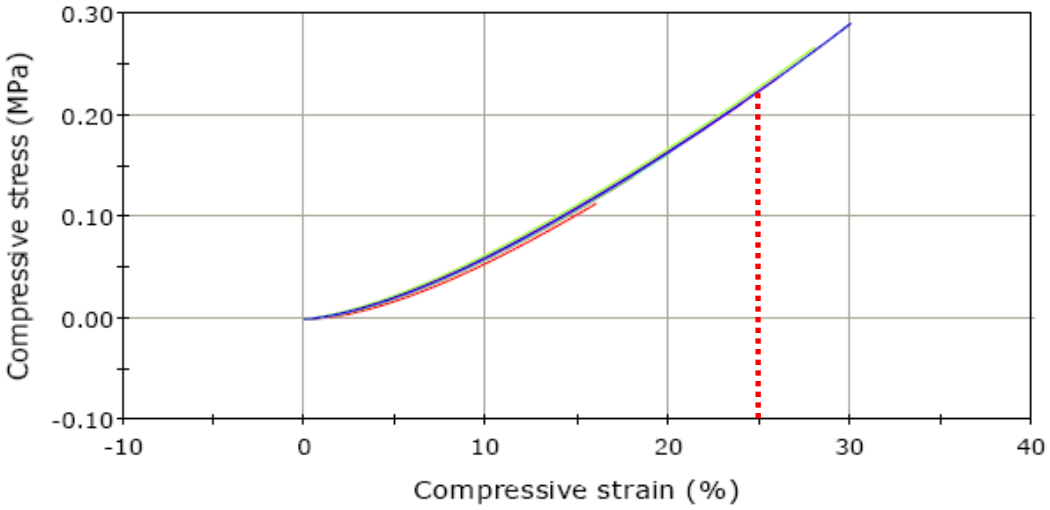

Fig 3.3.2a: An example of a stress vs strain graph obtained from the Instron 3345. The Young's Modulus was obtained at the point of 25% compressive strain to standardize mechanical testing data.

b. Calculation of Swelling Pressure (Hoop Stress) of Silicone NP

A close up photo of the silicone NP was taken with a CASIO EX-Z50 camera before and after compression (Fig 3.3.2b). The width of the disc before and after compression was measured using the Image J software (http://rsbweb.nih.gov/ij/). The transverse strain was then calculated by taking the ratio of the maximum change in width after compression over the original width of the silicone disc. To obtain the hoop stress at a particular axial compression, the generalized Hooke's law was used:

$$\varepsilon_\theta = \frac{1}{E}[\ \sigma_\theta - \nu(\sigma_r + \sigma_a)]$$

where

$$\nu = -\frac{\varepsilon_{trans}}{\varepsilon_{axial}}$$

E: Young's Modulus
ν: Poisson's ratio
ε: Strain
σ: Stress
θ: Circumferential Direction
r: Radial Direction
a: Axial Direction

We assume σ_r to be 0, σ_a is obtained from the Instron 3345, E is calculated as stated in 4.3.2a, ν and ε_θ are calculated using the Image J software.

A study by Glover *et al.* showed that the swelling pressure of the NP of a porcine model was 0.05MPa (Glover et al 1991). Thus, the objective of this experiment was to determine the axial compression that would give a 0.05MPa swelling pressure of the silicone NP. Following that, another 4 discs from the same batch were subjected to the same axial compression to determine the pooled average swelling pressure.

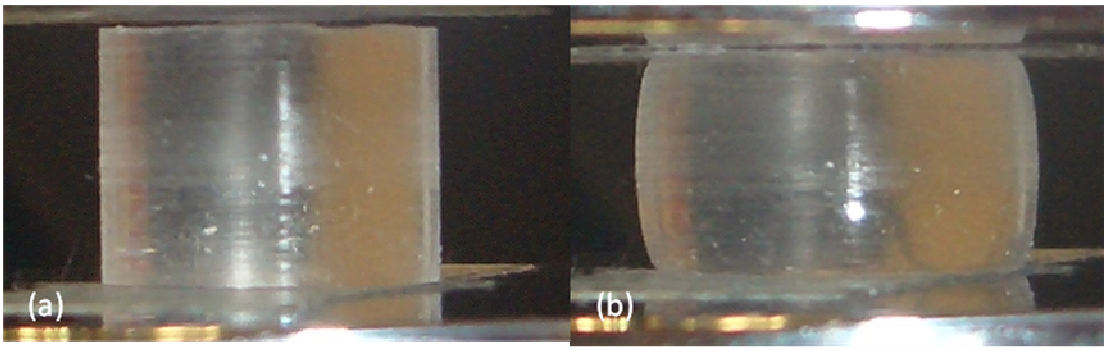

Fig 3.3.2b: silicone disc before (left) and after (right) compression

c. Effects of Ethylene Oxide Sterilization on the Mechanical Properties of the Silicone NP

The silicone discs underwent 25% axial compression before and after ethylene oxide sterilization. The Young's modulus of the disc at 25% axial compression was used to determine if this method of sterilization would have an effect on the mechanical properties on the silicone disc.

d. Effects of Cyclic Loading on the Mechanical Properties of the Silicone Nucleus Pulposus

2 batches of 5 silicone discs each were subjected to 25% compression at a rate of 0.25 Hz for 30 minutes each day, with a 1 second interval between each cycle. The discs were then allowed to recover for 23.5 hrs before the compressions were repeated again. The experiment was carried out for 3 consecutive days, amounting to 360 cycles per day, or 1080 cycles over 3 days. Mechanical testing was done on the discs each day, before and after each set of cyclic loading to obtain the Young's modulus.

e. Standardizing of Hoop Strain between Batches of Silicone Nucleus Pulposus

5 silicone discs from each batch were subjected to different percentages of axial compression to determine the hoop strain experienced. A close up photo of the silicone NP was taken with a CASIO EX-Z50 camera before and after compression (Fig 3.3.2b). The width of the disc before and after compression was measured using the Image J software (http://rsbweb.nih.gov/ij/). The hoop strain was then calculated by taking the ratio of the maximum change in width after compression over the original width of the silicone disc.

3.3.3 Preparing Combined Silk Scaffolds

The combined silk scaffolds are made up of a knitted silk skeleton with freeze dried silk covering the large holes within the knitted silk structure. Silk fibres were knitted using a knitting machine (Fig 4.3.3a) and the loose ends were held by inserting a K wire (Buhler, Uzwil, Switzerland) through the loops (Fig 4.3.3b). Sceracin, a protein

coating that causes immunogenic reactions when implanted was removed by boiling the silk in 0.1% Na_2CO_3 solution for 60 minutes.

To make the silk solution for freeze drying, sceracin was removed as stated above and dissolved in a solution of $CaCl_2$, 99% ethanol and water in a molar ratio of 1:2:8 at 80^{o}C for 15 minutes, to obtain a 10% silk solution. The silk solution was allowed to cool, put into a dialysis tubing with a molecular weight cut-off of 3500 daltons and dialysed in ddH_2O overnight. The silk solution was filtered before a small amount was characterized by freeze drying. The silk solution was then diluted to a concentration of 2% and the knitted silk scaffold immersed, to be freeze dried (Fig 3.3.3c).

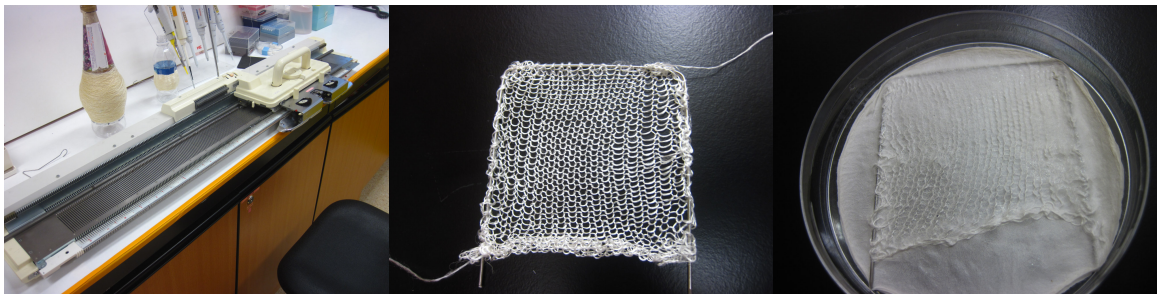

(a) (b) (c)

Fig 3.3.3: (a):Image of knitting machine; (b):Image of knitted silk scaffold; (c):Image of combined silk scaffold.

3.3.4 Fabrication of the Simulated IVD-like Construct

Strips of combined silk scaffolds measuring 50mm by 7mm was cut out and was used as substrates for the BMSC cell-sheets to adhere on and to simulate the lamellae structure of the AF when wrapped around the silicone NP.

a. Harvesting of BMSC Cell-Sheets

The harvesting of cells from tissue culture polystyrene (TCPS) usually involves harsh enzymatic conditions or mechanical methods that have deleterious effects on the cells and extracellular matrix. A method using a temperature responsive polymer, poly(N-isopropylacrylamide), (poly-NIPAAm) coated on the surface of normal TCPS to lift off the entire cell sheet would eliminate the problems faced by current cell harvest methods (Tsuda et al 2005,Okano et al 1995,Kushida et al 1999). 2 week old BMSC cell-sheets were cultured according to the protocol state in Section 4.1.3, but done on TCPS coated with poly-NIPAAm (Cellseed, Tokyo, Japan). It has been reported that this method allows the cell sheet to be harvested without any apparent damage to the ECM, and the cell sheet has improved re-adhesion properties to the new substrate (Canavan et al 2005).

Medium was removed from the well, and a CellShifter (Cellseed, Tokyo, Japan) was placed on top of the cell-sheet and incubated at 25^{o}C for 5 minutes. A pair of forceps was used to remove the CellShifter with the cell-sheet attached and transferred to the combined silk scaffold and left for 1 minute. The CellShifter was removed with a pair of forceps leaving behind the cell-sheet on the combined silk scaffold. The detached cell sheet would then be allowed to adhere to the combined silk scaffold.

b. Assembling the Silk AF and Silicone NP into the Simulated IVD-like Construct

The silk AF is made up of 3 strips of combined silk scaffold with only the centre strip having 2 BMSC cell-sheets attached to it, one on each side (Fig 4.3.4b). The 3 strips

of silk scaffolds would then be wrapped around the silicone NP and a suture be used to stitch the loose ends together (Fig 3.3.4b).

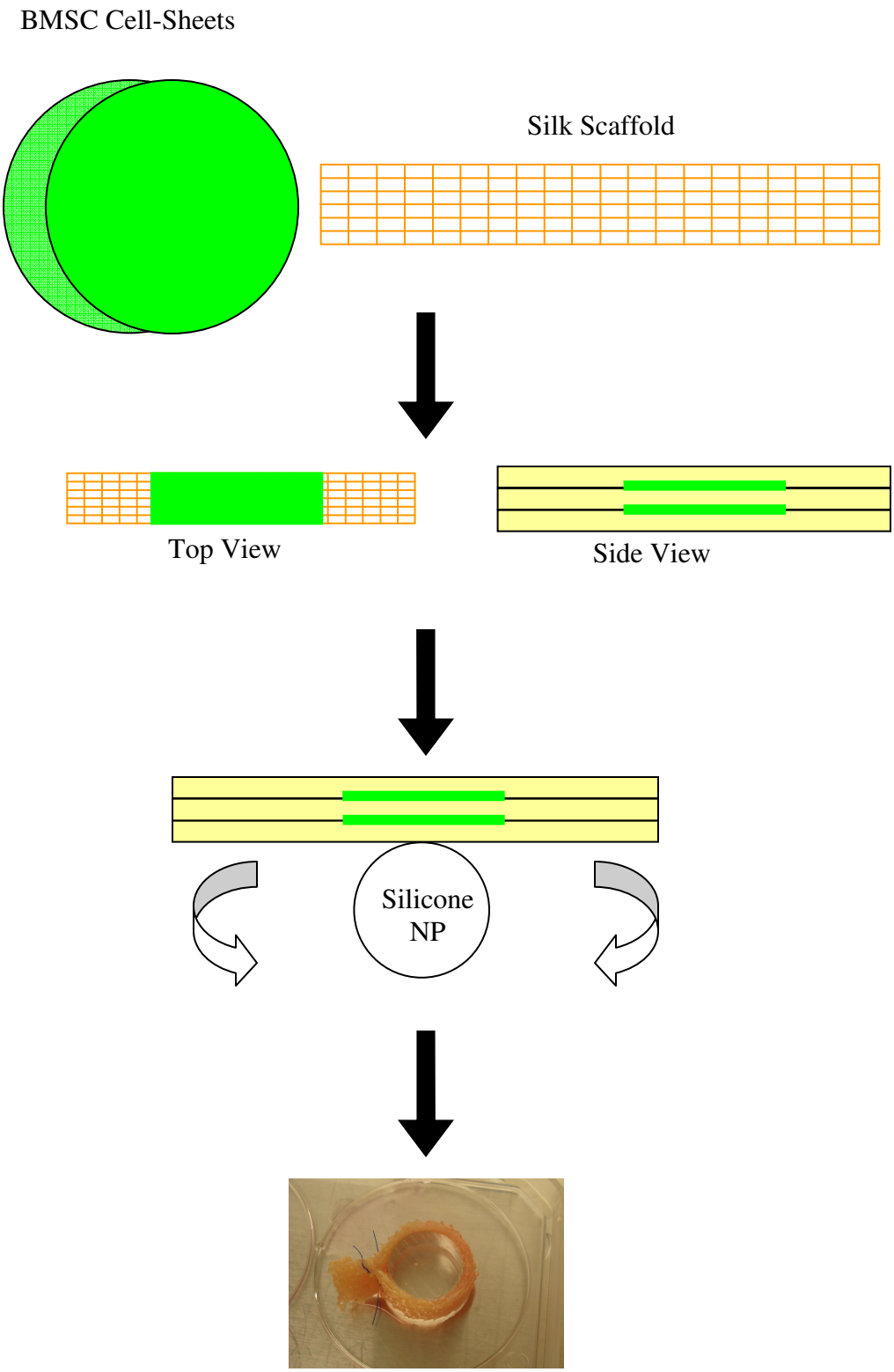

Fig 3.3.4b: Drawings illustrating Assembling of IVD Construct

1

3.3.5 Investigation of Simulated IVD-like Construct in Static Culture Conditions

a. Alamar Blue Cell-Sheet Viability Assessment

The viability of the cells present within the simulated IVD-like constructs was determined using the Alamar Blue colorimetric assay (Invitrogen, CA). The cells were incubated in medium supplemented with 10% (v/v) Alamar Blue dye for 3 hours. One hundred microliters of medium from each sample was read at 570/600nm in a microplate reader (Sunnyvale, CA). Medium supplemented with 10% Alamar Blue dye was used as a negative control and the percentage of Alamar Blue dye reduction was calculated according to the formula stated in Appendix A1. A percentage reduction of Alamar Blue dye would indicate that the cells assayed are viable.

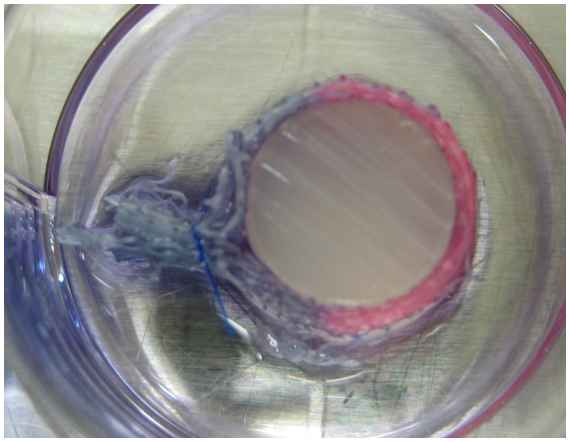

Fig 3.3.5a: Image of the Simulated IVD-like construct after Alamar Blue assay. Pink regions show the cell localization, blue regions have no cells.

b. SDS-PAGE Collagen Type I Quantification

The simulated IVD-like constructs were washed twice with 1xPBS after the Alamar Blue assay and digested with porcine gastric mucosa pepsin (2500 U/mg; Roche Diagnostics Asia Pacific, Singapore) in a final concentration of 0.25mg/mL. Samples were incubated at room temperature (RT) for 1h with gentle shaking followed by

sonication of the solution until all cell fragments have broken up followed by 1hr incubation at RT. After the incubation step, the samples were neutralized with 0.1 N NaOH. The samples were analyzed by SDS-PAGE under non-reducing conditions (See et al 2008). A SDS gel made up of 5% stacking and 7% resolving components were used (Appendix A4). The gel was run at 50V for 45 minutes and 180V for 95 minutes. Collagen bands were stained using SilverQuest kit (Invitrogen, Carlsbad, CA) according to the manufacturer's protocol (Appendix A3). Densitometric analysis of wet gels was performed on the GS-800 Calibrated Densitometer (Bio-Rad Laboratories, Hercules, CA) with the Quantity One v4.5.2 image analysis software (Bio-Rad Laboratories, Hercules, CA).

c. Histological Staining (H&E, ALcian Blue, Safranin-O)

The constructs were washed in 1xPBS, fixed in 10% neutral buffered formalin overnight, dehydrated in a progressively increasing ethanol gradient and then embedded in paraffin. 10μm thick sections were cut and collected on silane-coated slides for immunohistochemical analysis. Before staning, the sections were rehydrated a progressively decreasing ethanol gradient. The H&E staining technique was performed as follows: the samples were staining for 5 minutes with hematoxylin, washed with tap water and soaked in 0.2% (v/v) ammonium hydroxide for 30 seconds. They were washed in tap water and soaked in Eosin for 15 seconds. The slides were dehydrated before application of a coverslip. Alcian Blue staining technique was performed as follows: the samples where stained for 30 mins with Alcian Blue, washed for 3 min with ddH_2O, stained for 10 min with nuclear fast red and washed for 3 min with ddH_2O. The slides

were dehydrated before the application of a coverslip. Safranin O/fast green staining technique was performed as follows: the samples were stained for 3 min with iron hematoxylin, washed for 3 min with ddH_2O, stained for 3 min with fast green. They were washed in acetic acid for 5 sec and stained for 3 min with Safranin O. The slides were dehydrated before application of a coverslip.

d. Immunohistochemical Staining for Collagen Type I and Type II

The constructs were washed in 1xPBS, fixed in 10% neutral buffered formalin overnight and then embedded in paraffin. 10 μm thick sections were cut and collected on gelatin treated silane-coated slides for immunohistochemical analysis.

Immunohistochemistry study was carried out as follows: after deparaffinization and rehydration, endogenous peroxidase in the samples was first blocked with hydrogen peroxide for 15 min before pepsin treatment for 20 min. Monoclonal antibodies of collagen type I (Sigma-Aldrich, St Louis, MO) of dilution factor 1:500, collagen type II (Chemicon Inc., Temecuela, CA) of dilution factor 1:500; and control mouse IgG isotype (Zymed Laboratories Inc. San Francisco, CA) of dilution factor 1:2500 were applied for an hour followed by incubation with biotinylated goat anti-mouse (Lab Vision Corporation, Fremont, CA) for 30 min. Streptavidin peroxidase was added for 45 min and 3,30-diaminobenzidine was used as a chromogenic agent and counterstaining was done with hematoxylin. Between each step, the slides were washed with 1xPBS. The slides were dehydrated before application of a coverslip.

e. DNA Quantification

DNA content measured spectrophotometrically using the Hoechst 33258 method (Toh et al 2005). The fluorescence measurement of Hoechst 33258 dye was performed using a fluorescence plate reader (FLUOstar Optima, BMG Labtechnologies, Offenburg, Germany). Calf thymus DNA was used for construction of the standard curve for DNA quantification.

f. RNA Extraction and Real-Time PCR Analysis

Total RNA was extracted using Trizol® reagent (Invitrogen, Grand Island, NY) and purified using the RNeasy Mini Kit (Qiagen, Valencia, CA). RNA concentration was determined using NanoDrop (NanoDrop Technologies, Wilmington, DE) and complementary DNA synthesis was carried out using 100 ng of total RNA according to the manufacturer's protocol for SuperScript II reverse transcriptase with oligo(dT) primers. Real-Time PCR was done using 2µl of cDNA, 10µl of SYBR Green Master Mix (Qiagen, Valencia, CA) and the optimized concentration of primers, topped up to 20µl with nuclease free water. All reactions were performed on the real-time Mx3000P (Stratagene, CA, USA). The thermal cycling program for all PCRs was the following: 95ºC for 15 min, followed by 40 cycles of amplifications, consisted of denaturation step at 94ºC for 15 sec, an annealing step at 55ºC for 30 sec and an extension step at 72ºC for 30 sec. The genes analysed were Sox9, collagen type I (Col I), collagen type II (Col II), aggrecan, biglycan and decorin. Primer sequence for GAPDH and Collagen Type I (Col I) were previously described (Fan et al 2008). Remaining primers were designed using the Oligo 6.0 program and are listed in Table 4.3.5f. The level of expression of the target

gene, normalized to GAPDH, was then calculated using the 2^{Δ}Ct formula (Livak, & Schmittgen 2001) with reference to the respective control groups which are set to 1.

Gene	Primer Sequence	Product Size	Accession no
Sox9	F: 5' CTT CAT GAA GAT GAC CGA CGA G 3' R: 5' CTC TTC GCT CTC CTT CTT GAG G 3'	181bp	AY598935
Collagen Type II	F: 5' AAG AGC GGT GAC TAC TGG ATA G 3' R: 5' TGC TGT CTC CAT AGC TGA AGT 3'	214bp	D83228
Aggrecan	F: 5' GTG AAA GGT GTT GTG TTC CAC T 3' R: 5' TGG GGT ACC TGA CAG TCT GAT 3'	190bp	L38480
Biglycan	F: 5' ATG GCC TGA AGC TCA ACT ACC T 3' R: 5' ATC ATC CGG ATC TGG TTG TG 3'	187bp	AF020290
Decorin	F: 5' CCT TCT CTT ACG GAA CTA CAT C 3' R: 5' TGA AAC TCA GAC CCA ACT TAG 3'	103bp	U03394.1

Table 3.3.5f: Self Designed Primer Sequences for Assessment of Genes associated with IVD

3.3.6 Statistical Analysis

All data is expressed as mean ± standard deviation (SD). All statistical analysis was performed by pair-wise comparison of experimental categories using two-tailed, unpaired student t-test. A p-value <0.05 was considered significant. Statistical analysis was performed using Graph Pad Software (San Diego, CA).

3.4 Phase IV - Bioreactor Studies on Simulated IVD-like Construct

3.4.1 Design Concept of the Bioreactor

Under physiological conditions, NP cells within the IVD are compressed while the AF cells undergo a concentric tensile and radial compression stress due to the radial bulging of the NP. There have been several bioreactor systems designed with the aim to provide mechanical stimulus for IVD regeneration. However, most work involving mechanical stimulus uses hydrostatic (Reza, & Nicoll 2008) and hydrodynamic (Gokorsch et al 2004) pressure on IVD cells. However, these methods of mechanical stimulus do not accurately represent the physiological conditions experienced within the body. Therefore a bioreactor was designed to compress the silicone NP substitute, causing it to bulge in the radial direction to better mimic the physiological forced experienced by the AF.

3.4.2 Development of a Bioreactor to Compress Simulated IVD-like Assembly

The prototype consists of a water tight chamber and a moving platen to compress the simulated IVD-like assembly (Fig 3.4.2, see Appendix A5 for detailed Solidworks drawings). In order for the rotating motor to exert uniaxial compression onto the sample, a coupling is designed to transform the rotation into uniaxial motion. All the parts were made of stainless steel except the chamber case which was made up of acrylic. The bioreactor was made water-tight using rubber O-rings.

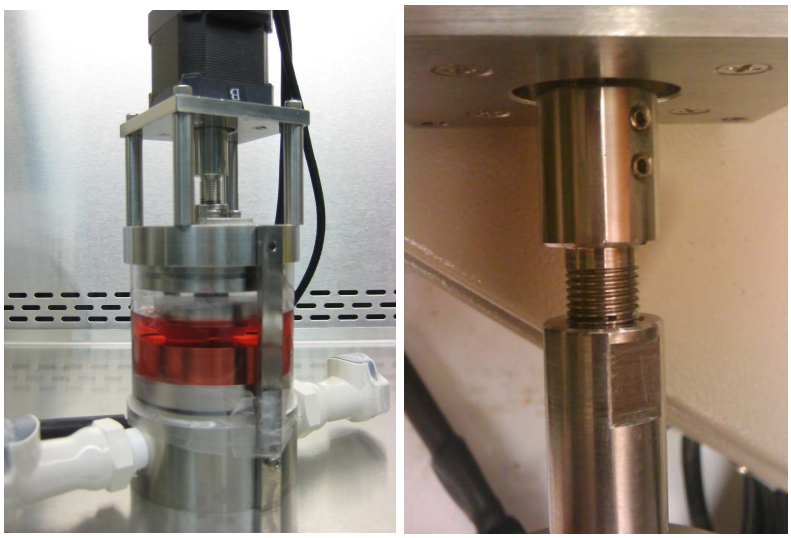

Fig 3.4.2: Picture of assembled bioreactor (left) and coupling to transform rotation into linear motion (right)

a. Software Programming

The software controller for the bioreactor was designed to be able to control 8 motors at once with the capacity to vary the following parameters:

1. Linear distance of compression
2. Duration of experiment
3. Frequency of each compressive cycle
4. Run Time Interval (Duration in which cyclic compressions will occur)
5. Wait Time Interval (Duration of rest between each round of compression)

3.4.3 Compression Regime and Culture Conditions for Simulated IVD-like Construct

A rehabilitative regime was chosen for the stimulation of the simulated IVD-like construct. The rehabilitative regime is based on gradually increasing the forces on the cells. This would ensure that the cells are conditioned, and produce the appropriate ECM

to be able to withstand larger forces. The assembly was compressed at 0.25Hz, for 15 minutes a day, for 4 weeks. The compression was increased gradually each week starting from 5% axial compression followed by 11% for the 2nd week, 18% for the 3rd and finally, 25% for the duration of the 4th week. The simulated IVD-like constructs was cultured in LG-DMEM supplemented with 15% FBS, 1% penicillin/streptomysin, and 50µg/ml of L-Asc. Medium was changed once a week.

3.4.4 Investigation of Simulated IVD-like Construct in Dynamic Culture Conditions

a. Alamar Blue Cell-Sheet Viability Assessment

The viability of the cells present within the simulated IVD-like constructs was determined using the Alamar Blue colorimetric assay (Invitrogen, CA). The cells were incubated in medium supplemented with 20% (v/v) Alamar Blue dye for 1 h. One hundred microliters of medium from each sample was read at 570/600nm in a microplate reader (Sunnyvale, CA). Medium supplemented with 20% Alamar Blue dye was used as a negative control and the percentage of Alamar Blue dye reduction was calculated according to the formula stated in Appendix A1. A percentage reduction of Alamar Blue dye would indicate that the cells assayed are viable.

b. SDS-PAGE Collagen Type I Quantification and Immunoblotting for Collagen Type II

The simulated IVD-like constructs were washed twice with 1xPBS after the Alamar Blue assay and digested with porcine gastric mucosa pepsin (2500 U/mg; Roche Diagnostics Asia Pacific, Singapore) in a final concentration of 0.25mg/mL. Samples were incubated at room temperature (RT) for 1h with gentle shaking followed by

sonication of the solution until all cell fragments have broken up followed by 1hr incubation at RT. After the incubation step, the samples were neutralized with 0.1 N NaOH. The samples were analyzed by SDS-PAGE under non-reducing conditions (See et al 2008). A SDS gel made up of 5% stacking and 7% resolving components were used (Appendix A4). The gel was run at 50V for 45 minutes and 180V for 95 minutes. Collagen bands were stained using SilverQuest kit (Invitrogen, Carlsbad, CA) according to the manufacturer's protocol (Appendix A3). Densitometric analysis of wet gels was performed on the GS-800 Calibrated Densitometer (Bio-Rad Laboratories, Hercules, CA) with the Quantity One v4.5.2 image analysis software (Bio-Rad Laboratories, Hercules, CA). For western immunoblotting, the sameple were subjected to SDS-PAGE and transferred to a nitrocellulose membrane. Primary antibodies for collagen type II (mouse anti-human Col II, MAB8887; Chemicon International, CA, USA) were used at 1:1000 dilutions. The signal was detected with chemiluminescence (Amersham™ ECL Plus Western Blotting Detection System; GE Healthcare., Buckinghamshire, UK) and captured with a VersaDoc Imaging System model 5000 (Bio-Rad Laboratories, Hercules, CA).

c. Histological Staining (H&E, Alcian Blue, Safranin-O)

The constructs were washed in 1xPBS, fixed in 10% neutral buffered formalin overnight, dehydrated in a progressively increasing ethanol gradient and then embedded in paraffin. 5 μm thick sections were cut and collected on silane-coated slides for immunohistochemical analysis. Before staning, the sections were rehydrated a progressively decreasing ethanol gradient. The H&E staining technique was performed as

follows: the samples were staining for 5 minutes with hematoxylin, washed with tap water and soaked in 0.2% (v/v) ammonium hydroxide for 30 seconds. They were washed in tap water and soaked in Eosin for 15 seconds. The slides were dehydrated before application of a coverslip. Alcian Blue staining technique was performed as follows: the samples where stained for 30 mins with Alcian Blue, washed for 3 min with ddH_2O, stained for 10 min with nuclear fast red and washed for 3 min with ddH_2O. The slides were dehydrated before the application of a coverslip. The Safranin O/fast green staining technique was performed as follows: the samples were stained for 3 min with iron hematoxylin, washed for 3 min with ddH_2O, stained for 3 min with fast green. They were washed in acetic acid for 5 sec and stained for 3 min with Safranin O. The slides were dehydrated before application of a coverslip.

d. Immunohistochemical Staining for Collagen Type I and Type II

The constructs were washed in 1xPBS, fixed in 10% neutral buffered formalin overnight and then embedded in paraffin. 5 μm thick sections were cut and collected on silane-coated slides for immunohistochemical analysis.

Immunohistochemistry study was carried out as follows: after deparaffinization and rehydration, endogenous peroxidase in the samples was first blocked with hydrogen peroxide for 15 min before pepsin treatment for 20 min. Monoclonal antibodies of collagen type I (Sigma-Aldrich, St Louis, MO) of dilution factor 1:500, collagen type II (Chemicon Inc., Temecuela, CA) of dilution factor 1:500; and control mouse IgG isotype (Zymed Laboratories Inc. San Francisco, CA) of dilution factor 1:2500 were applied for an hour followed by incubation with biotinylated goat anti-mouse (Lab Vision

Corporation, Fremont, CA) for 30 min. Streptavidin peroxidase was added for 45 min and 3,30-diaminobenzidine was used as a chromogenic agent and counterstaining was done with hematoxylin. Between each step, the slides were washed with 1xPBS. The slides were dehydrated before application of a coverslip.

e. DNA Quantification

DNA content measured spectrophotometrically using the Hoechst 33258 method (Toh et al 2005). The fluorescence measurement of Hoechst 33258 dye was performed using a fluorescence plate reader (FLUOstar Optima, BMG Labtechnologies, Offenburg, Germany). Calf thymus DNA was used for construction of the standard curve for DNA quantification.

f. RNA Extraction and Real-Time PCR Analysis

Total RNA was extracted using Trizol® reagent (Invitrogen, Grand Island, NY) and purified using the RNeasy Mini Kit (Qiagen, Valencia, CA). RNA concentration was determined using NanoDrop (NanoDrop Technologies, Wilmington, DE) and complementary DNA synthesis was carried out using 100 ng of total RNA according to the manufacturer's protocol for SuperScript II reverse transcriptase with oligo(dT) primers. Real-Time PCR was done using 2µl of cDNA, 10µl of SYBR Green Master Mix (Qiagen, Valencia, CA) and the optimized concentration of primers, topped up to 20µl with nuclease free water. All reactions were performed on the real-time Mx3000P (Stratagene, CA, USA). The thermal cycling program for all PCRs was the following:

95ºC for 15 min, followed by 40 cycles of amplifications, consisted of denaturation step at 94ºC for 15 sec, an annealing step at 55ºC for 30 sec and an extension step at 72ºC for 30 sec. . The genes analysed were Sox9, collagen type I (Col I), collagen type II (Col II), aggrecan, biglycan and decorin. Primer sequence for GAPDH and Collagen Type I (Col I) were previously described (Fan et al 2008). Remaining primers were designed using the Oligo 6.0 program and are listed in Table 4.3.5f. The level of expression of the target gene, normalized to GAPDH, was then calculated using the 2^{Δ}Ct formula (Livak, & Schmittgen 2001) with reference to the respective control groups which are set to 1.

3.4.5 Statistical Analysis

All data is expressed as mean ± standard deviation (SD). All statistical analysis was performed by pair-wise comparison of experimental categories using two-tailed, unpaired student t-test. A *p*-value <0.05 was considered significant. Statistical analysis was performed using Graph Pad Software (San Diego, CA).

CHAPTER 4

RESULTS

4.1 Phase I – Fabrication and Characterization of BMSC Cell-Sheet

4.1.1 Investigation on the Suitability of DexS to Aid BMSC Cell-Sheet Formation

a. SDS-PAGE Collagen Type I Quantification

From the SDS-PAGE results, it was shown that MMC using inert, negatively charged dextran sulphate for a period of 2 days was able to greatly enhance the collagen type I deposition on the cell layer (Fig 4.1.1a top). However, when another experiment was performed to determine the suitability of using MMC for long term culture on BMSCs, the SDS-PAGE gel results did not show an increase in collagen type I deposition for treatment C (twice DexS treated) over treatment A (once DexS treated) or B. In fact, treatment B (no DexS treatment) had the densest band, indicating more collagen type I deposition on the cell layer.

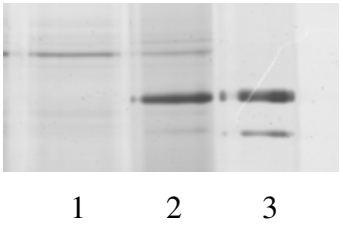

1: L-Asc
2: L-Asc + DexS
3: Collagen Type I standard

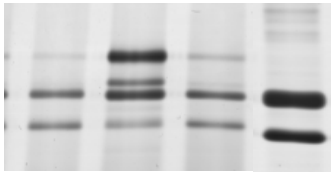

1: Treatment A
2: Treatment B
3: Treatment C
4: Collagen Type I standard

Fig 4.1.1a: (top) MMC treatment to aid Collagen Type I deposition (bottom) Collagen type I deposition does not increase after MMC treatment

b. Alamar Blue Cell-Sheet Viability Assessment between DexS and non DexS treated Cell-Sheets

From the data obtained from the Alamar Blue assay (Fig 4.1.1b), the cells in the cell-sheet were shown to remain viable during the 3 weeks of culture. There was no significant difference between the results when the cells were initially seeded, but the cell-sheets supplemented with L-Asc and DexS showed a significant decrease in the overall viability as compared to the ones only supplemented with only L-Asc.

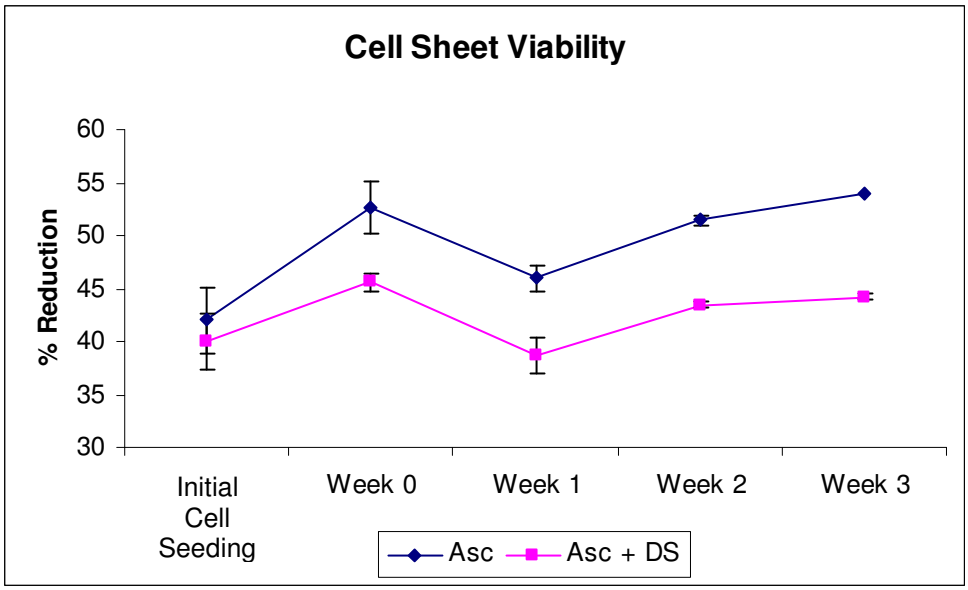

Fig 4.1.1b: Figure showing a significant decrease of cell-sheet viability between cultures supplemented with L-Asc and DexS (last 2 days) when compared to cultures with only L-Asc throughout

4.1.2 Technique to Accurately Quantify Collagen Content in Hyperconfluent Culture

a. Collagen Structure Unaffected by Sonication Treatment

Pepsin treatment of the cell layer destroys non collagenous components while leaving fibrillar collagens intact. Cell layers that just reach 100% confluence could be

entirely digested without the aid of sonication, therefore a comparison was done to prove that sonication did not affect the collagen structure as shown in Fig 4.1.2a. The Alamar Blue analysis showed no significant difference in cell numbers between samples that were not going to be sonicated and the samples that were going to be sonicated (Fig 4.1.2a). Densitometry showed no significant difference in collagen deposition between the sonicated sample and the un-sonicated sample of both BMSCs and fibroblasts (Fig 4.1.2a(b, c)).

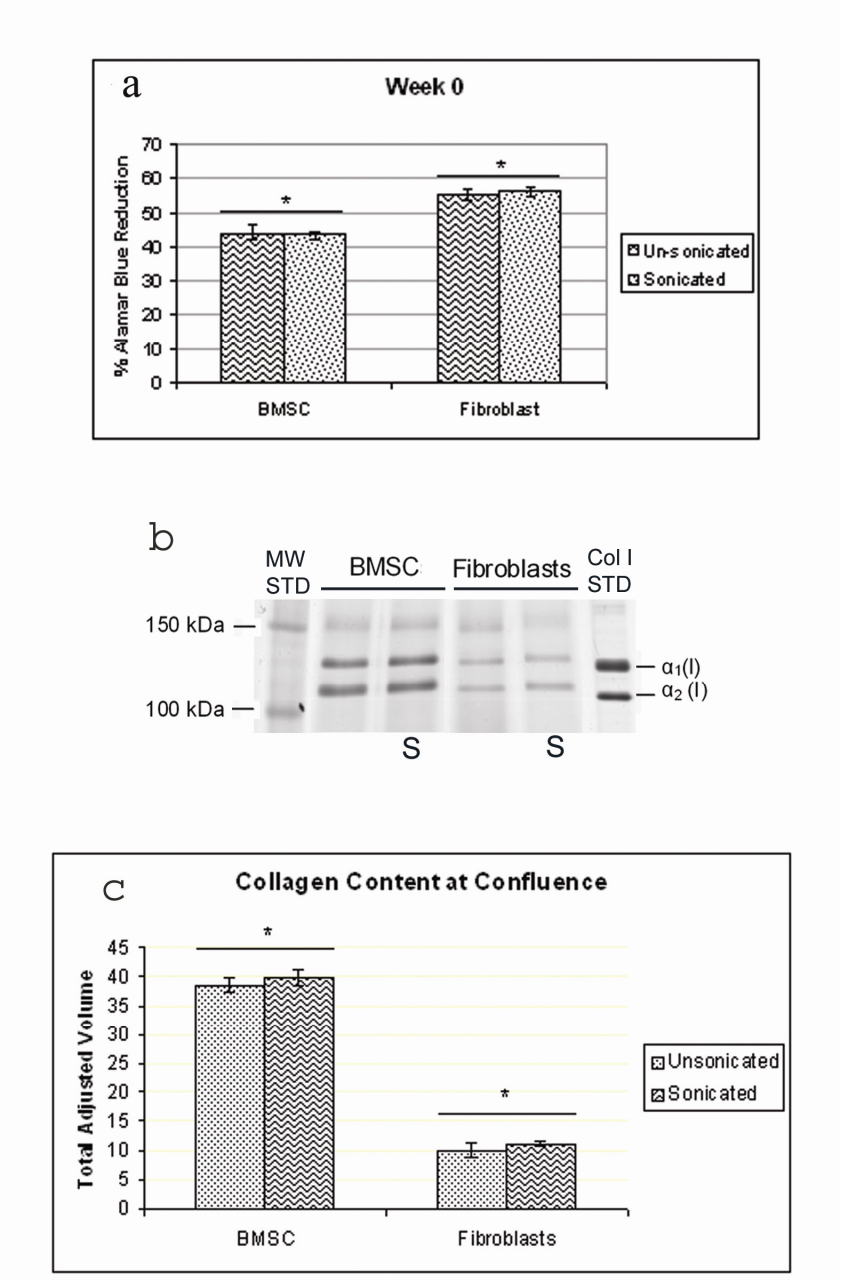

Fig 4.1.2a: (a) Alamar Blue analysis of sample wells shows no significant difference in cell numbers between sonicated and unsonicated samples of both BMSCs and fibroblasts at confluence; (b) Sonication does not affect collagen structure in both rabbit derived BMSCs and fibroblasts. Silver stained SDS-PAGE of peptic collagen extracts from the cell layer at 100% confluence. No difference observed in intensity and location of bands between sonicated and un-sonicated samples. MW STD, molecular weight ladder; BMSCs, bone marrow stromal cells; S, sonicated samples; (c) Graph showing the collagen quantified with and without sonication for both BMSCs and fibroblasts. Cells

were grown till confluence for this study. The results obtained are not statistically different *, $p>0.05$

b. Collagen Quantification in Hyperconfluent Culture Aided by Sonication

Although pepsin is able to destroy non collagenous components in early stages of culture, it is unable to efficiently destroy all non collagenous components in hyperconfluent cell cultures. But total destruction of all non collagenous components was achieved with the aid of a sonication step during the digestion process. The Alamar Blue analysis showed that there was no significant difference in cell numbers between the samples that were going to be sonicated and samples that were not going to be sonicated (Fig 4.1.2b(a)). Densitometry showed a significant difference in the density of collagen bands of samples obtained by culturing the cells for another 2 weeks after 100% confluence (Fig 4.1.2b(b)). The bands that have a significant difference are the collagen I crosslinking bands, β_{11}, β_{12}, and collagen I main chain bands, α_1 and α_2. This can be seen from the results of both the BMSC and fibroblasts cells. Results of the densitometric analysis of the gel bands show that the increase in collagen detected is stastically significant (Fig 4.1.2b(c)).

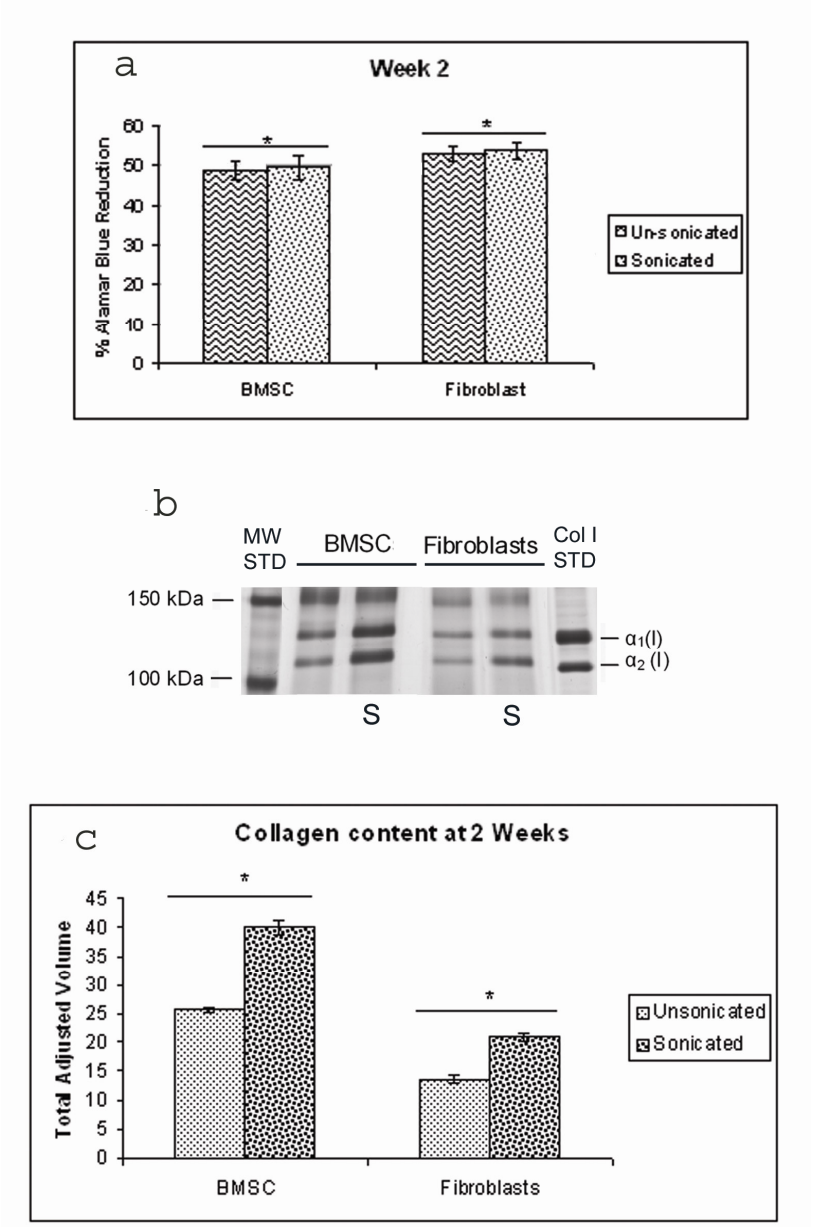

Fig 5.1.2b: (a) Alamar Blue analysis of sample wells shows no significant difference in cell numbers between sonicated and unsonicated samples of both BMSCs and fibroblasts at 2 weeks post confluence. *, $p>0.05$; (b) Sonication releases collagen that is trapped within cell layer fragments even after peptic digestion in both rabbit derived BMSCs and fibroblasts. Silver stained SDS-PAGE of peptic collagen extracts from the cell layer 2 weeks after 100% confluence. An obvious difference can be observed in intensity between sonicated and un-sonicated samples. Collagen fibrils are completely released by sonication. MW STD, molecular weight ladder; BMSCs, bone marrow stromal cells; S, sonicated samples; (c) Graph showing the increase in collagen quantified by sonication with both BMSCs and fibroblasts. Cells were grown till 2 weeks post confluence for this study. The results obtained are statistically different. *, $p<0.05$.

4.1.3 Investigation of BMSC Cell-Sheet Growth Post-Confluence

a. SDS-PAGE Collagen Type I Quantification

The results were obtained after densitometric analysis of the SDS-PAGE bands, followed by normalizing the data with the DNA content of the cell-sheets. The results show a steady increase of collagen type I deposition after each week.

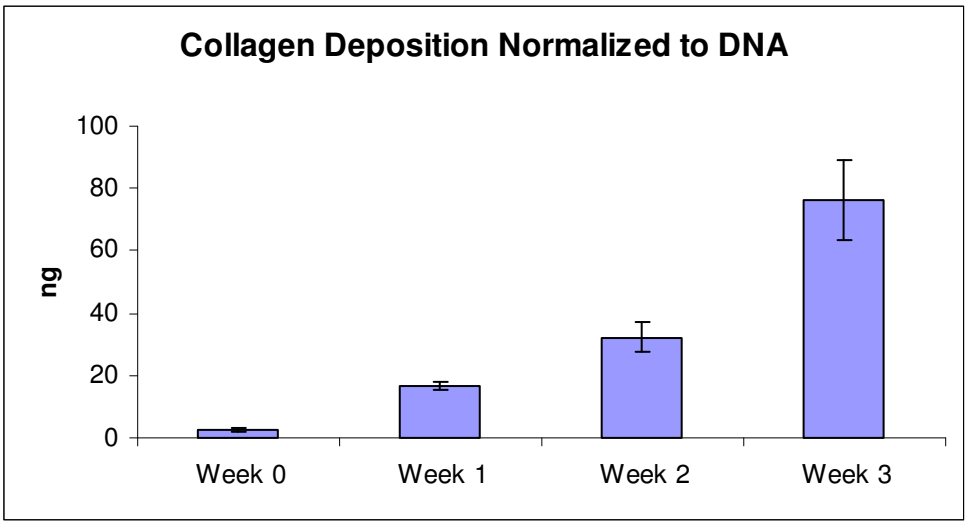

Fig 4.1.3a: Results of collagen type I deposition at weekly time points

b. Immunofluorescence for Cell-Sheet Thickness Assessment using Confocal Microscopy

It was observed that the hyperconfluent cell-sheet grew progressively thicker from 36.7 ± 2.1μm at week 0 to 78.5 ± 4.5 μm at week 3 with significant changes occurring between the 1st 2 weeks.

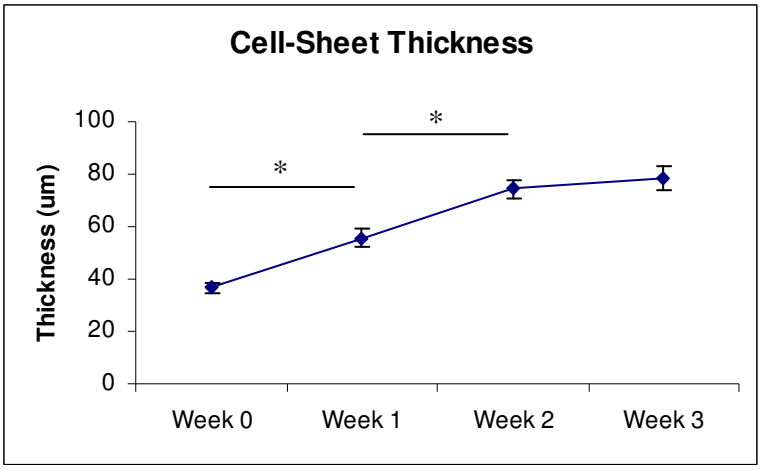

Fig 4.1.3b: Confocal microscopy results for cell-sheet thickness at weekly time points

c. SEM Analysis

The morphology of 2 week old cell-sheets was observed by phase contrast microscopy and SEM images. The results show that cell conformation and, indeed, individual cells cannot be distinguished by phase contrast and scanning electron microscopy (Fig 4.1.3c).

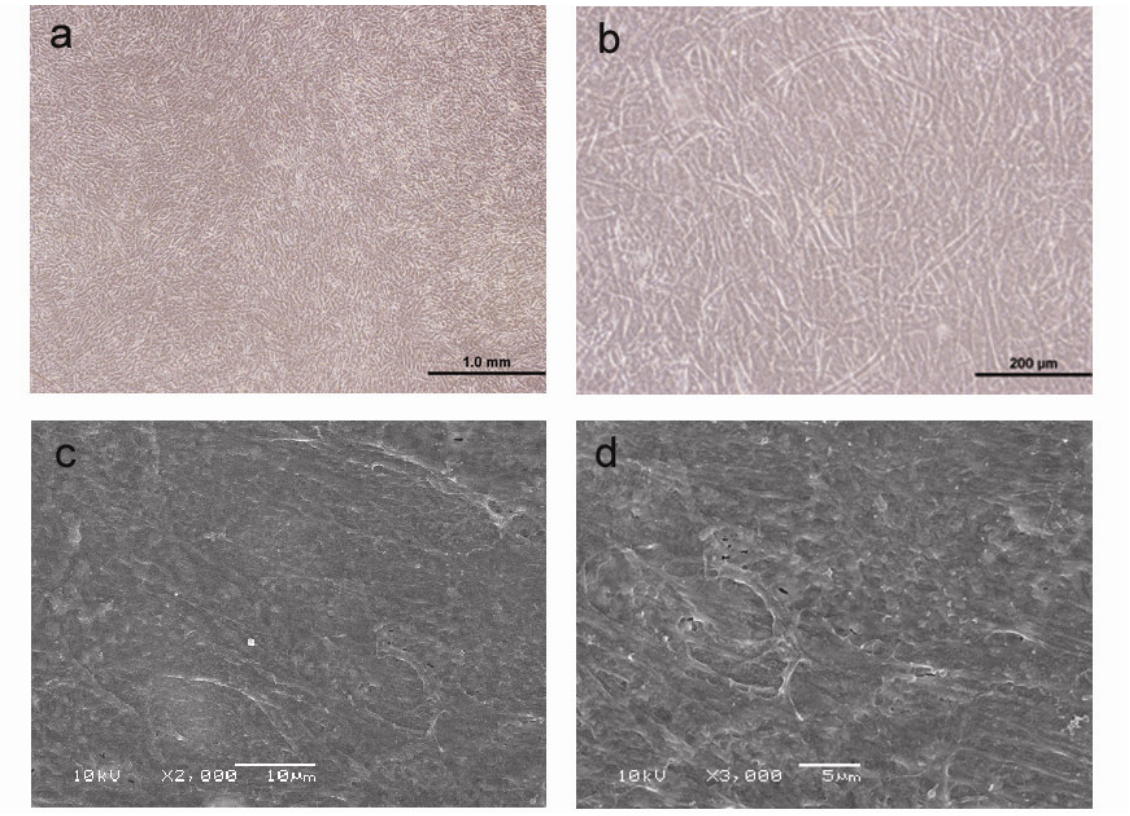

Fig 4.1.3c: Phase contrast (a, b) and SEM (c, d) images of 2 week old cell-sheets showing very dense mesh-like structures. (a) scale bars = 1mm; (b) scale bars = 200µm; (c) scale bars = 10µm; (d) scale bars = 5µm.

4.2 Phase II – Characterization of BMSC Cell-Sheet Multipotentiality and Comparison between Conventional BMSC Differentiation Protocols

4.2.1 Assessment of Adipogenic Differentiation of BMSC Cell-Sheets

a. Histochemical staining of Adipocytes

After 3 weeks of adipogenic differentiation, Oil Red O staining showed that both CI and CSI cultures had visible cytoplasmic lipid droplets formations within the cells (Fig 4.2.1a). Cytoplasmic lipid droplet formation was observed as early as the end of the 1st cycle of induction. After each cycle, the number and size of lipid droplets increased.

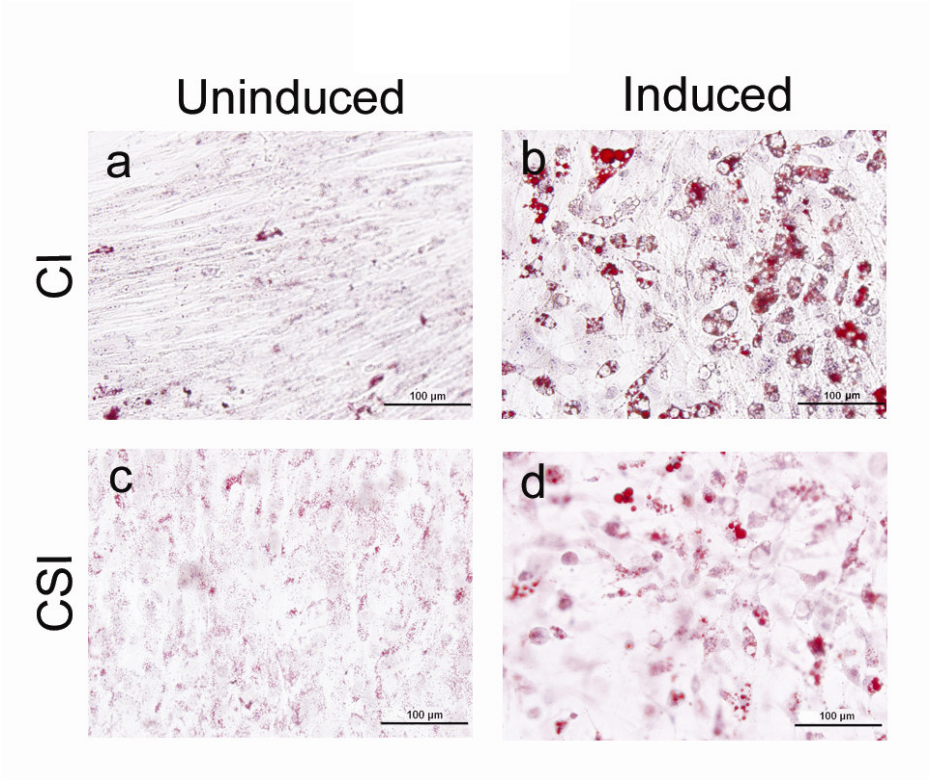

Fig 4.2.1a: Oil Red-O with hematoxylin counterstain of CI and CSI cultures compared to their NI cultures. CI and CSI cultures had large cytoplasmic lipid droplets (b, d) but the non-induced controls did not have any positive stain (a, c). Scale bars = 100µm.

b. Gene Expression of Adipogenic Differentiation Cultures

In both CI and CSI cultures, when compared to their respective NI cultures, mRNA expression levels of PPARγ2 and aP2 were significantly upregulated while leptin was significantly downregulated. The mRNA expression level of PPARγ2 and aP2 for CI cultures compared to the respective NI cultures resulted in a 3.1 ± 1.4 fold and 118 ± 63 fold increase respectively (Fig 4.2.1b(a)), while the CSI cultures compared to its respective NI culture had a 3.1 ± 0.2 and 65.6 ± 4.5 fold increase (Fig 4.2.1b(b)). Leptin mRNA expression levels on the other hand was markedly downregulated in both CI and CSI cultures, at 0.004 and 0.08 fold respectively. Comparing the mRNA expression levels between CI and CSI cultures, CSI cultures had a slight increase in PPARγ2 and aP2 expression of 1.27 ± 0.07 and 1.24 ± 0.08 fold respectively, but leptin mRNA expression was significantly higher at 10.7 ± 2.2 fold (Fig 4.2.1b(c)).

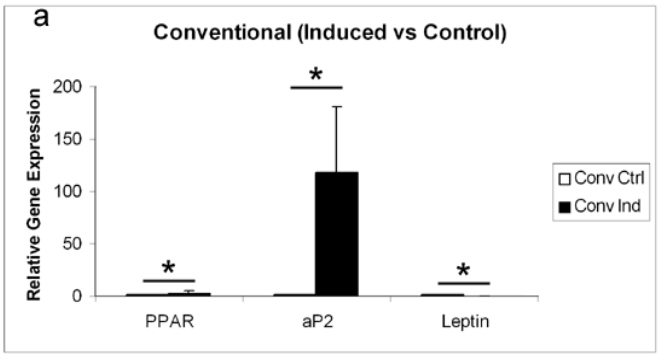

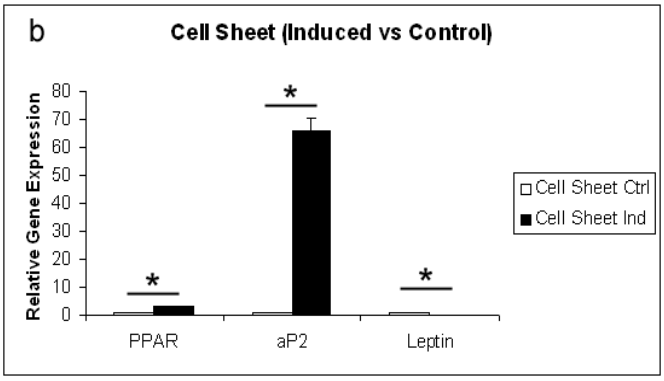

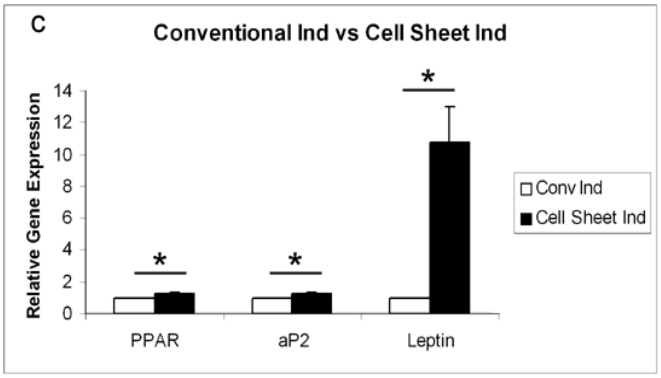

Fig 4.2.1b: Real Time RT-PCR of adipogenic genes (PPARγ2, aP2 and leptin) results compared between CI and CSI with their respective NI cultures (a, b) followed by a comparision of the gene expression between CI and CSI cultures (c). The level of expression of each target gene was normalized to GAPDH and calculated using the 2^{Δ}Ct formula with reference to the respective control groups, which are set to 1. For (a, b), PPARγ2 and aP2 was significantly upregulated while leptin was significantly downregulated. *p<0.05

4.2.2 Assessment of Chondrogenic Differentiation of BMSC Cell-Sheets

a. Histological and Immunohistochemical assessment of pellet cultures

After 3 weeks of chondrogenic differentiation, Safranin-O staining showed that both CSI and CI micromass cultures had rich amounts of glycosaminoglycans, and immunohistochemical staining for collagen type I and II showed that both cultures had a small amount of collagen type I matrix and a large content of collagen type II matrix (Fig 4.2.2a) when compared to the respective NI cultures which had predominantly collagen type I matrix. However, collagen type II matrix was barely detectable.

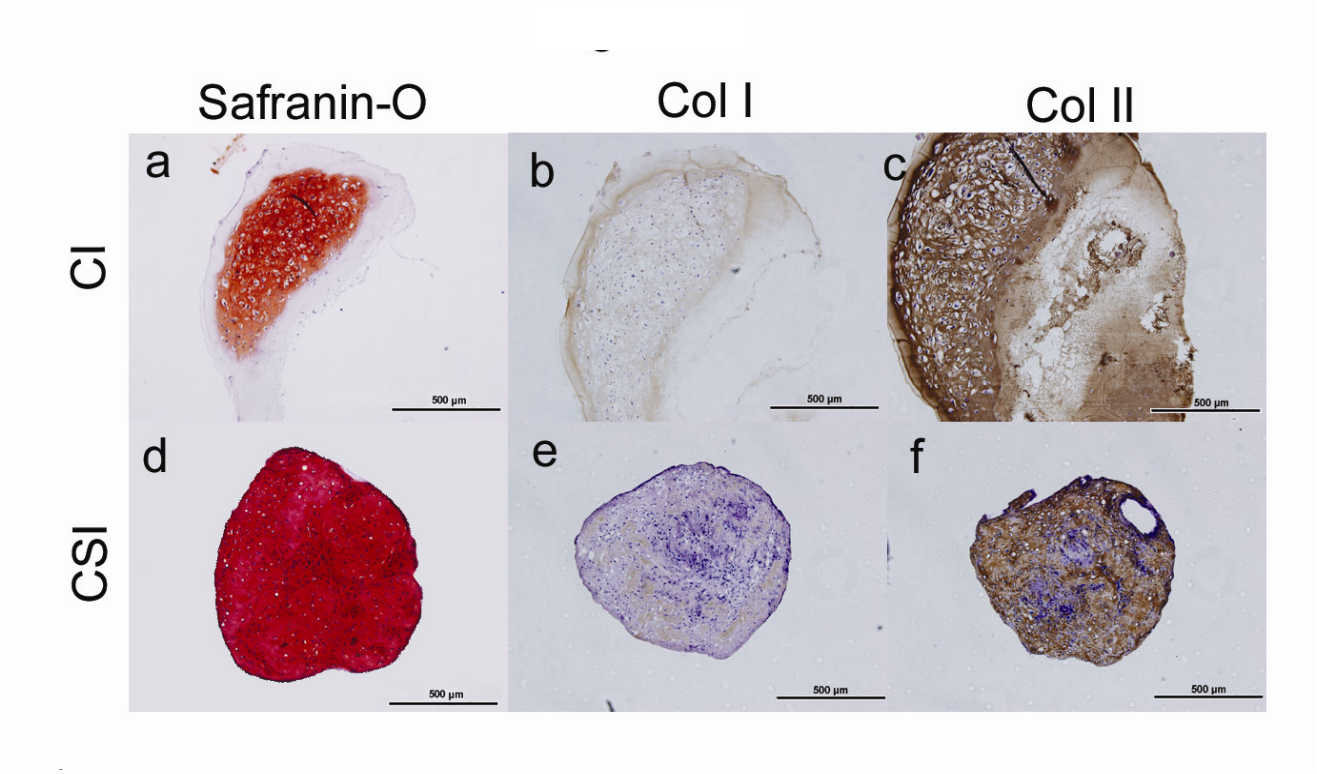

Fig 4.2.2a: Safranin-O with fast green counter stain of CI and CSI micromass pellets (a, d). Immunohistochemical staining of Col I (b, e) and Col II (c, f) showed that both induced micromass pellet cultures had strong Col II staining and very weak Col I staining. Scale bars = 500µm.

b. Gene Expression of Chondrogenic Differentiation Cultures

In both CSI and CI micromass cultures, when compared to their respective NI cultures, mRNA expression of Sox9, aggrecan and collagen type II were significantly upregulated. The mRNA expression level of Sox9, aggrecan and Col I for CI micromass cultures compared to the respective NI cultures resulted in a 18 ± 2.7, 215 ± 69 and 17.7 ± 3.4 fold increase respectively (Fig 4.2.2b(a)), while the CSI cultures compared to its respective NI culture had a 24.5 ± 9.2, 102 ± 31 and 4.26 ± 0.65 fold increase (Fig 4.2.2b(b)). On the other hand, collagen type II mRNA expression levels could not be quantified as both NI micromass cultures of CI and CSI did not have a measurable C_t value. The EtBr gel results distinctly showed that for both NI cultures, no collagen type II product was formed, while a thick band was found for both CI and CSI cultures (Fig 4.2.2b(c)). Comparing the mRNA expression levels between CI and CSI micromass cultures, CSI cultures had increases in all 4 gene expression of 5.4 ± 2.0, 18.3 ± 5.5, 15.6 ± 7.4 and 2.56 ± 0.4 fold for Sox9, aggrecan, collagen type II and collagen type I respectively (Fig 4.2.2b(d)).

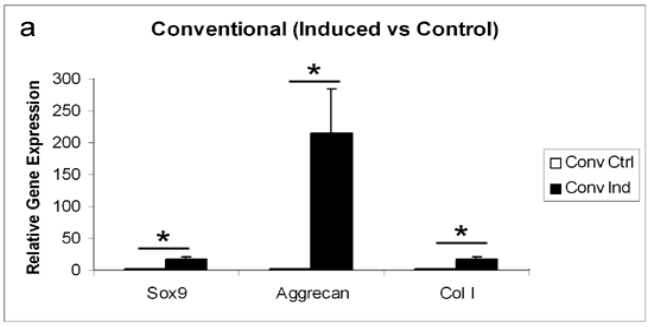

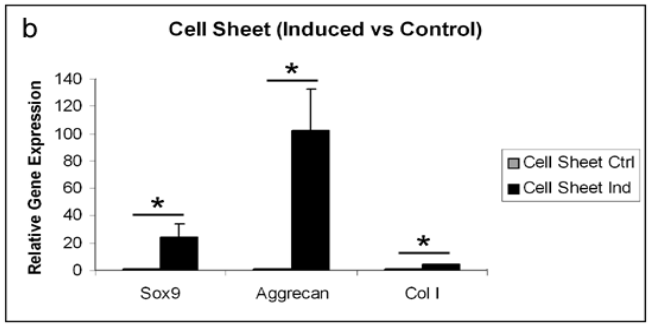

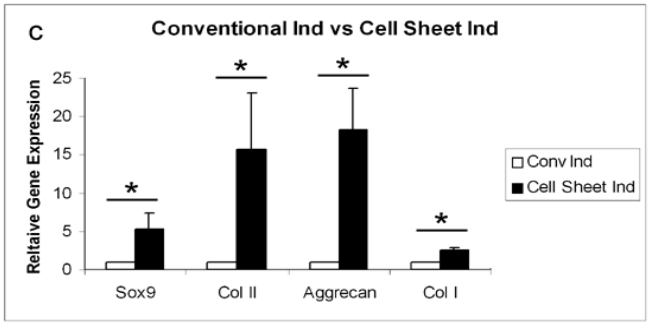

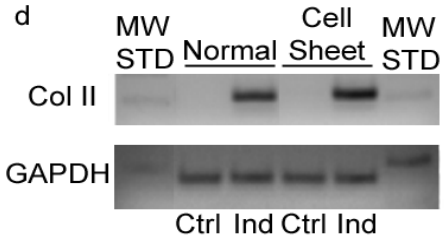

Fig 4.2.2b: Real Time RT-PCR of chondrogenic genes (Sox9, Aggrecan, Col I and Col II) results compared between CI and CSI with their respective NI cultures (a, b). A comparison of gene expression was done between CI and CSI cultures (c). The level of expression of each target gene was normalized to GAPDH and calculated using the 2^{Δ}Ct formula with reference to the respective control groups, which are set to 1. Ethidium bromine gel of Col II products (d) showed close to no expression of Col II products for NI cultures. All 4 genes in induced micromass pellets were significantly upregulated. *p<0.05.

4.2.3 Assessment of Osteogenic Differentiation of BMSC Cell-Sheets

a. Histochemical staining of Osteocytes

After 4 weeks of osteogenic differentiation, Alizarin Red S staining showed that both CI and CSI cultures had calcium deposits when cultured in osteogenic induction media, whereas no calcium deposits were found in the NI cultures (Fig 4.2.3a).

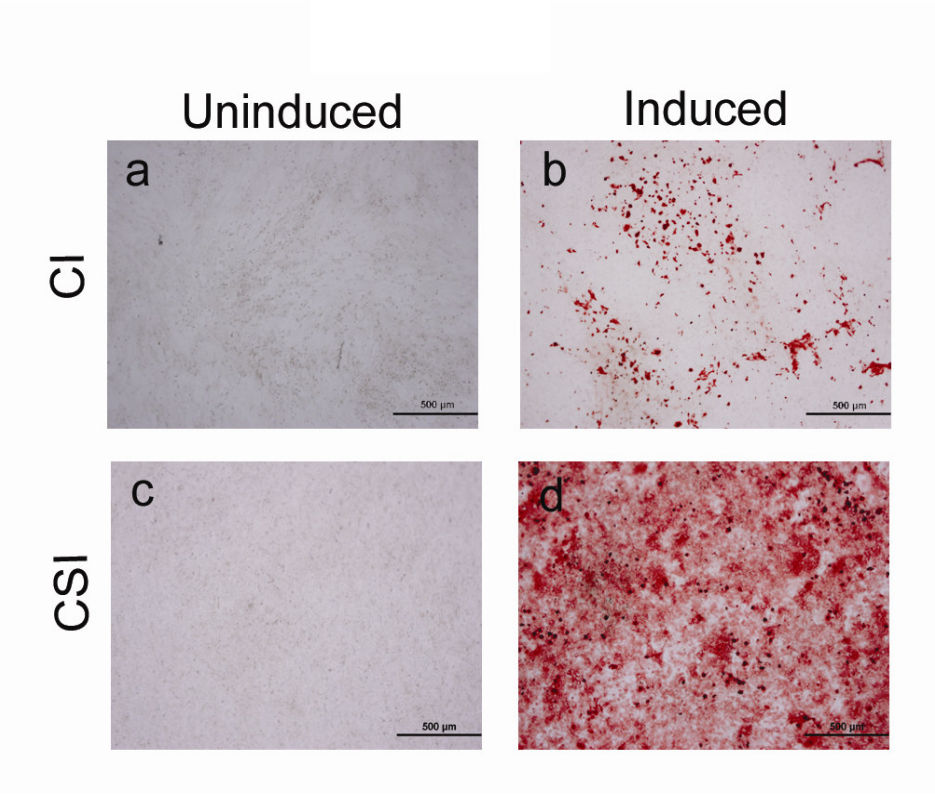

Fig 4.2.3a: Alizarin Red staining of CI and CSI cultures compared to their NI cultures. Both NI cultures did not have any stain (a, c) and the positive staining of CSI cultures (d) is visibly much more than in CI cultures (b). Scale bars = 500µm.

b. Gene Expression of Osteogenic Differentiation Cultures

In osteogenic medium, mRNA levels of Runx2, Collagen type I (Col I), Osteopontin (OPN) and Osteonectin (ON) from CSI and CI cultures were upregulated as compared to the NI cultures. At the end of the 4 week induction period, the mRNA level of Runx2 in the CI cultures was 5.6 ± 1.3 fold higher when compared to the respective NI

culture. Col I was 4.7 ± 0.1 fold higher while OPN and ON was upregulated by a factor of 1.56 ± 0.5 and 2.55 ± 0.25 respectively. The mRNA level of Runx2 in the CSI cultures was 3.3 ± 0.8 fold higher when compared to the respective NI culture. Col I was 4.27 ± 1.44 fold higher while OPN, and ON was both upregulated by a factor of 3.5 ± 0.8 and ± 0.7 respectively. CI cultures had a higher upregulation of Runx2 and a lower upregulation of the OPN gene, while CSI cultures had a lower upregulation of Runx2 and higher upregulation of the OPN gene. When the mRNA expression levels of these genes were compared between CI and CSI cultures, it was found that CSI cultures expressed significantly more osteogenic specific genes than CI cultures (Fig 4.2.3b).

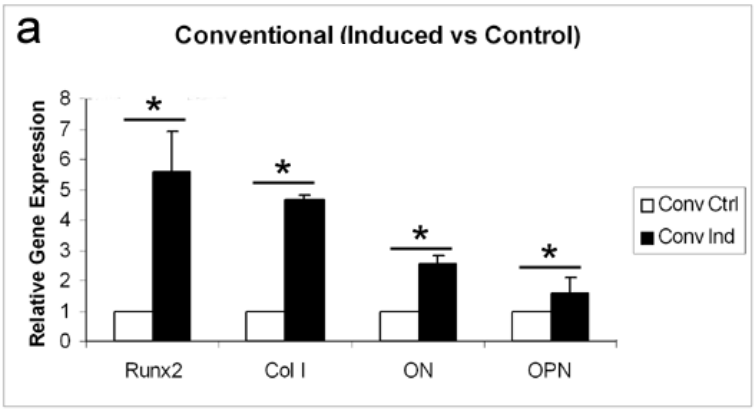

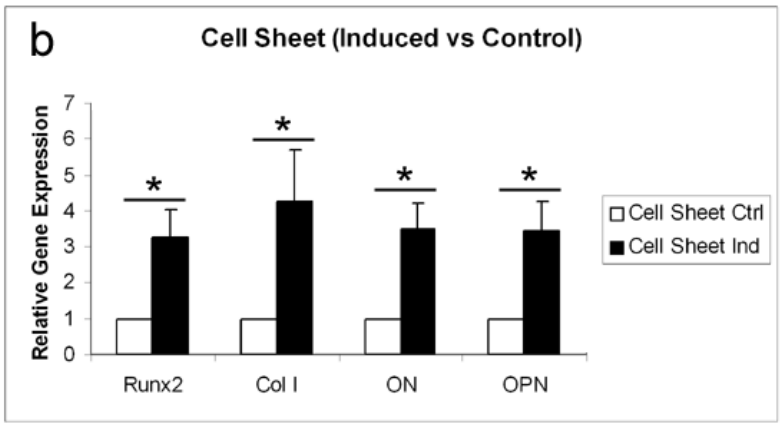

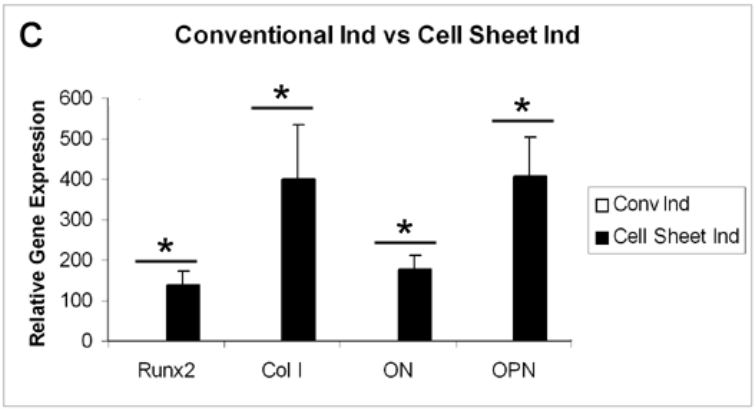

Fig 4.2.3b: Real Time RT-PCR of osteogenic genes (Runx2, Col I, ON and OPN) results compared between CI and CSI with their respective NI cultures (a, b), followed by a comparision of the gene expression between CI and CSI cultures (c). The level of expression of each target gene was normalized to GAPDH and calculated using the $2^{\Delta}Ct$ formula with reference to the respective control groups, which are set to 1. In all graphs, all 4 genes tested were significantly upregulated. *$p<0.05$

4.3 Phase III – Fabrication and Verification of a Simulated IVD-like Assembly

4.3.1 Characterization of Silicone Nucleus Pulposus

a. Calculation of Swelling Pressure (Hoop Stress) of Silicone NP

The swelling pressure of the silicone NP was calculated from 16% to 30% axial compression to determine the optimal axial compression that would give a swelling pressure of 0.05MPa. It was determined that a 25% axial compression gave an average swelling pressure of 0.0505 ± 0.0023 MPa. (Detailed calculations are shown in Appendix A6).

b. Effects of Ethylene Oxide Sterilization on the Mechanical Properties of the Silicone NP

Despite using the same protocol to fabricate 6 batches of silicone cylinders, the average Young's Modulus at 25% compression of batches A to F varies from as low as 1.04MPa to a high of 1.32MPa (details in Appendix A7). However, the Young's Modulus at 25% compression after ethylene oxide sterilization showed no significant change ($p>0.05$) from the pre-sterilized values for all 6 batches (Fig 4.3.1b).

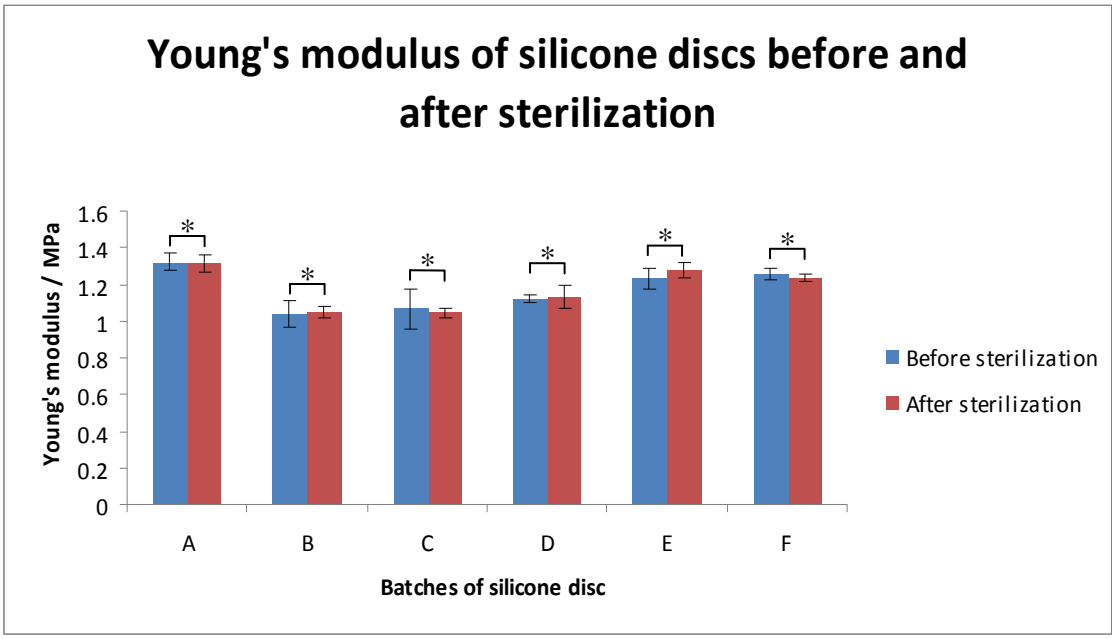

Fig 4.3.1b: No significant difference of Young's Modulus at 25% axial compression within each Silicone NP batch before and after sterilization. *p>0.05

c. Effects of Cyclic Loading on the Mechanical Properties of the Silicone Nucleus Pulposus

The Young's Modulus of the silicone discs from both batch B and batch D (Fig 4.3.1c) did not differ significantly after each day of the cyclic loading tests when tested with a 25% axial compression. The Young's Modulus of the discs was also not significantly different before and after the entire 3 day experiment (details in Appendix A8).

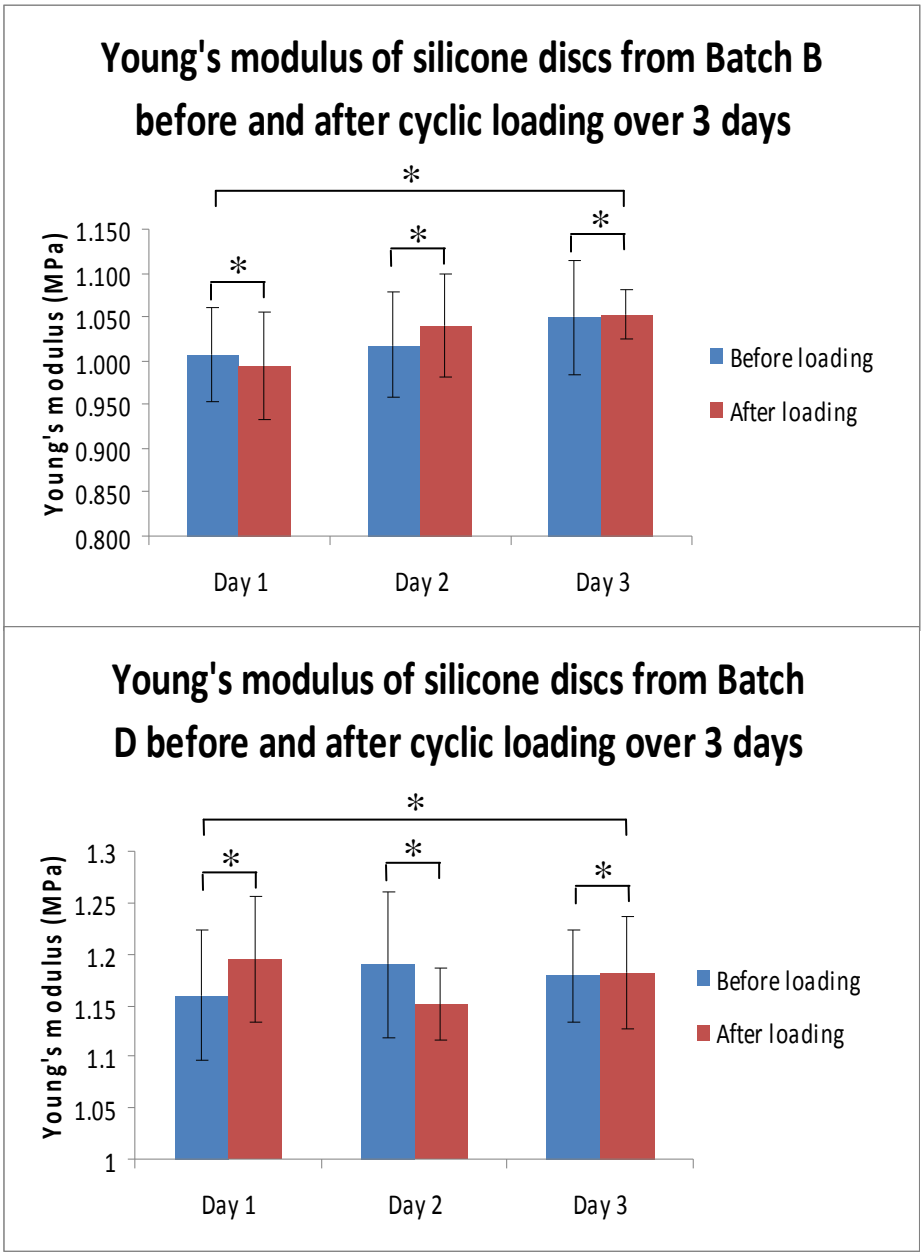

Fig 4.3.1c: Experiment done to show that the Young's Modulus of the silicone discs from batch B (top) and batch D (bottom) do not change significantly after cyclic loading. *p>0.05

d. Standardizing of Hoop Strain between Batches of Silicone Nucleus Pulposus

The hoop strain of Batch A was calculated to be 14.7±0.4% at a 25% axial compression. Batches B and D required a 23% axial compression to attain a 14.7±0.5%

and 14.6±0.4% hoop strain respectively, which batches C, E and F required a 24% axial compression to attain a 15.1±0.3%, 15.0±0.6% and 15.0±0.8% hoop strain respectively (details of results in Appendix A9). The hoop strain of batches B to F was not significantly different from that of batch A.

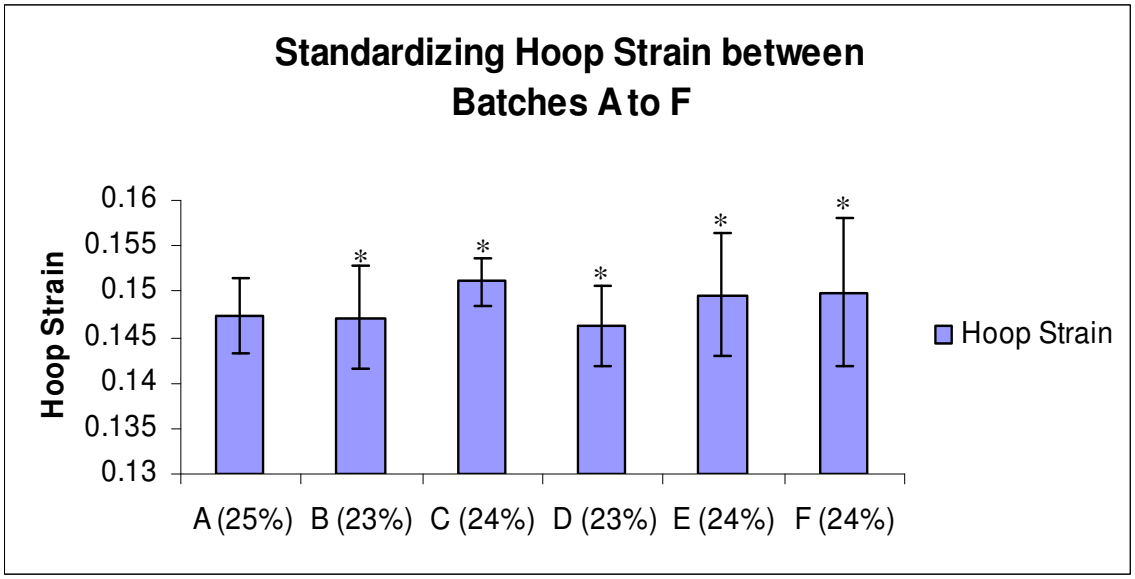

Fig 4.3.1d: Hoop strain of batches A to F. Batch B and D require 23% axial compression while batch C, E and F require 24% axial compression to attain a similar hoop strain profile to batch A. * p>0.05 when tested against batch A.

4.3.2 Investigation of Simulated IVD-like Assembly in Static Culture Conditions

a. Alamar Blue Simulated IVD-like Assembly Viability Assessment

From the data obtained from the Alamar Blue assay (Fig 4.3.2a), the cells in the simulated IVD-like construct were shown to remain viable during the 4 weeks of static culture.

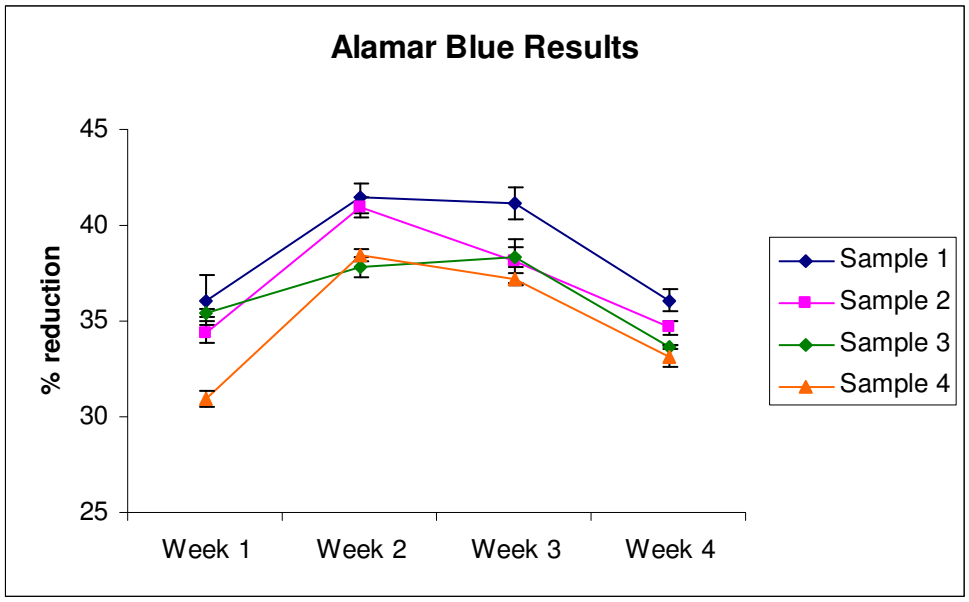

Fig 4.3.2a: Cells within the simulated IVD-like construct remain viable after 4 weeks of static culture

b. Histological Staining (H&E, Alcian Blue, Safranin-O)

After 4 weeks of static culture of the simulated IVD-like assembly, H&E staining showed that the cell-sheets adhered to the scaffolds (Fig 4.3.2b(a,d)). Alcian Blue staining was positive but Safranin-O was negative (Fig 4.3.2b(b,c,e,f). The results show that the GAG present within the ECM was poorly sulphated.

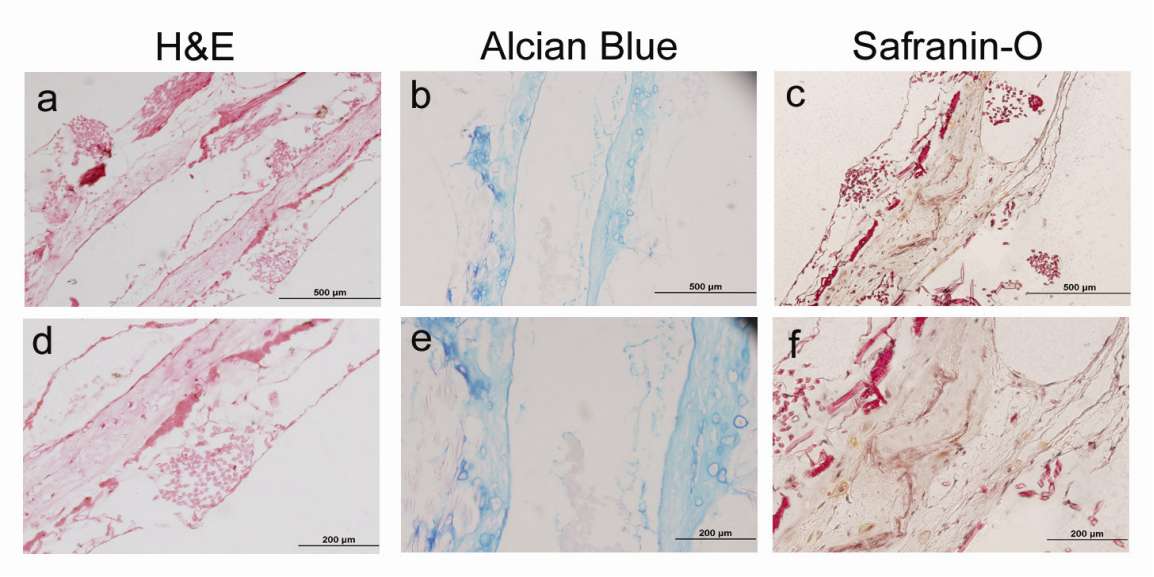

Fig 4.3.2b: H&E (a,d), Alcian blue (b,e) and Safranin-O (c,f) staining of simulated IVD-like assembly after 4 weeks of static culture. Scale bars = 500µm (a,b,c) and 200µm (d,e,f)

c. Immunohistochemical Staining for Collagen Type I and Type II

After 4 weeks of static culture of the simulated IVD-like assembly, immunohistochemical staining of collagen type I and collagen type II indicate that both types of collagen are found within the ECM (Fig 4.3.2c). There was no specific localization of both collagen types.

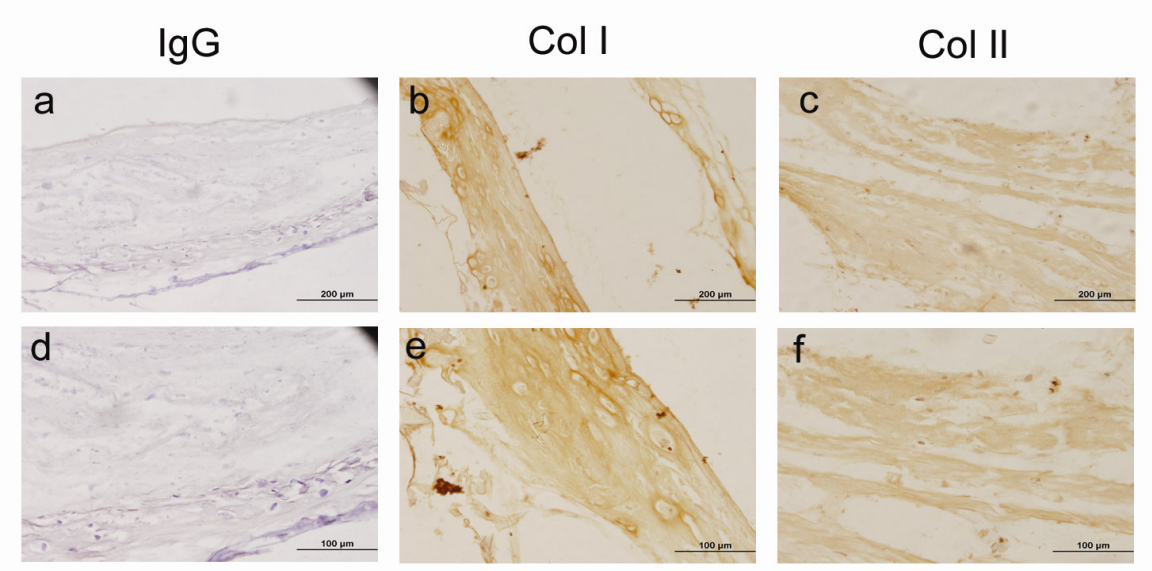

Fig 4.3.2c: Immunohistochemical staining of the simulated IVD-like assembly after 4 weeks static culture. (a,d): IgG control; (b,e): Col I; (c,f): Col II. Scale bars = 200µm (a,b,c) and 100µm (d,e,f).

d. Analysis of ECM for Collagen Type I Composition

SDS-PAGE was used to analyze the composition of the ECM of the cell-sheets before transplantation and after 4 weeks of static culture. It was shown that collagen type I content decreased over the 4 weeks of static culture (Fig 4.3.2d).

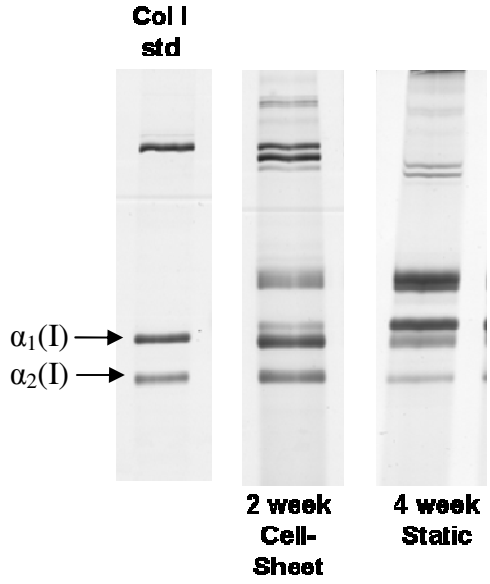

Fig 4.3.2d: SDS-PAGE to determine ECM composition of 2 week old cell-sheets and 4 week static culture of simulated IVD-like assembly. 4 week static cultures showed a decrease in collagen type I expression.

4.4 Phase IV – Bioreactor Studies of Simulated IVD-like Assembly

4.4.1 Investigation of Simulated IVD-like Construct in Dynamic Culture Conditions

a. Alamar Blue Simulated IVD-like Assembly Viability Assessment (Static vs Dynamic)

The results of the Alamar Blue assay show that the cells cultured in static and dynamic conditions remain viable over the 4 week period (Fig 4.4.1a). However, after week 2, the metabolic rate of the cells cultured under dynamic conditions begins to drop, and at week 4, the cells within the dynamic culture have a distinctly lower metabolic rate than the static control cultures.

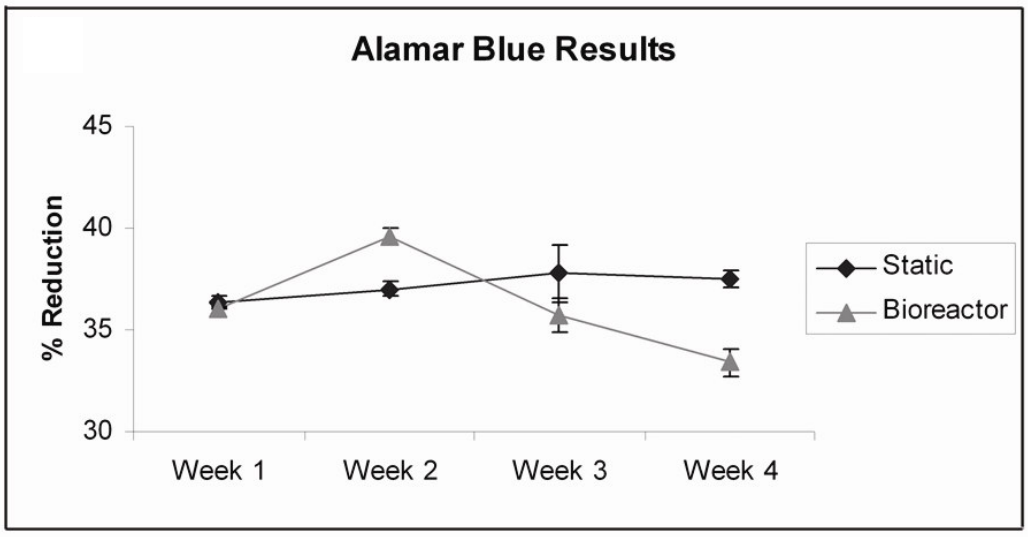

Fig 4.4.1a: Cells of both the static and dynamic cultures remain viable and metabolically active over 4 weeks. However, the metabolic rate of the cells within the dynamic cultures begins to decrease after the 2nd week.

b. SDS-PAGE Collagen Type I and Immunoblot for Collagen Type II

The results of the SDS-PAGE indicate a decrease in the amount of collagen type I within the ECM of the assemblies within the dynamic culture at Week 2 and Week 4. When compared to the static control, the composition of collagen type I in the ECM was also reduced. For collagen type II immunoblot, it is shown that the deposition of collagen

type II occurs in both the static culture and dynamic culture after 4 weeks. However, at 2 weeks, deposition of collagen type II was barely detected.

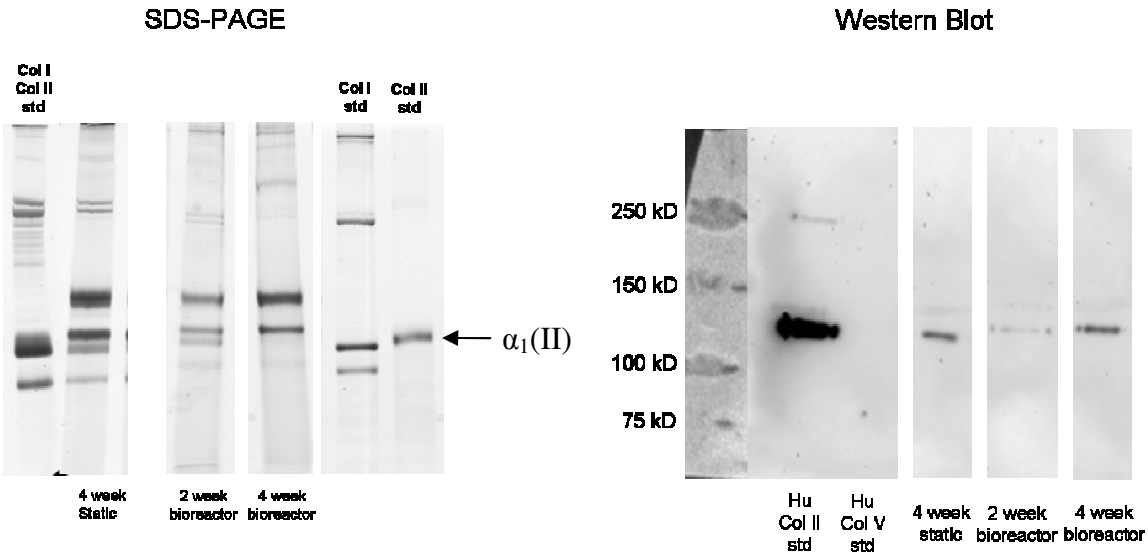

Fig 4.4.1b: SDS-PAGE collagen type I and type II between 4 weeks static culture and 2 weeks/4 weeks dynamic culture. Collagen type I deposition decreased over the 4 week dynamic culture period. Collagen type II was detected in both 4 week static and 4 week dynamic culture

c. Histological Staining (H&E, Alcian Blue, Safranin-O)

After 2 weeks and 4 weeks of dynamic culture, the simulated IVD-like assembly was sacrificed for histological analysis. H&E staining showed that the cell-sheets adhered well to the scaffolds (Fig 4.4.1c(a,d)). Both Alcian Blue and Safranin-O staining was positive at both 2 weeks and 4 weeks of dynamic culture (Fig 4.4.1c(b,c,e,f). The results show that the GAG present within the ECM became more sulphated from dynamic stimulation.

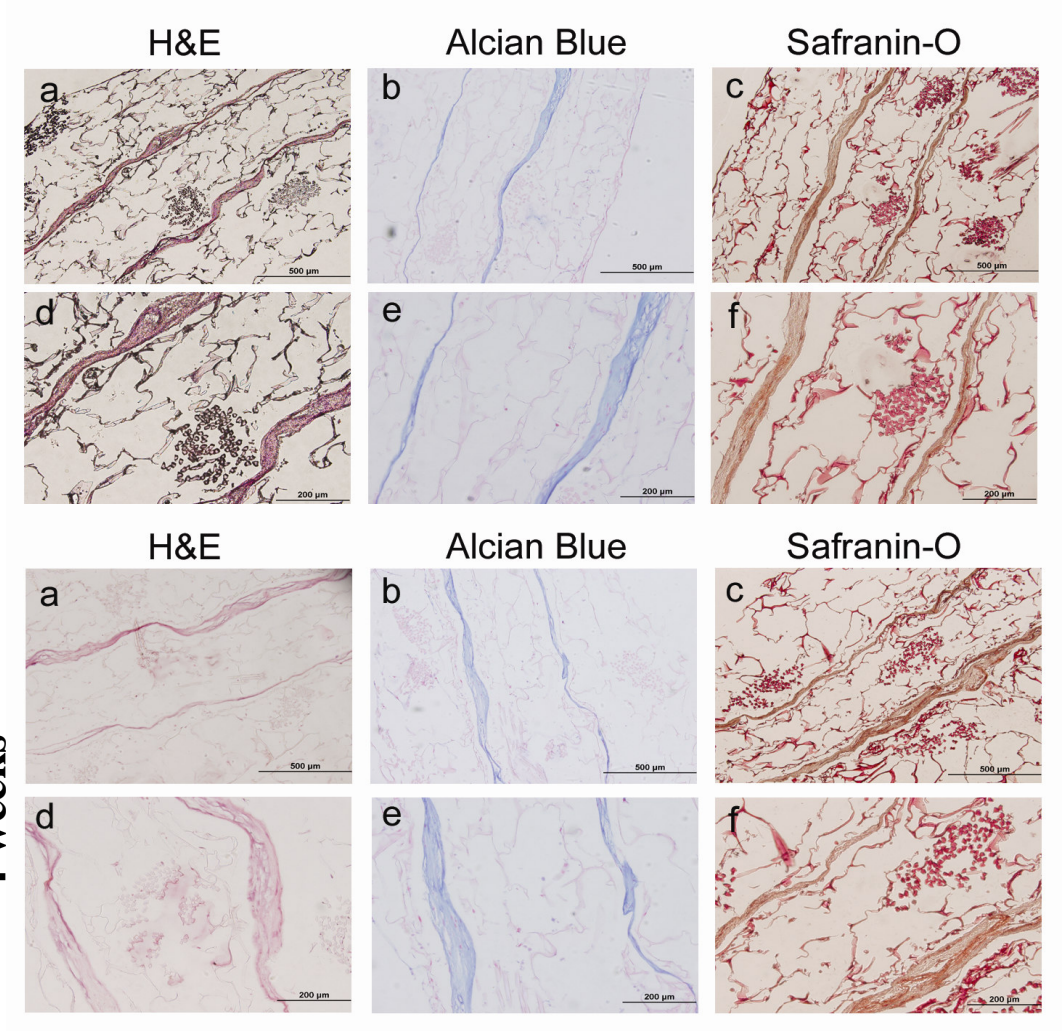

Fig 4.4.1c: H&E (a,d), Alcian blue (b,e) and Safranin-O (c,f) staining of simulated IVD-like assembly after 2 weeks and 4 weeks of dynamic culture. Scale bars = 500µm (a,b,c) and 200µm (d,e,f)

d. Immunohistochemical Staining for Collagen Type I and Type II

After 2 weeks and 4 weeks of dynamic culture, the simulated IVD-like assembly was sacrificed for immunohistochemical staining analysis. It is concluded that both collagen type I and collagen type II are present at both the 2 week and 4 week timepoint.

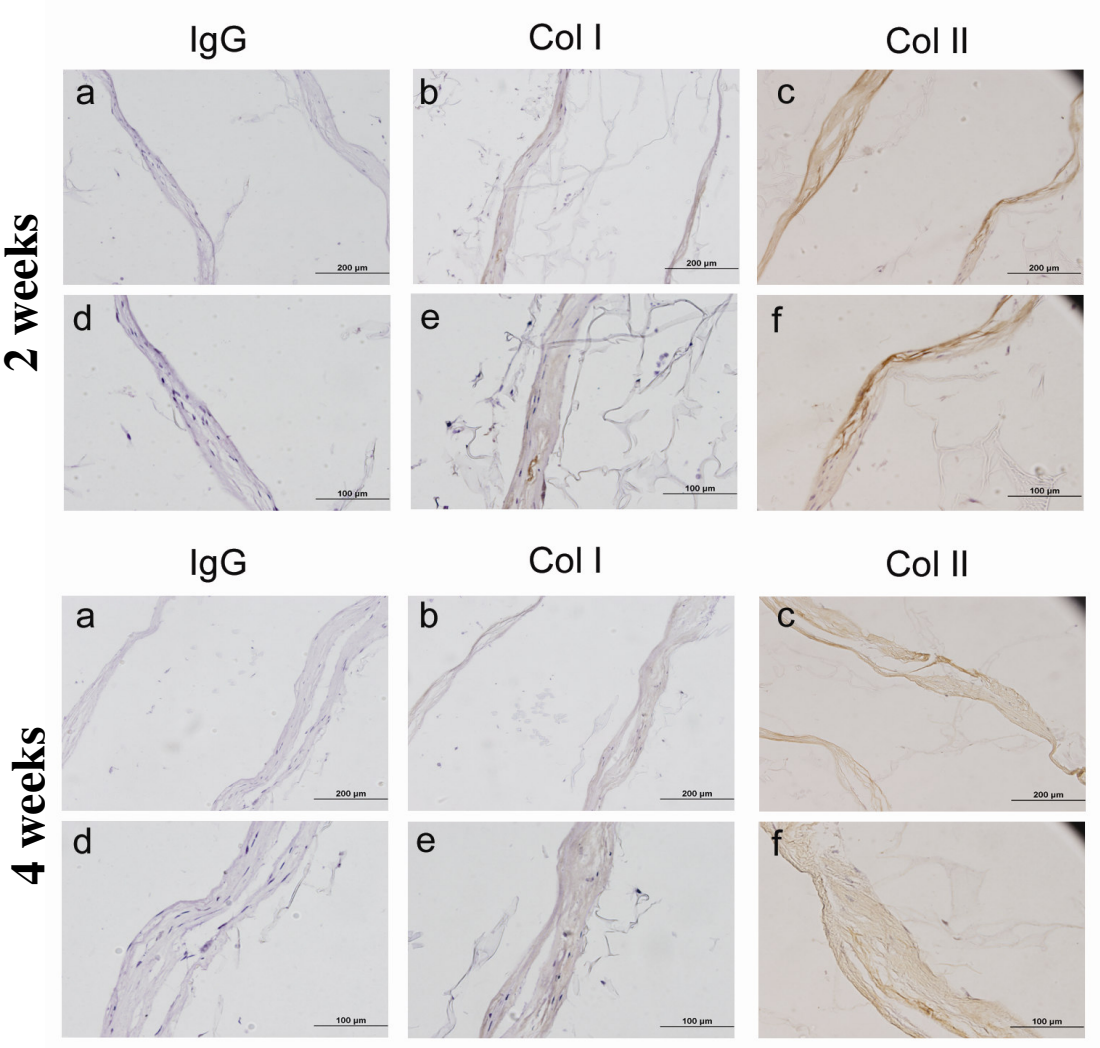

Fig 4.4.1d: Immunohistochemical staining of the simulated IVD-like assembly after 2 weeks (top) and 4 weeks (bottom) of dynamic culture. (a,d): IgG control; (b,e): Col I; (c,f): Col II. Scale bars = 200µm (a,b,c) and 100µm (d,e,f).

e. Real-Time PCR Analysis between Static and Dynamic Cultures of the Simulated IVD-like Assembly

After 4 weeks of dynamic culture in the bioreactor, the mRNA expression levels of Sox9, collagen type I (Col I), aggrecan (Aggr) and decorin (Dec) were upregulated when compared to the mRNA expression levels of the IVD-like assemblies in 4 weeks of static culture. The mRNA expression level of Sox9 after 4 weeks of dynamic culture was

2.68 ± 0.7 fold higher when compared to the 4 week static cultures. Col I mRNA expression level was 2.00 ± 0.4 fold higher while aggrecan and decorin was upregulated by a factor of 6.54 ± 1.2 and 3.96 ± 1.2 respectively. The only gene that was significantly upregulated by the 2 week dynamic culture period when compared to the 4 week static culture was collagen type II (Col II). The mRNA expression level of collagen type II was upregulated by a factor of 4.10 ± 0.9 at the 2 week dynamic culture time point and further upregulated to 8.55 ± 2.6 folds by the 4 week dynamic culture period. However, the gene expression of biglycan did not show can significant upregulation even after 4 weeks of dynamic culture.

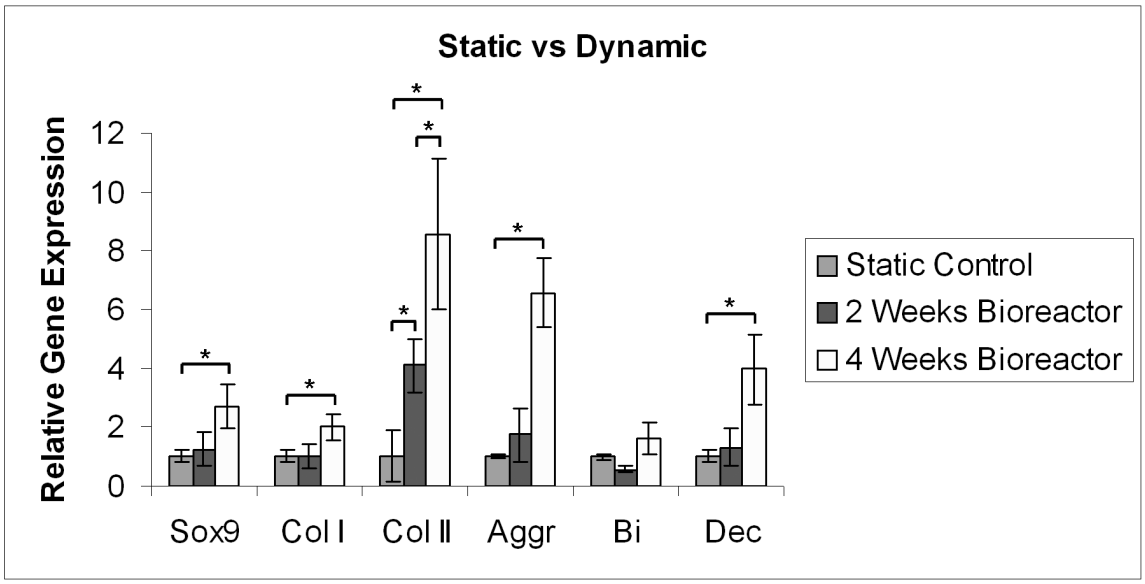

Fig 4.4.1e: Real Time RT-PCR results of common IVD genes (Sox9, Col I, Col II, Aggr, Bi, Dec) compared between 2 week and 4 week dynamic cultures against 4 week static cultures. The level of expression of each target gene was normalized to GAPDH and calculated using the 2^{Δ}Ct formula with reference to the control group, which are set to 1. At week 2, only Col II was upregulated, but at week 4, all the genes but biglycan were upregulated and Col II was further upregulated. *p<0.05

CHAPTER 5

DISCUSSION

5.1 Phase I – Fabrication and Characterization of BMSC Cell-Sheet

Fabrication of a stable engineered tissue depends largely on the formation of the ECM. An integral part of the ECM is made up of collagen. Research has shown that L-Asc accelerated procollagen processing to collagen and therefore enhanced the rate of collagen synthesis over long term culture (Hata, & Senoo 1989). In a more recent *in vitro* study, it was shown that collagen deposition was enhanced by using EVE on top of adding L-Asc (Lareu et al 2007). EVE was achieved by adding DexS, an inert macromolecular crowder to the culture media. The study showed that the enhanced ECM formation was also due to an acceleration of procollagen conversion. The experiment using L-Asc together with EVE to improve collagen deposition was done on terminally differentiated cells in short term *in vitro* culture. With an increasing interest in formation of a robust BMSC cell-sheet, it is important that we characterize the effects of L-Asc together with EVE in long term cultures on BMSCs and using the better technique to fabricate and characterize the BMSC cell-sheet process. Hence this study was conducted with these aims in mind.

In order to characterize the effects of L-Asc together with EVE on BMSCs in long term culture, we followed the procedures in delivering a pulse of EVE for 2 days just before harvesting for assessment (Lareu et al 2007). Alamar blue cell viability assay and SDS-PAGE quantification of collagen deposition was evaluated. The L-Asc together with EVE treated cultures were compared to the ones with only L-Asc treatment.

The experimental results show that EVE was able to improve the efficiency of collagen type I deposition on the BMSC cell layer at confluence (Fig 4.1.1a (top)). However, when the experiment was extended in an attempt to use EVE in pulses

(Treatment C) to further improve the collagen type I deposition, the results was not comparable to that of the wells of only L-Asc treatment (Treatment B). Moreover, the results from the Alamar Blue assay also showed that cultures that are treated with DexS have a significantly lower viability when compared to the non DexS treated cultures (Fig 4.1.1b). It was concluded that the BMSCs treated with EVE had an improved efficiency of collagen deposition, but the technique is ineffective in pulses. Since the viability of the cells was significantly reduced after treatment with EVE, it is not a feasible technique to aid in improving the existing fabrication method of a cell-sheet.

The technique of using pepsin digestion for assessment of collagen content in short term cultures are accurate. However, this technique is not robust enough to digest hyperconfluent cell layers from long term cultures, as shown in Fig 4.1.2b. Therefore, to accurately quantify the collagen content within the hyperconfluent cell layers, we have shown in our results, (Fig 4.1.2a) that sonication does not affect the structure and concentration of collagen from short term subconfluent cell cultures, and also, successfully shown that sonication of the fragments left behind after peptic digestion aids to breakdown the cell sheet fragments. The breakdown of the indigestible cell sheet fragments release the collagen fibrils that were trapped within the fragments, as shown in our results. (Fig 4.1.2b) The maintenance of collagen without obvious denaturation and peptic cleavage, and the increase in yield of insoluble collagen content is consistent with previous results (Takahashi et al 1991), thus showing that we have improved upon current methods of collagen quantification for assessment of tissue engineered cell sheets.

For the 2nd part of Phase 1, we wanted to characterize the BMSC cell-sheet growth profile at weekly time points, as there has not been any such study performed

previously. Ouyang et al. 2006 published data using 2-3 week old BMSC cell-sheets to revitalize grafts of bone and tendon, Wang et al. 2008 used 1 week old BMSC cell-sheet fragments to improve cardiac functions after myocardial infarct and Akahane et al. 2008 used the cell-sheets at confluence for bone formation at an ectopic site. However, they did not report any work done to characterize the growth of the BMSC cell-sheets during the fabrication period, hence was our motivation for these series of experiments.

We have successfully cultured rabbit BMSCs to hyperconfluent cell-sheets using L-Asc as the only additive to the culture medium. The cells in the cell-sheet were shown to remain viable throughout the 3-week culture period and no significant change in cell number was observed. It was also observed that the cells continue to produce collagen throughout the period of study and the cell-sheet grew progressively thicker, ie from an initial 36.7 ± 2.1μm at week 0 to 78.5 ± 4.5 μm at week three. The morphology of the cell-sheet was observed through phase contrast microscopy and SEM images (Fig 4.1.3c), and it was found that the cells were arranged randomly in a dense mesh-like tissue.

When we compared the BMSC cell-sheet fabrication technique presented by Wang et al. 2008, we found out that they did not use L-Asc during the cell-sheet fabrication period. Our rational of using L-Asc was to improve ECM deposition using the fabrication period; however, their group had a higher seeding density of 5×10^4 cells/cm^2 as compared to ours which was seeded at 3×10^4 cells/cm^2. The 67% increase in the number of cells seeded might have made up for the lack of use of L-Asc for the cell-sheet fabrication to obtain an ECM structure robust enough for transplantation. Conversely, Akahane et al. 2008 had a very low seeding density of 1×10^4 cells/cm^2, and their group had used L-Asc at a concentration of 82μg/ml immediately after seeding the cells.

Despite using L-Asc, it still took approximately 14 days to reach confluence. When compared with our fabrication protocol, the seeding density of 3 x 10^4 cells/cm^2 was able to reach confluence in 1-2 days without the use of L-Asc.

When compared to the other reports using cell-sheets, we've managed to fabricate a cell-sheet using a lower cell seeding density and yet form a robust ECM structure within the shortest time.

5.2 Phase II – Characterization of BMSC Cell-Sheet Multipotentiality and Comparison between Conventional BMSC Differentiation Protocols

Due to their multilineage potential, BMSCs are widely used in the field of tissue engineering (Dezawa 2008,Lin et al 2008,Wang et al 2005,Ge et al 2005,Liu et al 2008,Altman et al 2002). Primary cultures of BMSCs grow in dense colonies. To obtain sufficient cell numbers to culture BMSC cell-sheets, a commonly used method is to use trypsin to disrupt the ECM and cell-cell adhesion proteins so that the cells can be suspended and re-plated with more space to proliferate. When sufficient cell numbers are obtained, the cells are trypsinized and seeded to form cell-sheets. Trypsin is less of a concern during cell-sheet formation stage because the cells can recover from the damage caused by the trypsin treatment during the period of cell-sheet formation. However, once the cell-sheet is formed, use of the trypsinization method should be avoided. A preferred method is the use of thermosensitive polymers to harvest the cell-sheets for transplantation. This method also alleviates the problem associated with loss of cell numbers due to single cell suspension seeding before transplantation.

The use of cell-sheets have generally been limited to terminally differentiated cells for various tissue engineering approaches to aid in the repair and regeneration of a specific tissue (Shimizu et al 2003,Michel et al 1999). There have been reports claiming the use of BMSC cell-sheets for cartilage (Zhang et al 2009) and bone tissue engineering (Zhou et al 2010), however, the reported method of fabrication of the cell-sheets involved differentiating the BMSCs and culturing them till cell-sheets form. These methods are similar to using terminally differentiated cells to fabricate cell-sheets. There have also been studies done using BMSCs cultured to form cell-sheets that are used for bone and

tendon tissue engineering (Ouyang et al 2006) and recently, for improving cardiac function after an infarction (Wang et al 2008). These reported methods involve culturing the BMSCs till they form cell-sheets before they are differentiated to osteocytes, or directly injected into the infarct heart. With the growing interest in the use of BMSC cell-sheets for therapeutic applications, it is essential to characterize the multilineage differentiation capability of BMSC that are cultured into hyperconfluent cell-sheets. Hence this study was performed with such an aim in mind.

In order to characterize the retention capacity of the multilineage property of the BMSC after being cultured to a hyperconfluent cell-sheet, we followed well established standard procedures and differentiated the BMSC in the cell-sheets into osteogenic, chondrogenic and adipogenic lineages (Pittenger et al 1999,Zou et al 2008,Nöth et al 2002). mRNA levels of key transcription factors and lineage specific proteins explicit for all three mesenchymal lineages under osteogenic, adipogenic, and chondrogenic conditions were evaluated. Their expression levels were compared with conventional differentiated cultures. Immunohistochemical and histochemical staining of cell layers and sections were also performed to demonstrate the presence of critical morphological structures and protein deposition of each mesenchymal lineage.

Differentiation of BMSCs into osteogenic, adipogenic and chondrogenic lineages required a specific cocktail of supplements to be added to the basal medium. Osteogenic differentiation medium has been well documented. Supplements of dexamathasone, L-Ascorbic acid and β-glycerolphosphate are essential to direct uncommitted BMSCs down the osteogenic lineage (Jaiswal et al 1997). Studies have shown that BMSCs cultured in the presence of serum and L-Ascorbic acid spontaneously differentiate into osteoblasts

(Franceschi et al 1994,Matsumoto et al 1991), and BMPs are able to stimulate the differentiation process (Yamaguchi et al 1996).

The results show that this combination of these 4 supplements was able to upregulate osteogenic specific genes, ie. Runx2 (a key transcription factor associated with osteoblast differentiation), ON (a key calcium binding glycoprotein), OPN (an anchor of osteoclasts to bone) and Col I (Reinholt et al 1990) were all upregulated. This is in agreement with previous publications (Zou et al 2008,Guillot et al 2008) that had indicated the upregulation of these genes. The osteogenic gene expression (ie. early phase: Runx2 and ON; late phase: Col I and OPN) of CI and CSI cultures showed increases with respect to their respective NI cultures. These results also indicate that there were more cells in the CSI culture that expressed late stage osteogenic genes as compared to the CI cultures. Between the CI and CSI cultures, the mRNA expression levels of all 4 genes in the CSI cultures were significantly higher when compared to that of the CI cultures. The difference in Alizarin Red S staining showed that CSI cultures deposited significantly more calcium on the cell layer. However, CI and CSI cultures had vastly different cell numbers, we were not able to normalize the calcium deposited to make a comparison between the CI and CSI cultures. Nevertheless, the cell-sheet cultures retained their osteogenic differentiative capacity despite being cultured beyond 2 weeks post confluence.

Adipogenic differentiation induction medium which contains isobutyl-methylxanthine, insulin, dexamathasone, and indomethacin has the ability to direct BMSCs towards the adipogenic lineage. This has been well documented (Nöth et al 2002). Recently, adipogenic induction has been shown to be effective when done in

phases, ie alternating between induction and maintenance medium (Janderová et al 2003,Nakamura et al 2003). Our results showed that for both CI and CSI cultures, mRNA expression levels for PPARγ2 - which is upregulated early in adipocyte differentiation (Chawla et al 1994,Tontonoz et al 1994) and aP2 - a late adipogenic marker (Fink et al 2004), were both significantly upregulated when compared to the respective controls. The data obtained was substantiated by the positive staining of the cytoplasmic lipid droplets using Oil Red O. The downregulation of leptin mRNA in both adipogenic induced cultures were also in agreement with previous reports which showed that leptin enhances osteogenesis and inhibits adipogenesis (Thomas et al 1999,Yang et al 2008,Chang et al 2006). When mRNA expression levels of the two adipogenic induced cultures were compared, there was barely any significant difference observed between both sets of data. It can be hypothesized that although the ECM found within the cell-sheet did not provide additional cues to enhance differentiation of BMSC into adipocytes, it was able to preserve the adipogenic potential of the BMSC. This hypothesis is in agreement with a previous study which showed that adipogenic potential of late passage BMSCs was retained when cultured on denatured collagen type I matrix (Mauney et al 2005). However, more extensive studies are required to determine the possible biological cues found within the secreted cell-sheet ECM that was able to aid the retention of BMSC adipogenic potential.

Chondrogenic differentiation involves culturing MSCs in micromass cultures with TGF-β3 to induce differentiation towards the chondrogenic lineage. Sox9 - an early marker for chondrogenesis (Lefebvre, & de Crombrugghe 1998), is also a direct activator of the chondrocyte specific ECM gene collagen type II (Lefebvre et al 1997) along with

aggrecan - a major structural component of cartilage. The mRNA expressions of these genes were upregulated in both CI and CSI induced micromass cultures. Histological staining using Safranin-O and immunohistological staining of collagen type I and II all showed that the micromass pellets had differentiated towards the chondrogenic lineage. When the mRNA expressions of the three genes were compared between CI and CSI pellet cultures, it was observed that the level of all three genes from the CSI cultures had a higher expression level than those in CI cultures. This study demonstrated that the gene expressions of chondrogenic modified micromass pellet culture using an entire cell-sheet when compared to conventional micromass pellet culture using single cells was extensively upregulated. It is hypothesized that this was due to the ECM within the cell-sheet that was able to provide the appropriate biological cues, ie suitable microenvironment and ideal cell - cytokine/growth factor interactions to differentiate the BMSCs into chondrocytes. In a published study by Hickok et al (1998), it was shown that close spatial relationships of neighbouring BMSC will give rise to better cell to cell and cell to matrix interactions which facilitates chondrogenic differentiation (Hickok et al 1998). It has also been reported that BMP plays an important role in initiating chondrogenic differentiation in BMSCs (Bosnakovski et al 2006,Schmitt et al 2003). It is believed that CSI pellets provided a culture system where the cells already had well established cell - cell and extensive cell - matrix interactions, and as stated previously, the BMPs that are bound to the ECM of the cell-sheet would be able to provide the ideal cues to differentiate the BMSCs into chondrocytes (Suzawa et al 1999).

There has been a study by Akahane et al, 2008 that reports BMSC cell-sheets at confluence to tend towards the osteogenic lineage. The report states that alkaline

phosphatase activity, alkaline phosphatase staining and osteocalcin contents indicate the BMSC cell-sheet tendency towards the osteogenic lineage. However, the reported method of cell-sheet fabrication had dexamethasone and β-glycerophosphate added. These are known additives for osteogenic differentiation of BMSCs, which might have induced the upregulation of the osteogenic markers detected in the report. Thus it cannot be concluded that BMSC cell-sheets tended towards the osteogenic lineage.

We have shown conclusively that 2 week old BMSC cell-sheets retain their multipotentiality. Our results also show that the BMSCs within the cell-sheet might have an enhanced differentiation capability, particularly in the case of osteogenic and chondrogenic lineages when compared to differentiated cell cultures following conventional induction protocols, but more studies will have to be done to confirm this hypothesis. Hence, it is possible to use BMSC cell-sheets for more complex tissue engineering applications that require more than one cell type.

5.3 Phase III – Fabrication and Verification of a Simulated IVD-like Assembly

The inner core of the IVD is consists of a turgid tissue called the nucleus pulposus. This tissue contains high proteoglycan, and causes it to exhibit a high affinity for water due to its highly negative sulfated charge (Revell et al 2007). The nucleus pulposus is also filled with Type II collagen, in random orientation. Studies have shown previously that the NP exhibits viscoelastic properties under physiological compression (Bader, & Rochefort 2008). It is "fluidlike" and relaxes to near zero stress under transient condition, while behaving like an "elastic solid" under dynamic loading (Iatridis et al 1996). In order to fabricate the simulated IVD-like assembly, a suitable NP-like substitute had to be fabricated.

The mechanical properties of the NP-like substitute have to remain constant after sterilization and dynamic compression. Dow Corning's Slygard 184 Elastomer kit was chosen as the material for the NP-like substitute due to its viscoelastic properties and biocompatibility (Brown et al 2005). The 1st part of this study was to determine a fabrication protocol to produce NP-like substitutes that had similar mechanical properties to the actual porcine NP (Glover et al 1991), and conduct further mechanical tests on its suitability for use in a compression bioreactor. The 2nd part of this study involved fabricating the entire simulated IVD-like construct using the silicone NP-like substitute wrapped with alternating layers of silk scaffolds and BMSC cell-sheets to simulate the AF, to determine the feasibility of the entire assembly to regenerate the AF.

In order to determine the axial compression needed to produce a 0.05 MPa bulging pressure (Glover et al 1991), the silicone NP-like substitute was compressed in the axial direction from 15% to 30% and the bulging pressure calculated using the

formula stated in Appendix A6. It was determined that a 25% axial compression of the NP-like substitute resulted in a radial bulging pressure of 0.0505 ± 0.0023 MPa.

The next characterization step was to determine if the mechanical properties of NP-like substitute would change after undergoing ethylene oxide sterilization. The Young's modulus of the NP-like substitute at 25% axial compression will be used to determine if the mechanical properties have changed. 6 batches of NP-like substitutes were fabricated using the same protocol and sterilized using ethylene oxide. From the data of the Young's modulus, we concluded that ethylene oxide sterilization did not affect the mechanical properties of the silicone NP-like substitute. However, it is observed that the Young's modulus was significantly different within batches even though the fabrication process was consistent (Fig 4.3.1b).

The next characterization experiment was to determine if the mechanical properties of the silicone NP-like substitute would change after cyclic loading. The experiment, done on Batch B and D was conducted over 3 consecutive days, was done for 15mins each day with a 25% axial compression at a frequency of 0.25Hz. The Young's modulus of the NP-like substitute at 25% axial compression was calculated before and after each day of cyclic compression. The results show that the Young's modulus of the NP-like substitute did not significantly different after each day and after the 3 consecutive days of cyclic loading (Fig 4.3.1c).

From the experiments conducted thus far, the NP-like substitutes have been shown to have desirable material properties to function within the simulated IVD-like assembly. However, the inability to have a consistent Young's modulus between batches presented a problem in standardizing the bulging pressure. It was then decided that

keeping the hoop strain constant would be more attainable. The final experiment was performed to obtain the axial compression of each batch that was needed to give a 14.7±0.4% hoop strain (derived from a 25% axial compression of Batch A). The results of the experiment (Fig 4.3.1d) showed that Batches B and D required a 23% axial compression to attain a 14.7±0.5% and 14.6±0.4% hoop strain respectively, which batches C, E and F required a 24% axial compression to attain a 15.1±0.3%, 15.0±0.6% and 15.0±0.8% hoop strain respectively (details of results in Appendix A9).

It can be concluded that the Dow Corning Sylgard 184 Elastomer Kit was able to fabricate the NP-like substitutes with suitable mechanical properties in a 20:1 (elastomer:harderner) ratio. The mechanical properties of the NP-like substitutes remained constant after ethylene oxide sterilization and 3 consecutive days of cyclic loading and an axial compression of between 23% to 25% (depending on Batch) was required standardize the hoop strain of each batch at 14.7%.

After successfully fabricating the NP-like substitute, the simulated IVD-like assembly was fabricated using 2 week old BMSC cell-sheets and combined silk scaffolds as the simulated AF (Fig 3.3.4). The simulated IVD-like assembly was cultured for 4 weeks in static conditions using only LG-DMEM supplemented with 15% FBS, 1% penicillin/streptomycin, 1% L-Glutamine and 50μg/ml L-Asc. The feasibility of the simulated IVD-like assembly to aid IVD regeneration was verified by a series of assays.

The results of the Alamar Blue assay confirmed that cells within the BMSC cell-sheet of the simulated IVD-like assembly remained viable throughout the 4 week static culture period (Fig 4.3.2a). Histological staining of sections of the simulated IVD-like assembly showed the localization of the cells and ECM in between layers of the silk

scaffold. The staining showed that the BMSC cell-sheets had adhered onto the silk scaffolds. However, there was no evidence that the cells from the cell-sheet migrated into the pores of the silk scaffold. The positive Alcian Blue and negative Safranin-O staining (Fig 4.3.2b) of the sections showed that the GAG present within the ECM was poorly sulphated mucopolysaccharide (Chan et al 2001). Immunohistological staining of collagen type I and collagen type II the sections show evidence of both collagen types within the ECM (Fig 4.3.2c). Further analysis of the collagen content within the ECM of the simulated IVD-like assembly shows evidence of a decrease in collagen type I detected within the ECM. Before transplantation into the simulated IVD-like assembly, the ECM was made up of mainly of collagen type I. However, after 4 weeks of static culture in the simulated IVD-like assembly, the amount of collagen type I detected within the ECM decreased as shown in the SDS-PAGE gel (Fig 4.3.2d). This might suggest that the ECM composition is going through extensive remodeling as shown by the immunohistochemical staining results. The positive staining for collagen type II suggest that the ECM is tending towards that of the inner AF where collagen type II makes up a larger proportion of the ECM (Beard et al 1981). Since there have been no distinct markers that can be used to differentiate IVD cells from cartilage cells, we also felt that this hypothesis is also in agreement with previous studies that have shown that silk scaffolds are suitable for cartilage tissue engineering (Wang et al 2005,Hofmann et al 2006).

The remodeling of the ECM might be due to the change in the substrate that the cells attach on. The cell-sheets were initially attached onto poly-NIPAAm coated surfaces and we hypothesize that the change in the substrate when transplanted onto the silk

scaffolds caused a biochemical alteration of the cells in the cell-sheet which in turn caused the remodeling of the ECM. We also hypothesize that the remodeling of the ECM is partially due to the radial compressive force experienced by the cell-sheet due to the wrapping of the silk scaffolds around the silicone NP. This hypothesis is somewhat in agreement with previous studies that have shown that cyclic compression can induce BMSCs to undergo chondrogenesis (Huang et al 2004) and an increase in compressive load in AF cells causes matrix remodeling expression (Wenger et al 2005). However, more experiments have to be done to determine the molecular mechanisms that caused this extensive change in the ECM composition over a period of 4 weeks.

Recently, there has been a report that attempted to regenerate the AF using BMSCs seeded onto aligned, electrospun poly(ε-caprolactone) (PCL) (Nerurkar et al 2009). The group had concluded that structural hierarchy of the AF was attained by the aligned nanofibres, and after seeding the scaffolds with BMSCs and culturing then in chondrogenic differentiation medium for 10 weeks, the construct was suitable for AF regeneration. However, one contradictory point in the study was that it seemed that with the use of aligned scaffolds, the aim was to regenerate the outer AF, but the medium of choice had been used extensively for chondrogenic differentiation. This would cause the BMSCs to differentiate towards the chondrogenic lineage and deposit extracellular matrix similar to the inner AF and NP. The group had also reported an increase in collagen deposition over the 10 week culture duration. However, the exact composition of collagen type was not determined in this study. It has been extensively reported that the outer AF is made up of mainly collagen type I and to a much lesser extent, collagen type II and the amount of collagen type I fibres decrease and collagen type II fibres increase

gradually near the NP (Bruehlmann et al 2002), thus it cannot be concluded if the group was attempting to regenerate the inner or outer AF. This group also reported the lack of BMSC migration into the electrospun scaffolds due to the small pore size and dense nanofibre packing of the scaffolds. Therefore, although the study done by this group to mimic the native structural hierarchy of the outer AF seems promising, we were not able to determine if their goal was to regenerate the inner or outer AF.

In this phase of experiments, we have shown that the cell-sheets transplanted into the simulated IVD-like assembly remains viable and go through extensive extracellular matrix remodeling throughout the 4 week static culture period. There was a significant decrease in collagen type I composition within the ECM, coupled by the detection of collagen type II by immunohistochemical analysis, it seems that the composition of the ECM found within the 4 week static cultured simulated IVD-like assembly might be that found between the inner and outer AF. However, the exact cause and mechanism for the ECM remodeling has yet to be determined.

5.4 Phase IV – Bioreactor Studies of Simulated IVD-like Assembly

There have been a number of reports using mechanical stimulus to try to achieve increased IVD cell proliferation, increased mRNA expression and matrix deposition of the related proteins (Iwashina et al 2006,Miyamoto et al 2005,Wenger et al 2005). It is hypothesized that stress fibres within the cells detect the mechanical stimulus and adapt accordingly. When the NP within the IVD is compressed, the AF cells undergo a concentric tensile and radial compression stress due to the radial bulging of the NP. Recent work involving mechanical stimulus to regenerate the AF uses hydrostatic (Reza, & Nicoll 2008) and hydrodynamic (Gokorsch et al 2004) pressure on the AF cells. Dynamic hydrostatic pressure was shown to enhance deposition and organization of the ECM from the cells derived from the outer AF, however, the cells from the inner AF was not as responsive (Reza, & Nicoll 2008). Hydrodynamic pressure on AF cells seeded within agarose also induced the cells to produce more ECM, mainly sGAG (Gokorsch et al 2004). A more recent report showed that the application of a 10% equibiaxial cyclic tensile strain was able to increase collagen and sGAG synthesis of previously compressed AF cells (Hee et al 2010). However, these methods of application of mechanical stimulus do not accurately represent the physiological conditions experienced when forces are transmitted throughout the IVD. Moreover, these studies all involve the use of AF cells where it would not be feasible to obtain healthy autologous AF cells as it would involve taking a biopsy of a healthy AF from which to extract the cells. This would mean that a healthy AF would have to be punctured and thereby damaging structure and mechanical function.

With these limitations in mind, a bioreactor was designed to be able to apply and control cyclic axial compression, applied on a silicone NP-substitute. The silicone NP-substitute would translate the axial force into a hoop strain in the radial direction to stimulate an AF-like assembly made up of BMSC cell-sheets seeded onto silk scaffolds. The unique facets of this study design was to use a rehabilitative stimulation regime and a silicone NP substitute to mimic the physiological transmission of forces to the BMSC cell-sheets and silk scaffolds that make up the simulated AF.

The results from the Alamar Blue assay suggest that the cells were able to survive the dynamic culture conditions. However, cellular activity of the BMSCs within cell-sheet of the mechanically stimulated simulated IVD-like assembly initially increased till Week 2 and then decreased after that. The viability of the mechanically stimulated cells ended up being significantly reduced when compared to the static control (Fig 5.4.1a). This might be due to the loss of cell viability of the BMSC as they are induced to differentiate (Yamashita et al 2009,Nuttelman et al 2004) or driven to cell dearh by the compressive forces experienced (Kroeber et al 2002).

There have been no reports on markers and genes specific to the IVD. A previous study has shown that AF cells express cartilage-specific matrix proteins albeit with quantitative differences when compared to articular chondrocytes (Poiraudeau et al 1999). Therefore, most of the studies that have been conducted, use chondrogenic genes (Chang et al 2007,Korecki et al 2009,Kuh et al 2009). The ECM of the AF provides strength and distributes load over large parts of the AF. The assembly of the ECM is catalyzed by both biglycan and decorin. A diminished function of these molecules will lead to a loss of mechanical properties of the collagen network and results in the inability of the AF to

resist the hoop stresses delivered by the NP (Bron et al 2009). At 2 weeks of dynamic culture in the bioreactor, only collagen type II mRNA was significantly upregulated over the static control group. However, after 4 weeks of dynamic culture, the mRNA expression of all these genes except biglycan became significantly upregulated when compared to the static control group (Fig 4.4.1e). Histological staining using Alcian Blue and Safranin-O showed that the GAG within the ECM of the simulated IVD-like assembly has become more sulphated due to the mechanical stimulation of the entire assembly (Fig 4.4.1c). These histological results are in agreement to a study done by (Leung et al 2009) on IVD growth and degeneration. Immunohistological staining of collagen type I and II also confirm the presence of both types of collagen within the ECM of the simulated IVD-like assemblies cultured in the bioreactor (Fig 4.4.1d).

Pepsin digestion was done to extract and quantify the collagen found within the ECM of the samples. SDS-PAGE analysis was done to detect collagen type I and an immunoblot was done to detect collagen type II. Collagen type II could not be accurately quantified by SDS-PAGE as the collagen type II α1 chain is expected to co-migrate with the collagen type V α2 chain. After 2 weeks of dynamic culture, the amount of collagen type I detected in the SDS-PAGE gel and collagen type II detected in the western immunoblot was lesser than the static control even though the collagen type II gene expression was already significantly upregulated. However, after 4 weeks of dynamic culture, the amount of collagen type I found within the ECM was significantly decreased while a strong signal of collagen type II was detected in the immunoblot. This showed that there was a large increase in collagen type II deposition had occurred during the 3rd and 4th week of dynamic culture (Fig 4.4.1b). The collagen composition profile is similar

to that of the inner AF where collagen type II makes up a larger proportion of the ECM over collagen type I (Beard et al 1981). When in collagen composition profile was compared against the static control, it was found that the ECM continued to go through extensive matrix remodeling to a point where there was barely any collagen type I. The presence of collagen type V bands might play an important role in the remodeling of the ECM, however, the specific functional role of collagen type V in the AF has not been reported.

Most studies are done using AF cells with various methods of mechanical stimulation with a wide range of magnitudes, frequencies and durations (Hee et al 2010,Reza, & Nicoll 2008,Gokorsch et al 2004,Gokorsch et al 2005,Iwashina et al 2006), thus it would not be feasible to compare the reported results obtained with the one we have presented. Very recently, there has been a study done using BMSCs seeded onto aligned nanofibres to regenerate the AF (Nerurkar et al 2009), and the same group subsequently used dynamic culture conditions to further enhance cell infiltration into the scaffolds (Nerurkar et al 2010). The group reported that culturing the constructs in chondrogenic differentiation medium on an orbital shaker for 6 weeks followed by another 6 weeks of static culture also improved the sGAG and collagen deposition when compared to 12 weeks of dynamic and 12 weeks of static culture. However, like in their previous report, there was no mention of the composition of the collagen type within the ECM nor was there any gene expression analysis done to determine if the seeded BMSCs had begun to differentiate towards a particular mesenchyme lineage.

None of the previous studies have attempted to regenerate the AF by stimulating the cells with forces as it would experience within the native IVD. Our method of using a

cylindrical silicone NP to translate an external axial force to the AF (radial compressive and circumferential tensile) to induce the BMSC cell-sheets to adopt an AF-like morphology and biochemistry is unique. However, our data is in agreement with previous reports, that some form of compression or increase in pressure was able stimulate the cells to produce more ECM to improve the regeneration of the AF.

5.5 Summary

In summary, although this is just a preliminary study using BMSC cell-sheets as a cell source, fabricated into a simulated IVD-like assembly and mechanically stimulated by a bioreactor in attempt to regenerate the inner AF. We have managed to show conclusively that the cells within the BMSC cell-sheet were able to survive the rehabilitative regime in the bioreactor. Not only did the cells survive, the gene expression and protein deposition results obtained indicate that the ECM found within the simulated IVD-like assembly after dynamic culture was capable of regenerating a tissue structure similar to that found in the native inner AF (Bron et al 2009,Reza, & Nicoll 2008,Wan et al 2008).

CHAPTER 6

CONCLUSION

6. CONCLUSION

The findings from Phase I established the method of growing the BMSC cell-sheet. The cell-sheet growth profile was also successfully characterized. During the course of characterizing the cell-sheet growth profile, a novel method to enhance the accuracy of collagen quantification was also discovered.

In Phase II, the multipotency of the BMSCs of 2 week old BMSC cell-sheets was examined. The 2 week old cell-sheets were differentiated into the 3 main mesenchymal lineages; adipogenic, chondrogenic and osteogenic lineage. It was found that despite 2 weeks of hyperconfluent culture to form the cell-sheet, the BMSCs still retained the multipotency to these 3 lineages, contrary to previous findings that BMSC self differentiate in hyperconfluent conditions.

In Phase III, a fabrication protocol was established to fabricate a silicone NP-like substitute. The fabricated silicone NP-like substitute was found to retain its mechanical properties after ethylene oxide sterilization and consecutive days of cyclic loading. A simulated IVD-like assembly was fabricated using the pre-fabricated silicone as the NP substitute and alternating layers of BMSC cell-sheet and silk scaffold as the AF. It was shown that the simulated IVD-like assembly remained viable after 4 weeks of static culture and the composition of the ECM was made up of both collagen types I and II. The ECM formed is similar to what is expected between the inner and outer AF.

In Phase IV, a bioreactor was fabricated to compress the simulated IVD-like assembly as in physiological conditions. The results illustrated that a rehabilitative mechanical stimulation from the bioreactor was able to induce the cells within the cell-

sheet to adopt a discogenic gene expression and remodel the ECM in a profile similar to that of the inner AF.

Collectively, this doctoral work has satisfied all the stated objectives in each phase, and to a certain extent, the hypothesis. To successfully regenerate the AF, the appropriate cell source, scaffold and mechanical stimulation would have to come together. A mechanically stimulated simulated IVD-like assembly was successfully fabricated to improve the inner AF regeneration.

CHAPTER 7

RECOMMENDATIONS

7. RECOMMENDATIONS

The main aim of this study was to determine if a novel method of fabricating a simulated IVD-like assembly would be feasible in AF regeneration, and if the fabricated bioreactor that would simulate the *in vivo* physiological loading mechanism could enhance the AF regeneration.

During the 4 week dynamic culture period of the simulated IVD-like assembly in the bioreactor, there was no means possible to monitor the growth progress without having to sacrifice the assembly. It is recommended that a load cell be incorporated into the design of the bioreactor to monitor the forces experienced by the assembly real-time. It is hypothesized that if a more robust matrix is deposited by the cells, the load cell reading would be able to detect the change. Another recommendation would be to use chondrogenic induction medium supplemented with TGFβ3 in the bioreactor. It is hypothesized that the induction medium would enhance the efficiency of differentiation of BMSCs into the inner AF cells over mechanical stimulation alone.

Furthermore, the simulated IVD-like assembly was done using only 3 layers of scaffolds and 2 "lamellae" of BMSC cell-sheets. The mechanical stimulation caused a radial bulging throughout the entire assembly. It is recommended that more "lamellae" of BMSC cell-sheets can be added onto the assembly to try to regenerate the outer AF.

It was also observed that throughout the static and dynamic culture of the simulated IVD-like assembly, the cells within the cell-sheets did not migrate into the pores of the silk scaffolds. This would pose a problem in forming a robust tissue structure when the silk scaffolds start to degenerate. It is recommended that for the inner AF, the method of electrospraying BMSCs while electrospinning nanofibres can be used to form

scaffolds that are well populated with cells throughout the entire thickness. This would alleviate the problem of the cells from the cell-sheet not migrating into the pores of the scaffold. As for the outer AF, a novel method of electrospraying BMSCs while electrospinning aligned nanofibres can be used to mimic the aligned fibres found in the native outer AF. Alternating layers and directions of these electrosprayed-electrospun aligned scaffolds can be used to mimic the native lamellae of the IVD. On top of these, the inner AF and the outer AF can be cultured in media containing TGFβ3 and bFGF respectively to differentiate the BMSCs towards the chondrogenic and fibroblastic lineage.

From the analysis of the SDS-PAGE results of the ECM in the simulated IVD-like assembly, collagen type V was deposited in large amounts. However the function of collagen type V in the AF has not been determined. It would be beneficial to determine if collagen type V was responsible for the down regulation of collagen type I deposition or if it is a precursor to collagen type II deposition. It might possibly be a marker for inner AF cells.

Finally, it is widely reported that articular cartilage cells and IVD cells are different in morphology and phenotype. However, there are no markers that have been discovered to positively differentiate IVD cells from those from the articular cartilage, thus all studies have been using chondrogenic markers to prove that a discogenic phenotype was obtained. Without a series of markers unique in expression from other cell types, the work done to regenerate the IVD would always not be completely conclusive.

CHAPTER 8

REFERENCES

8. References

Aguiar DJ, Johnson SL, Oegema TR. Notochordal cells interact with nucleus pulposus cells: regulation of proteoglycan synthesis. Exp Cell Res 1999;246(1):129-37.

Alini M, Eisenstein SM, Ito K, Little C, Kettler AA, Masuda K et al. Are animal models useful for studying human disc disorders/degeneration? Eur Spine J 2008;17(1):2-19.

Altman GH, Horan RL, Lu HH, Moreau J, Martin I, Richmond JC et al. Silk matrix for tissue engineered anterior cruciate ligaments. Biomaterials 2002;23(20):4131-41.

Altman GH, Lu HH, Horan RL, Calabro T, Ryder D, Kaplan DL et al. Advanced bioreactor with controlled application of multi-dimensional strain for tissue engineering. J Biomech Eng 2002;124(6):742-9.

An HS, Takegami K, Kamada H, Nguyen CM, Thonar EJMA, Singh K et al. Intradiscal administration of osteogenic protein-1 increases intervertebral disc height and proteoglycan content in the nucleus pulposus in normal adolescent rabbits. Spine 2005;30(1):25-31; discussion 31.

An HS, Thonar EJMA, Masuda K. Biological repair of intervertebral disc. Spine 2003;28(15 Suppl):S86-92.

Bader RA, Rochefort WE. Rheological characterization of photopolymerized poly(vinyl alcohol) hydrogels for potential use in nucleus pulposus replacement. J Biomed Mater Res A 2008;86(2):494-501.

Banfi A, Muraglia A, Dozin B, Mastrogiacomo M, Cancedda R, Quarto R. Proliferation kinetics and differentiation potential of ex vivo expanded human bone marrow stromal cells: Implications for their use in cell therapy. Exp Hematol 2000;28(6):707-15.

Beard HK, Roberts S, O'Brien JP. Immunofluorescent staining for collagen and proteoglycan in normal and scoliotic intervertebral discs. J Bone Joint Surg Br 1981;63B(4):529-34.

Biering-Sørensen F. Low back trouble in a general population of 30-, 40-, 50-, and 60-year-old men and women. Study design, representativeness and basic results. Dan Med Bull 1982;29(6):289-99.

Boos N, Weissbach S, Rohrbach H, Weiler C, Spratt KF, Nerlich AG. Classification of age-related changes in lumbar intervertebral discs: 2002 Volvo Award in basic science. Spine 2002;27(23):2631-44.

Bosnakovski D, Mizuno M, Kim G, Takagi S, Okumur M, Fujinag T. Gene expression profile of bovine bone marrow mesenchymal stem cell during spontaneous chondrogenic differentiation in pellet culture system. Jpn J Vet Res 2006;53(3-4):127-39.

Bron JL, Helder MN, Meisel HJ, Van Royen BJ, Smit TH. Repair, regenerative and supportive therapies of the annulus fibrosus: achievements and challenges. Eur Spine J 2009;18(3):301-13.

Brown XQ, Ookawa K, Wong JY. Evaluation of polydimethylsiloxane scaffolds with physiologically-relevant elastic moduli: interplay of substrate mechanics and surface chemistry effects on vascular smooth muscle cell response. Biomaterials 2005;26(16):3123-9.

Bruehlmann SB, Rattner JB, Matyas JR, Duncan NA. Regional variations in the cellular matrix of the annulus fibrosus of the intervertebral disc. J Anat 2002;201(2):159-71.

Buckwalter JA. Aging and degeneration of the human intervertebral disc. Spine 1995;20(11):1307-14.

Canavan HE, Cheng X, Graham DJ, Ratner BD, Castner DG. Cell sheet detachment affects the extracellular matrix: a surface science study comparing thermal liftoff, enzymatic, and mechanical methods. J Biomed Mater Res A 2005;75(1):1-3.

Cassinelli EH, Hall RA, Kang JD. Biochemistry of intervertebral disc degeneration and the potential for gene therapy applications. Spine J 2001;1(3):205-14.

Chan A, Cooley MA, Collins AM. Mast cells in the rat liver are phenotypically heterogeneous and exhibit features of immaturity. Immunol Cell Biol 2001;79(1):35-40.

Chang G, Kim HJ, Kaplan D, Vunjak-Novakovic G, Kandel RA. Porous silk scaffolds can be used for tissue engineering annulus fibrosus. Eur Spine J 2007;16(11):1848-57.

Chang YJ, Shih DTB, Tseng CP, Hsieh TB, Lee DC, Hwang SM. Disparate mesenchyme-lineage tendencies in mesenchymal stem cells from human bone marrow and umbilical cord blood. Stem Cells 2006;24(3):679-85.

Chawla A, Schwarz EJ, Dimaculangan DD, Lazar MA. Peroxisome proliferator-activated receptor (PPAR) gamma: adipose-predominant expression and induction early in adipocyte differentiation. Endocrinology 1994;135(2):798-800.

Crock HV, Goldwasser M. Anatomic studies of the circulation in the region of the vertebral end-plate in adult Greyhound dogs. Spine 1984;9(7):702-6.

Dezawa M. Systematic neuronal and muscle induction systems in bone marrow stromal cells: the potential for tissue reconstruction in neurodegenerative and muscle degenerative diseases. Med Mol Morphol 2008;41(1):14-9.

Etebar S, Cahill DW. Risk factors for adjacent-segment failure following lumbar fixation with rigid instrumentation for degenerative instability. J Neurosurg 1999;90(2

Suppl):163-9.

Fan H, Liu H, Toh SL, Goh JCH. Enhanced differentiation of mesenchymal stem cells co-cultured with ligament fibroblasts on gelatin/silk fibroin hybrid scaffold. Biomaterials 2008;29(8):1017-27.

Fink T, Abildtrup L, Fogd K, Abdallah BM, Kassem M, Ebbesen P et al. Induction of adipocyte-like phenotype in human mesenchymal stem cells by hypoxia. Stem Cells 2004;22(7):1346-55.

Franceschi RT, Iyer BS, Cui Y. Effects of ascorbic acid on collagen matrix formation and osteoblast differentiation in murine MC3T3-E1 cells. J Bone Miner Res 1994;9(6):843-54.

Frymoyer JW, Cats-Baril WL. An overview of the incidences and costs of low back pain. Orthop Clin North Am 1991;22(2):263-71.

Fujioka N, Morimoto Y, Takeuchi K, Yoshioka M, Kikuchi M. Difference in infrared spectra from cultured cells dependent on cell-harvesting method. Appl Spectrosc 2003;57(2):241-3.

Ge Z, Goh JCH, Lee EH. Selection of cell source for ligament tissue engineering. Cell Transplant 2005;14(8):573-83.

Gertzbein SD, Hollopeter MR. Disc herniation after lumbar fusion. Spine 2002;27(16):E373-6.

Ghiselli G, Wang JC, Bhatia NN, Hsu WK, Dawson EG. Adjacent segment degeneration in the lumbar spine. J Bone Joint Surg Am 2004;86-A(7):1497-503.

Glover MG, Hargens AR, Mahmood MM, Gott S, Brown MD, Garfin SR. A new technique for the in vitro measurement of nucleus pulposus swelling pressure. J Orthop Res 1991;9(1):61-7.

Gokorsch S, Nehring D, Grottke C, Czermak P. Hydrodynamic stimulation and long term cultivation of nucleus pulposus cells: a new bioreactor system to induce extracellular matrix synthesis by nucleus pulposus cells dependent on intermittent hydrostatic pressure. Int J Artif Organs 2004;27(11):962-70.

Gokorsch S, Weber C, Wedler T, Czermak P. A stimulation unit for the application of mechanical strain on tissue engineered anulus fibrosus cells: a new system to induce extracellular matrix synthesis by anulus fibrosus cells dependent on cyclic mechanical strain. Int J Artif Organs 2005;28(12):1242-50.

Goupille P, Jayson MI, Valat JP, Freemont AJ. Matrix metalloproteinases: the clue to intervertebral disc degeneration? Spine 1998;23(14):1612-26.

Gruber HE, Stasky AA, Hanley EN. Characterization and phenotypic stability of human disc cells in vitro. Matrix Biol 1997;16(5):285-8.

Gruber HE, Ingram JA, Davis DE, Hanley EN. Increased cell senescence is associated with decreased cell proliferation in vivo in the degenerating human annulus. Spine J 2009;9(3):210-5.

Gruber HE, Ingram JA, Norton HJ, Hanley EN. Senescence in cells of the aging and degenerating intervertebral disc: immunolocalization of senescence-associated beta-galactosidase in human and sand rat discs. Spine 2007;32(3):321-7.

Guillot PV, De Bari C, Dell'accio F, Kurata H, Polak J, Fisk NM. Comparative osteogenic transcription profiling of various fetal and adult mesenchymal stem cell sources. Differentiation 2008;

Guiot BH, Fessler RG. Molecular biology of degenerative disc disease. Neurosurgery 2000;47(5):1034-40.

Haefeli M, Kalberer F, Saegesser D, Nerlich AG, Boos N, Paesold G. The course of macroscopic degeneration in the human lumbar intervertebral disc. Spine 2006;31(14):1522-31.

Handa T, Ishihara H, Ohshima H, Osada R, Tsuji H, Obata K. Effects of hydrostatic pressure on matrix synthesis and matrix metalloproteinase production in the human lumbar intervertebral disc. Spine 1997;22(10):1085-91.

Hassler O. The human intervertebral disc. A micro-angiographical study on its vascular supply at various ages. Acta Orthop Scand 1969;40(6):765-72.

Hata R, Senoo H. L-ascorbic acid 2-phosphate stimulates collagen accumulation, cell proliferation, and formation of a three-dimensional tissuelike substance by skin fibroblasts. J Cell Physiol 1989;138(1):8-16.

Hee HT, Zhang J, Wong HK. Effects of cyclic dynamic tensile strain on previously compressed inner annulus fibrosus and nucleus pulposus cells of human intervertebral disc-an in vitro study. J Orthop Res 2010;28(4):503-9.

Hickey DS, Hukins DW. X-ray diffraction studies of the arrangement of collagenous fibres in human fetal intervertebral disc. J Anat 1980;131(Pt 1):81-90.

Hickok NJ, Haas AR, Tuan RS. Regulation of chondrocyte differentiation and maturation. Microsc Res Tech 1998;43(2):174-90.

Hofmann S, Knecht S, Langer R, Kaplan DL, Vunjak-Novakovic G, Merkle HP et al. Cartilage-like tissue engineering using silk scaffolds and mesenchymal stem cells. Tissue

Eng 2006;12(10):2729-38.

Huang CYC, Hagar KL, Frost LE, Sun Y, Cheung HS. Effects of cyclic compressive loading on chondrogenesis of rabbit bone-marrow derived mesenchymal stem cells. Stem Cells 2004;22(3):313-23.

Hunter CJ, Matyas JR, Duncan NA. The notochordal cell in the nucleus pulposus: a review in the context of tissue engineering. Tissue Eng 2003;9(4):667-77.

Hutton WC, Toribatake Y, Elmer WA, Ganey TM, Tomita K, Whitesides TE. The effect of compressive force applied to the intervertebral disc in vivo. A study of proteoglycans and collagen. Spine 1998;23(23):2524-37.

Iatridis JC, Weidenbaum M, Setton LA, Mow VC. Is the nucleus pulposus a solid or a fluid? Mechanical behaviors of the nucleus pulposus of the human intervertebral disc. Spine 1996;21(10):1174-84.

Imai Y, Okuma M, An HS, Nakagawa K, Yamada M, Muehleman C et al. Restoration of disc height loss by recombinant human osteogenic protein-1 injection into intervertebral discs undergoing degeneration induced by an intradiscal injection of chondroitinase ABC. Spine 2007;32(11):1197-205.

Indrawattana N, Chen G, Tadokoro M, Shann LH, Ohgushi H, Tateishi T et al. Growth

factor combination for chondrogenic induction from human mesenchymal stem cell. Biochem Biophys Res Commun 2004;320(3):914-9.

Ishihara H, Urban JP. Effects of low oxygen concentrations and metabolic inhibitors on proteoglycan and protein synthesis rates in the intervertebral disc. J Orthop Res 1999;17(6):829-35.

Iwashina T, Mochida J, Miyazaki T, Watanabe T, Iwabuchi S, Ando K et al. Low-intensity pulsed ultrasound stimulates cell proliferation and proteoglycan production in rabbit intervertebral disc cells cultured in alginate. Biomaterials 2006;27(3):354-61.

Jaiswal N, Haynesworth SE, Caplan AI, Bruder SP. Osteogenic differentiation of purified, culture-expanded human mesenchymal stem cells in vitro. J Cell Biochem 1997;64(2):295-312.

Janderová L, McNeil M, Murrell AN, Mynatt RL, Smith SR. Human mesenchymal stem cells as an in vitro model for human adipogenesis. Obes Res 2003;11(1):65-74.

Johnstone B, Bayliss MT. The large proteoglycans of the human intervertebral disc. Changes in their biosynthesis and structure with age, topography, and pathology. Spine 1995;20(6):674-84.

Kang JD, Stefanovic-Racic M, McIntyre LA, Georgescu HI, Evans CH. Toward a

biochemical understanding of human intervertebral disc degeneration and herniation. Contributions of nitric oxide, interleukins, prostaglandin E2, and matrix metalloproteinases. Spine 1997;22(10):1065-73.

Kettler A, Wilke HJ. Review of existing grading systems for cervical or lumbar disc and facet joint degeneration. Eur Spine J 2006;15(6):705-18.

Kikuchi A, Okuhara M, Karikusa F, Sakurai Y, Okano T. Detailed method to remove cell layer using PIPAAm. J Biomater Sci Polym Ed 1998;9(12):1331-48.

Kim BS, Putnam AJ, Kulik TJ, Mooney DJ. Optimizing seeding and culture methods to engineer smooth muscle tissue on biodegradable polymer matrices. Biotechnol Bioeng 1998;57(1):46-54.

Kobayashi M, Squires GR, Mousa A, Tanzer M, Zukor DJ, Antoniou J et al. Role of interleukin-1 and tumor necrosis factor alpha in matrix degradation of human osteoarthritic cartilage. Arthritis Rheum 2005;52(1):128-35.

Korecki CL, Kuo CK, Tuan RS, Iatridis JC. Intervertebral disc cell response to dynamic compression is age and frequency dependent. J Orthop Res 2009;27(6):800-6.

Krismer M, Haid C, Rabl W. The contribution of anulus fibers to torque resistance. Spine 1996;21(22):2551-7.

Kroeber MW, Unglaub F, Wang H, Schmid C, Thomsen M, Nerlich A et al. New in vivo animal model to create intervertebral disc degeneration and to investigate the effects of therapeutic strategies to stimulate disc regeneration. Spine 2002;27(23):2684-90.

Kuh SU, Zhu Y, Li J, Tsai KJ, Fei Q, Hutton WC et al. A comparison of three cell types as potential candidates for intervertebral disc therapy: annulus fibrosus cells, chondrocytes, and bone marrow derived cells. Joint Bone Spine 2009;76(1):70-4.

Kushida A, Yamato M, Konno C, Kikuchi A, Sakurai Y, Okano T. Decrease in culture temperature releases monolayer endothelial cell sheets together with deposited fibronectin matrix from temperature-responsive culture surfaces. J Biomed Mater Res 1999;45(4):355-62.

Langer R, Vacanti JP. Tissue engineering. Science 1993;260(5110):920-6.

Lareu RR, Arsianti I, Subramhanya HK, Yanxian P, Raghunath M. In vitro enhancement of collagen matrix formation and crosslinking for applications in tissue engineering: a preliminary study. Tissue Eng 2007;13(2):385-91.

Lareu RR, Subramhanya KH, Peng Y, Benny P, Chen C, Wang Z et al. Collagen matrix deposition is dramatically enhanced in vitro when crowded with charged macromolecules: the biological relevance of the excluded volume effect. FEBS Lett 2007;581(14):2709-14.

Le Maitre CL, Hoyland JA, Freemont AJ. Catabolic cytokine expression in degenerate and herniated human intervertebral discs: IL-1beta and TNFalpha expression profile. Arthritis Res Ther 2007;9(4):R77.

Lefebvre V, Huang W, Harley VR, Goodfellow PN, de Crombrugghe B. SOX9 is a potent activator of the chondrocyte-specific enhancer of the pro alpha1(II) collagen gene. Mol Cell Biol 1997;17(4):2336-46.

Lefebvre V, de Crombrugghe B. Toward understanding SOX9 function in chondrocyte differentiation. Matrix Biol 1998;16(9):529-40.

Leung VYL, Chan WCW, Hung SC, Cheung KMC, Chan D. Matrix remodeling during intervertebral disc growth and degeneration detected by multichromatic FAST staining. J Histochem Cytochem 2009;57(3):249-56.

Li Y, Ma T, Kniss DA, Lasky LC, Yang ST. Effects of filtration seeding on cell density, spatial distribution, and proliferation in nonwoven fibrous matrices. Biotechnol Prog 2001;17(5):935-44.

Lin W, Chen X, Wang X, Liu J, Gu X. Adult rat bone marrow stromal cells differentiate into Schwann cell-like cells in vitro. In Vitro Cell Dev Biol Anim 2008;44(1-2):31-40.

Lipson SJ, Muir H. Experimental intervertebral disc degeneration: morphologic and proteoglycan changes over time. Arthritis Rheum 1981;24(1):12-21.

Liu H, Fan H, Wang Y, Toh SL, Goh JCH. The interaction between a combined knitted silk scaffold and microporous silk sponge with human mesenchymal stem cells for ligament tissue engineering. Biomaterials 2008;29(6):662-74.

Livak KJ, Schmittgen TD. Analysis of relative gene expression data using real-time quantitative PCR and the 2(-Delta Delta C(T)) Method. Methods 2001;25(4):402-8.

Lotz JC, Chin JR. Intervertebral disc cell death is dependent on the magnitude and duration of spinal loading. Spine 2000;25(12):1477-83.

Lyons G, Eisenstein SM, Sweet MB. Biochemical changes in intervertebral disc degeneration. Biochim Biophys Acta 1981;673(4):443-53.

Matsuda N, Shimizu T, Yamato M, Okano T. Tissue Engineering Based on Cell Sheet. Advanced Materials 2007;19:3089-99.

Matsumoto T, Igarashi C, Takeuchi Y, Harada S, Kikuchi T, Yamato H et al. Stimulation by 1,25-dihydroxyvitamin D3 of in vitro mineralization induced by osteoblast-like MC3T3-E1 cells. Bone 1991;12(1):27-32.

Mauney JR, Volloch V, Kaplan DL. Matrix-mediated retention of adipogenic differentiation potential by human adult bone marrow-derived mesenchymal stem cells during ex vivo expansion. Biomaterials 2005;26(31):6167-75.

Michel M, L'Heureux N, Pouliot R, Xu W, Auger FA, Germain L. Characterization of a new tissue-engineered human skin equivalent with hair. In Vitro Cell Dev Biol Anim 1999;35(6):318-26.

Miller JA, Schmatz C, Schultz AB. Lumbar disc degeneration: correlation with age, sex, and spine level in 600 autopsy specimens. Spine 1988;13(2):173-8.

Miyamoto K, An HS, Sah RL, Akeda K, Okuma M, Otten L et al. Exposure to pulsed low intensity ultrasound stimulates extracellular matrix metabolism of bovine intervertebral disc cells cultured in alginate beads. Spine 2005;30(21):2398-405.

Mizuno H, Roy AK, Vacanti CA, Kojima K, Ueda M, Bonassar LJ. Tissue-engineered composites of anulus fibrosus and nucleus pulposus for intervertebral disc replacement. Spine 2004;29(12):1290-7; discussion 1297.

Moore RJ. The vertebral end-plate: what do we know? Eur Spine J 2000;9(2):92-6.

Nakamura A, Akahane M, Shigematsu H, Tadokoro M, Morita Y, Ohgushi H et al. Cell sheet transplantation of cultured mesenchymal stem cells enhances bone formation in a

rat nonunion model. Bone 2010;46(2):418-24.

Nakamura T, Shiojima S, Hirai Y, Iwama T, Tsuruzoe N, Hirasawa A et al. Temporal gene expression changes during adipogenesis in human mesenchymal stem cells. Biochem Biophys Res Commun 2003;303(1):306-12.

Natarajan RN, Ke JH, Andersson GB. A model to study the disc degeneration process. Spine 1994;19(3):259-65.

Neidlinger-Wilke C, Würtz K, Urban JPG, Börm W, Arand M, Ignatius A et al. Regulation of gene expression in intervertebral disc cells by low and high hydrostatic pressure. Eur Spine J 2006;15 Suppl 3:S372-8.

Nerurkar NL, Sen S, Baker BM, Elliott DM, Mauck RL. Dynamic culture enhances stem cell infiltration and modulates extracellular matrix production on aligned electrospun nanofibrous scaffolds. Acta Biomater 2010;

Nerurkar NL, Baker BM, Sen S, Wible EE, Elliott DM, Mauck RL. Nanofibrous biologic laminates replicate the form and function of the annulus fibrosus. Nat Mater 2009;8(12):986-92.

Nishida K, Doita M, Takada T, Kakutani KI, Miyamoto H, Shimomura T et al. Sustained transgene expression in intervertebral disc cells in vivo mediated by microbubble-

enhanced ultrasound gene therapy. Spine 2006;31(13):1415-9.

Nishida K, Suzuki T, Kakutani K, Yurube T, Maeno K, Kurosaka M et al. Gene therapy approach for disc degeneration and associated spinal disorders. Eur Spine J 2008;17 Suppl 4:459-66.

Nuttelman CR, Tripodi MC, Anseth KS. In vitro osteogenic differentiation of human mesenchymal stem cells photoencapsulated in PEG hydrogels. J Biomed Mater Res A 2004;68(4):773-82.

Nöth U, Osyczka AM, Tuli R, Hickok NJ, Danielson KG, Tuan RS. Multilineage mesenchymal differentiation potential of human trabecular bone-derived cells. J Orthop Res 2002;20(5):1060-9.

O'Halloran DM, Pandit AS. Tissue-engineering approach to regenerating the intervertebral disc. Tissue Eng 2007;13(8):1927-54.

O'Neill CW, Kurgansky ME, Derby R, Ryan DP. Disc stimulation and patterns of referred pain. Spine 2002;27(24):2776-81.

Okano T, Yamada N, Okuhara M, Sakai H, Sakurai Y. Mechanism of cell detachment from temperature-modulated, hydrophilic-hydrophobic polymer surfaces. Biomaterials 1995;16(4):297-303.

Osada R, Ohshima H, Ishihara H, Yudoh K, Sakai K, Matsui H et al. Autocrine/paracrine mechanism of insulin-like growth factor-1 secretion, and the effect of insulin-like growth factor-1 on proteoglycan synthesis in bovine intervertebral discs. J Orthop Res 1996;14(5):690-9.

Ouyang HW, Cao T, Zou XH, Heng BC, Wang LL, Song XH et al. Mesenchymal stem cell sheets revitalize nonviable dense grafts: implications for repair of large-bone and tendon defects. Transplantation 2006;82(2):170-4.

Pfirrmann CW, Metzdorf A, Zanetti M, Hodler J, Boos N. Magnetic resonance classification of lumbar intervertebral disc degeneration. Spine 2001;26(17):1873-8.

Pittenger MF, Mackay AM, Beck SC, Jaiswal RK, Douglas R, Mosca JD et al. Multilineage potential of adult human mesenchymal stem cells. Science 1999;284(5411):143-7.

Poiraudeau S, Monteiro I, Anract P, Blanchard O, Revel M, Corvol MT. Phenotypic characteristics of rabbit intervertebral disc cells. Comparison with cartilage cells from the same animals. Spine 1999;24(9):837-44.

Raghunath M, Steinmann B, Delozier-Blanchet C, Extermann P, Superti-Furga A. Prenatal diagnosis of collagen disorders by direct biochemical analysis of chorionic villus

biopsies. Pediatr Res 1994;36(4):441-8.

Razaq S, Wilkins RJ, Urban JPG. The effect of extracellular pH on matrix turnover by cells of the bovine nucleus pulposus. Eur Spine J 2003;12(4):341-9.

Reinholt FP, Hultenby K, Oldberg A, Heinegård D. Osteopontin--a possible anchor of osteoclasts to bone. Proc Natl Acad Sci U S A 1990;87(12):4473-5.

Revell PA, Damien E, Di Silvio L, Gurav N, Longinotti C, Ambrosio L. Tissue engineered intervertebral disc repair in the pig using injectable polymers. J Mater Sci Mater Med 2007;18(2):303-8.

Reza AT, Nicoll SB. Hydrostatic pressure differentially regulates outer and inner annulus fibrosus cell matrix production in 3D scaffolds. Ann Biomed Eng 2008;36(2):204-13.

Richardson SM, Walker RV, Parker S, Rhodes NP, Hunt JA, Freemont AJ et al. Intervertebral disc cell-mediated mesenchymal stem cell differentiation. Stem Cells 2006;24(3):707-16.

Risbud MV, Albert TJ, Guttapalli A, Vresilovic EJ, Hillibrand AS, Vaccaro AR et al. Differentiation of mesenchymal stem cells towards a nucleus pulposus-like phenotype in vitro: implications for cell-based transplantation therapy. Spine 2004;29(23):2627-32.

Roberts S, Evans EH, Kletsas D, Jaffray DC, Eisenstein SM. Senescence in human intervertebral discs. Eur Spine J 2006;15 Suppl 3:S312-6.

Roberts S, Menage J, Urban JP. Biochemical and structural properties of the cartilage end-plate and its relation to the intervertebral disc. Spine 1989;14(2):166-74.

Roberts S, Urban JP, Evans H, Eisenstein SM. Transport properties of the human cartilage endplate in relation to its composition and calcification. Spine 1996;21(4):415-20.

Rong Y, Sugumaran G, Silbert JE, Spector M. Proteoglycans synthesized by canine intervertebral disc cells grown in a type I collagen-glycosaminoglycan matrix. Tissue Eng 2002;8(6):1037-47.

Sakai D, Mochida J, Yamamoto Y, Nomura T, Okuma M, Nishimura K et al. Transplantation of mesenchymal stem cells embedded in Atelocollagen gel to the intervertebral disc: a potential therapeutic model for disc degeneration. Biomaterials 2003;24(20):3531-41.

Sato M, Kikuchi M, Ishihara M, Asazuma T, Kikuchi T, Masuoka K et al. Tissue engineering of the intervertebral disc with cultured annulus fibrosus cells using atelocollagen honeycomb-shaped scaffold with a membrane seal (ACHMS scaffold). Med Biol Eng Comput 2003;41(3):365-71.

Schmitt B, Ringe J, Häupl T, Notter M, Manz R, Burmester GR et al. BMP2 initiates chondrogenic lineage development of adult human mesenchymal stem cells in high-density culture. Differentiation 2003;71(9-10):567-77.

Schwarzer AC, Aprill CN, Derby R, Fortin J, Kine G, Bogduk N. The prevalence and clinical features of internal disc disruption in patients with chronic low back pain. Spine 1995;20(17):1878-83.

See EYS, Toh SL, Goh JCH. Technique to accurately quantify collagen content in hyperconfluent cell culture. J Mol Histol 2008;39(6):643-7.

Seki S, Kawaguchi Y, Chiba K, Mikami Y, Kizawa H, Oya T et al. A functional SNP in CILP, encoding cartilage intermediate layer protein, is associated with susceptibility to lumbar disc disease. Nat Genet 2005;37(6):607-12.

Shim CS, Lee SH, Park CW, Choi WC, Choi G, Choi WG et al. Partial disc replacement with the PDN prosthetic disc nucleus device: early clinical results. J Spinal Disord Tech 2003;16(4):324-30.

Shimizu T, Yamato M, Kikuchi A, Okano T. Cell sheet engineering for myocardial tissue reconstruction. Biomaterials 2003;24(13):2309-16.

Steck E, Bertram H, Abel R, Chen B, Winter A, Richter W. Induction of intervertebral disc-like cells from adult mesenchymal stem cells. Stem Cells 2005;23(3):403-11.

Sun Y, Hurtig M, Pilliar RM, Grynpas M, Kandel RA. Characterization of nucleus pulposus-like tissue formed in vitro. J Orthop Res 2001;19(6):1078-84.

Suzawa M, Takeuchi Y, Fukumoto S, Kato S, Ueno N, Miyazono K et al. Extracellular matrix-associated bone morphogenetic proteins are essential for differentiation of murine osteoblastic cells in vitro. Endocrinology 1999;140(5):2125-33.

Takahashi S, Zhao M, Eng C. Isolation and characterization of insoluble collagen of dog hearts. Protein Expr Purif 1991;2(4):304-12.

Thomas T, Gori F, Khosla S, Jensen MD, Burguera B, Riggs BL. Leptin acts on human marrow stromal cells to enhance differentiation to osteoblasts and to inhibit differentiation to adipocytes. Endocrinology 1999;140(4):1630-8.

Thompson JP, Oegema TR, Bradford DS. Stimulation of mature canine intervertebral disc by growth factors. Spine 1991;16(3):253-60.

Thompson JP, Pearce RH, Schechter MT, Adams ME, Tsang IK, Bishop PB. Preliminary evaluation of a scheme for grading the gross morphology of the human intervertebral disc. Spine 1990;15(5):411-5.

Toh WS, Liu H, Heng BC, Rufaihah AJ, Ye CP, Cao T. Combined effects of TGFbeta1 and BMP2 in serum-free chondrogenic differentiation of mesenchymal stem cells induced hyaline-like cartilage formation. Growth Factors 2005;23(4):313-21.

Tontonoz P, Hu E, Spiegelman BM. Stimulation of adipogenesis in fibroblasts by PPAR gamma 2, a lipid-activated transcription factor. Cell 1994;79(7):1147-56.

Tsuda Y, Kikuchi A, Yamato M, Nakao A, Sakurai Y, Umezu M et al. The use of patterned dual thermoresponsive surfaces for the collective recovery as co-cultured cell sheets. Biomaterials 2005;26(14):1885-93.

Urban JPG, Smith S, Fairbank JCT. Nutrition of the intervertebral disc. Spine 2004;29(23):2700-9.

Van Eijk F, Saris DBF, Riesle J, Willems WJ, Van Blitterswijk CA, Verbout AJ et al. Tissue engineering of ligaments: a comparison of bone marrow stromal cells, anterior cruciate ligament, and skin fibroblasts as cell source. Tissue Eng 2004;10(5-6):893-903.

Waddell G. Low back pain: a twentieth century health care enigma. Spine 1996;21(24):2820-5.

Wallach CJ, Gilbertson LG, Kang JD. Gene therapy applications for intervertebral disc

degeneration. Spine 2003;28(15 Suppl):S93-8.

Walsh AJL, Bradford DS, Lotz JC. In vivo growth factor treatment of degenerated intervertebral discs. Spine 2004;29(2):156-63.

Wan Y, Feng G, Shen FH, Laurencin CT, Li X. Biphasic scaffold for annulus fibrosus tissue regeneration. Biomaterials 2008;29(6):643-52.

Wang CC, Chen CH, Lin WW, Hwang SM, Hsieh PCH, Lai PH et al. Direct intramyocardial injection of mesenchymal stem cell sheet fragments improves cardiac functions after infarction. Cardiovasc Res 2008;77(3):515-24.

Wang QW, Chen ZL, Piao YJ. Mesenchymal stem cells differentiate into tenocytes by bone morphogenetic protein (BMP) 12 gene transfer. J Biosci Bioeng 2005;100(4):418-22.

Wang Y, Kim UJ, Blasioli DJ, Kim HJ, Kaplan DL. In vitro cartilage tissue engineering with 3D porous aqueous-derived silk scaffolds and mesenchymal stem cells. Biomaterials 2005;26(34):7082-94.

Wenger KH, Woods JA, Holecek A, Eckstein EC, Robertson JT, Hasty KA. Matrix remodeling expression in anulus cells subjected to increased compressive load. Spine 2005;30(10):1122-6.

West JL, Bradford DS, Ogilvie JW. Results of spinal arthrodesis with pedicle screw-plate fixation. J Bone Joint Surg Am 1991;73(8):1179-84.

Wu YN, Yang Z, Hui JHP, Ouyang HW, Lee EH. Cartilaginous ECM component-modification of the micro-bead culture system for chondrogenic differentiation of mesenchymal stem cells. Biomaterials 2007;28(28):4056-67.

Yamaguchi A, Ishizuya T, Kintou N, Wada Y, Katagiri T, Wozney JM et al. Effects of BMP-2, BMP-4, and BMP-6 on osteoblastic differentiation of bone marrow-derived stromal cell lines, ST2 and MC3T3-G2/PA6. Biochem Biophys Res Commun 1996;220(2):366-71.

Yamashita A, Krawetz R, Rancourt DE. Loss of discordant cells during micro-mass differentiation of embryonic stem cells into the chondrocyte lineage. Cell Death Differ 2009;16(2):278-86.

Yang DC, Tsay HJ, Lin SY, Chiou SH, Li MJ, Chang TJ et al. cAMP/PKA regulates osteogenesis, adipogenesis and ratio of RANKL/OPG mRNA expression in mesenchymal stem cells by suppressing leptin. PLoS ONE 2008;3(2):e1540.

Zhang J, Liu L, Gao Z, Li L, Feng X, Wu W et al. Novel approach to engineer implantable nasal alar cartilage employing marrow precursor cell sheet and biodegradable

scaffold. J Oral Maxillofac Surg 2009;67(2):257-64.

Zhou W, Han C, Song Y, Yan X, Li D, Chai Z et al. The performance of bone marrow mesenchymal stem cell--implant complexes prepared by cell sheet engineering techniques. Biomaterials 2010;31(12):3212-21.

Zou L, Zou X, Chen L, Li H, Mygind T, Kassem M et al. Multilineage differentiation of porcine bone marrow stromal cells associated with specific gene expression pattern. J Orthop Res 2008;26(1):56-64.

CHAPTER 9

APPENDICES

9. APPENDICES

A1. Formula for Calculation of Alamar Blue Reduction

$$\% \text{ reduction} = \frac{(\varepsilon_{ox}\lambda_2)(A\lambda_1) - (\varepsilon_{ox}\lambda_1)(A\lambda_2)}{(\varepsilon_{red}\lambda_1)(A'\lambda_2) - (\varepsilon_{red}\lambda_2)(A'\lambda_1)} \times 100$$

λ_1=570nm, λ_2=600nm

($\varepsilon_{red}\lambda_1$) = 155677 (Molar extinction coefficient of reduced Alamar Blue™ at 570nm)

($\varepsilon_{red}\lambda_2$) = 14652 (Molar extinction coefficient of reduced Alamar Blue™ at 600nm)

($\varepsilon_{ox}\lambda_1$) = 80586 (Molar extinction coefficient of oxidized Alamar Blue™ at 570nm)

($\varepsilon_{ox}\lambda_2$) = 117216 (Molar extinction coefficient of oxidized Alamar Blue™ at 600nm)

($A\lambda_1$) = Absorbance of test wells at 570nm

($A\lambda_2$) = Absorbance of test wells at 600nm

($A'\lambda_1$) = Absorbance of negative control wells which contain medium plus Alamar Blue™ but to which no cells have been added at 570nm

($A'\lambda_2$) = Absorbance of negative control wells which contain medium plus Alamar Blue™ but to which no cells have been added at 600nm

A2. 3%/5% SDS Gel making Protocol

5% Separation Gel (1mm thickness) for Collagen

	1 Gel (µl)	2 Gel (µl)
30% Acrylamid/Bis (37.5 : 1)	830	1660
1.875M Tris (pH 8.8)	1000	2000
10% SDS	50	100
ddH_2O	3070	6140
APS (100mg/ml)	42	84
TEMED	5	10
Total	5ml	10ml

3% Stacking Gel

	1 Gel (µl)	2 Gel (µl)
30% Acrylamid/Bis (37.5 : 1)	200µl	400µl
1.25M Tris (pH 8.8)	200µl	400µl
10% SDS	33µl	66µl
ddH_2O	1550µl	3100µl
APS (100mg/ml)	17µl	33µl
TEMED	3µl	6µl
Total	2ml	4ml

1. Clean glass plates with 70% Ethanol and wipe dry.
    a. Assemble the gel making apparatus
2. Add the 5% resolving gel ingredients into the space between the 2 glass plates to
3. Overlay with 10% Ethanol to cut-off O_2 contact.
4. Leave for 30mins.
5. Alcohol and Resolving gel interface will disappear and reappear after 30mins, indicating that polymerization is complete.
6. Pour off Ethanol, wash with ddH_2O and use filter paper to absorb remaining traces of water.
7. Add APS and TEMED to 3% Stacking gel and pour it on top of the polymerized resolving gel and immediately insert the comb of choice.
    a. Leave for 10mins.

8. Remove comb gently

9. Wash with running buffer.

A3. Silver Staining Protocol

Step	Reagent	Volume				Fast Protocol	Basic Protocol
		1 mini gel	2 mini gels	1 big gel	2 big gels		
Fix	Ethanol (40%) Acetic Acid (10%) Water	50	100	150	300	1hr/overnight	1hr/overnight
Wash	Ethanol (30%) Water	50	100	150	300	Microwave 30sec Agitate 5mins	10mins
Sensitize	Ethanol Sensitizer Water	15 5 30	30 10 60	45 15 90	90 30 180	Microwave 30sec Agitate 2mins	10mins
1st Wash	Ethanol (30%) Water	50	100	150	300	N.A.	10mins
1st Wash	Water	50	100	150	300	Microwave 30sec Agitate 2mins	N.A.
2nd Wash	Water	50	100	150	300	Microwave 30sec Agitate 2mins	10mins
Stain	Stainer Water	0.5 49.5	1 99	1.5 148.5	3 297	Microwave 30sec Agitate 5mins	15mins
Wash	Water	50	100	150	300	1min	1min
Develop	Developer Developer enhancer Water	5 1 drop 45	10 1 drop 90	15 2 drops 135	30 4 drops 270	5-8mins or when dark bands start to show	5-8mins or when dark bands start to show
Stop	Stopper	5	10	15	30	Add directly to developing solution, pour on gel, 10mins	Add directly to developing solution, pour on gel, 10mins
Wash	Water	50	100	150	300	10mins	10mins

A4. 5%/7% SDS Gel making Protocol

7% Separation Gel

Reagents	1 Gel	2 Gels
30% Acrylamide/Bis (37.5:1)	1.167ml	2.333ml
1.875M Tris (pH 8.8)	1.25ml	2.5ml
10% SDS	50µl	100µl
ddH_20	2.32ml	4.64ml
APS	50µl	100µl
TEMED	2µl	4µl
Total	5ml	10ml

5% Stacking Gel

Reagents	1 Gel	2 Gels
30% Acrylamide/Bis (37.5:1)	0.415ml	0.83ml
1.25M Tris (pH 6.8)	0.315ml	0.63ml
10% SDS	25µl	50µl
ddH_2O	1.7ml	3.4ml
TEMED	2.5µl	5µl
APS (100mg/ml)	25µl	50µl
Total	2ml	4ml

A5. Solidworks Drawings of Bioreactor Parts

Assembly of Bioreactor

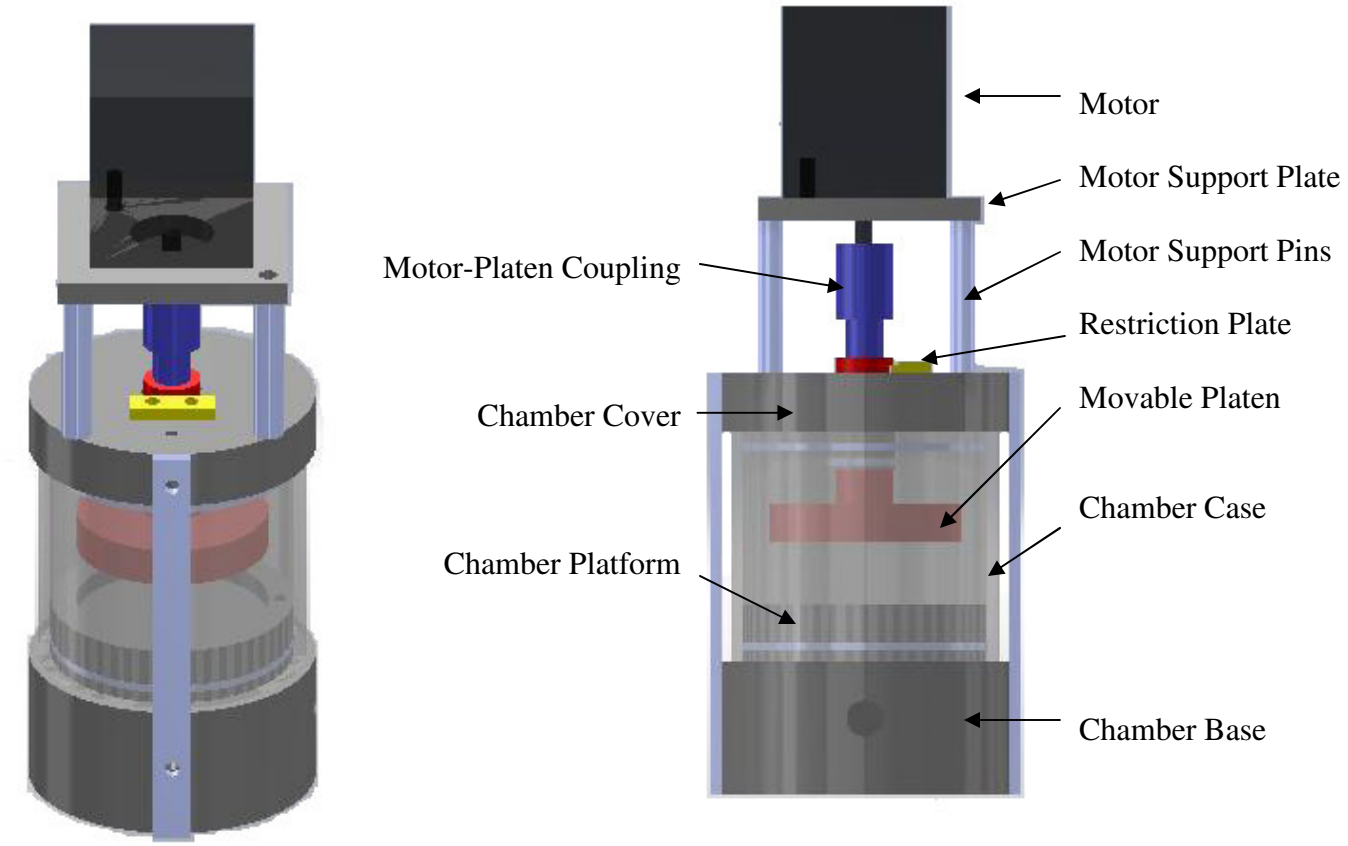

1 **CAD drawing of Motor Support Plate**

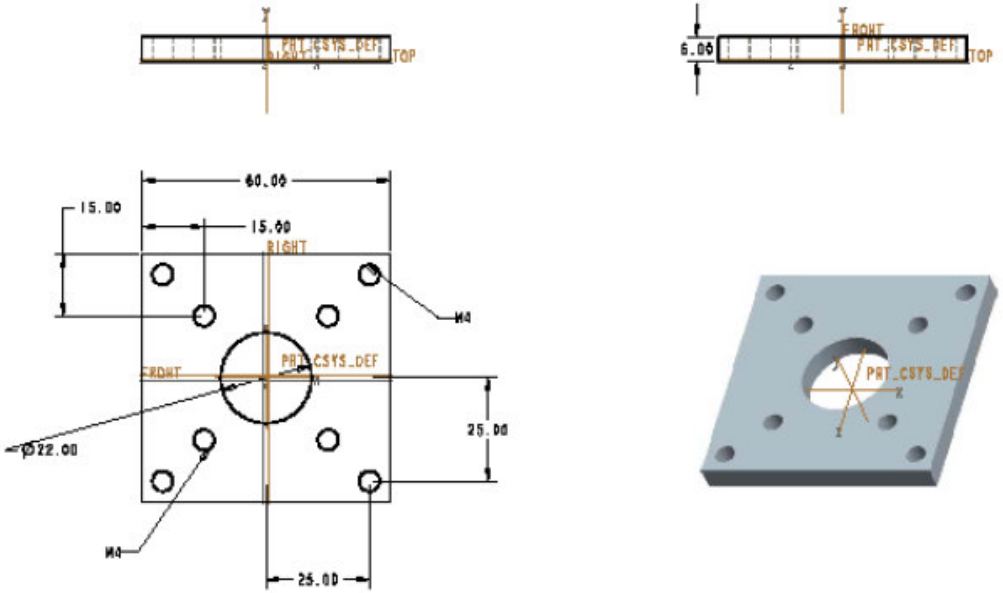

2

1 **CAD Drawing of Motor Support Pin**

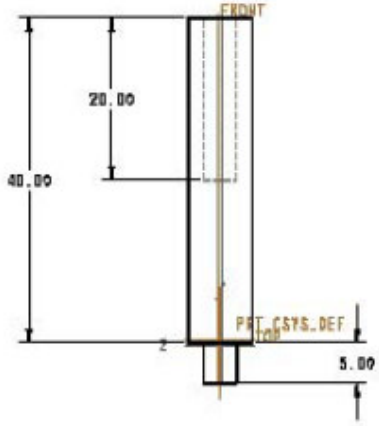

2

1 **CAD Drawing of Motor-Platen Coupling**

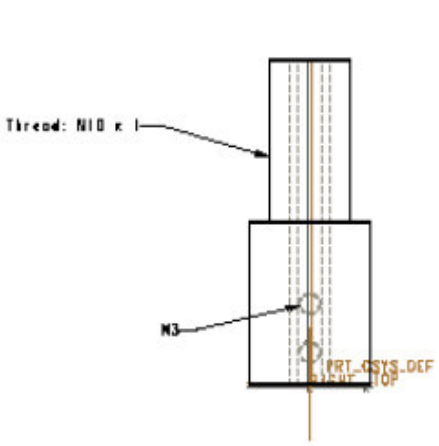

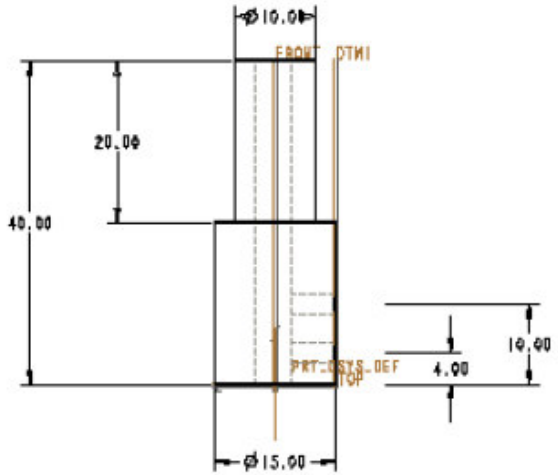

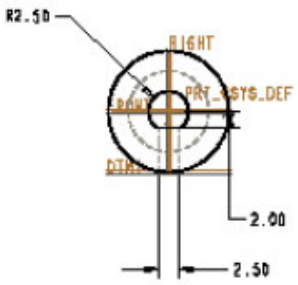

2

1 **CAD Drawing of Movable Platen**

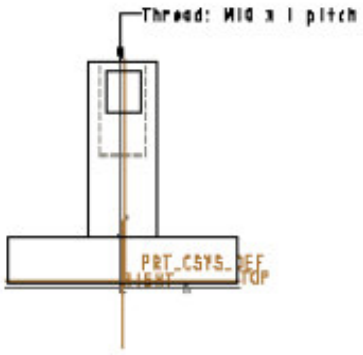

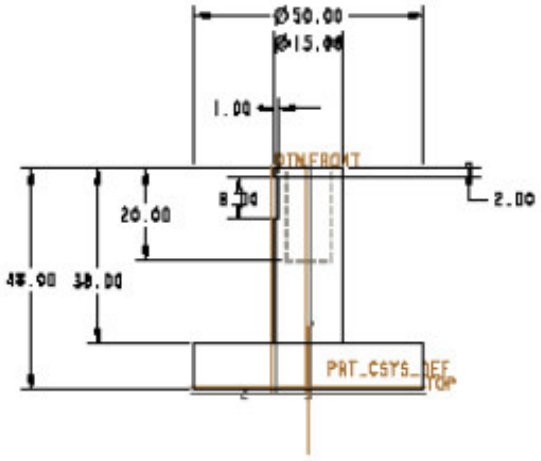

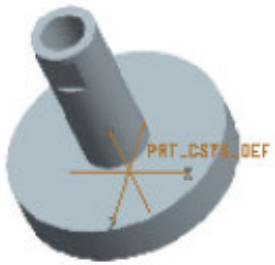

2

1 **CAD Drawing of Rotation Restriction Plate**

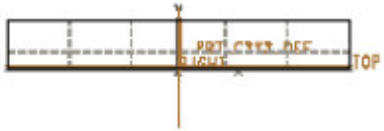

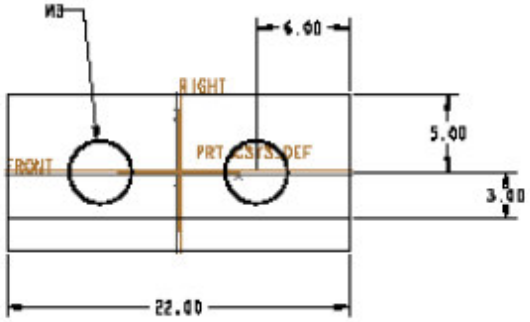

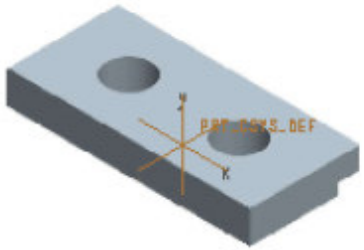

2

1 **CAD Drawing of Chamber Cover**

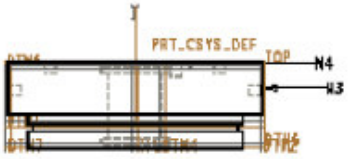

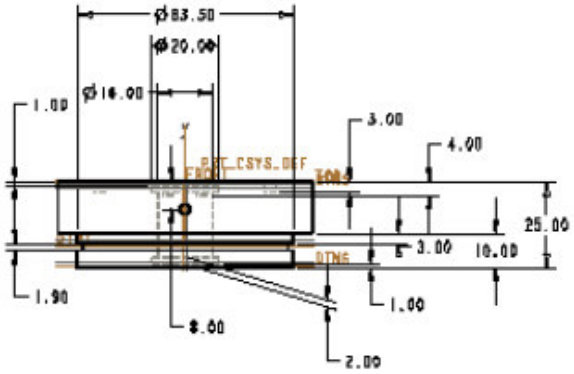

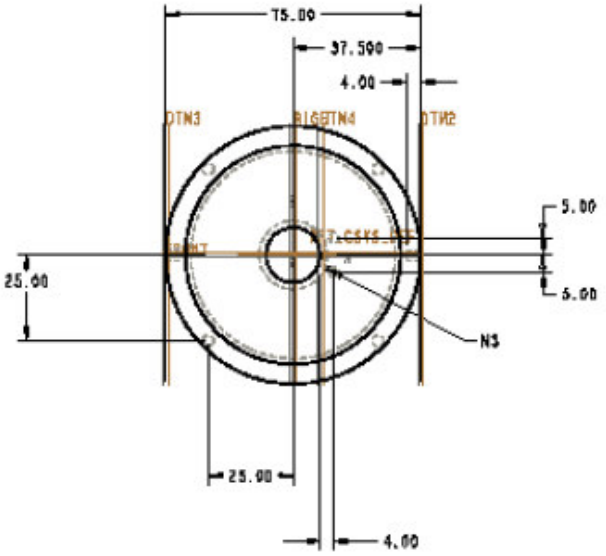

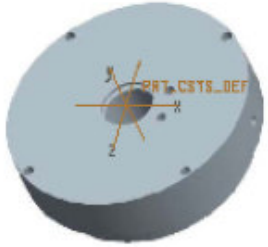

2

1 **CAD Drawing of Acrylic Chamber Case**

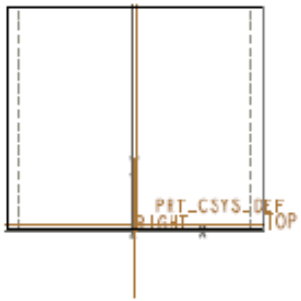

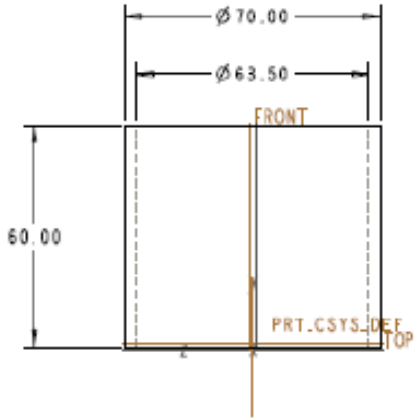

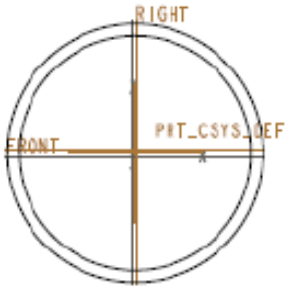

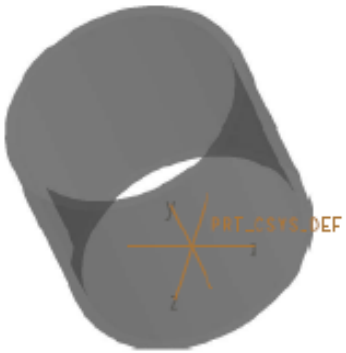

2

1 **CAD Drawing of Chamber Platform**

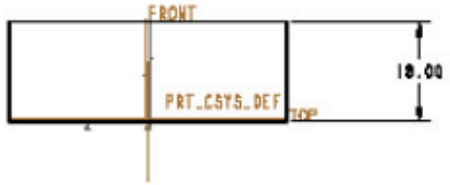

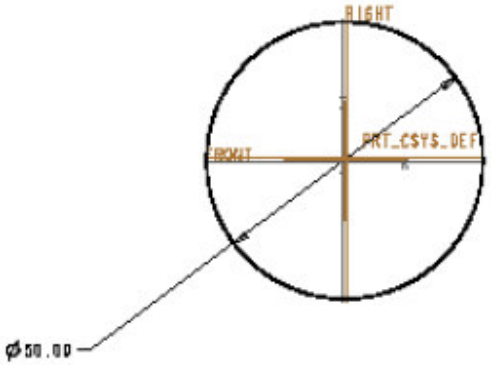

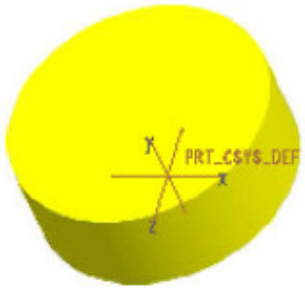

2

1 **CAD Drawing of Chamber Base**

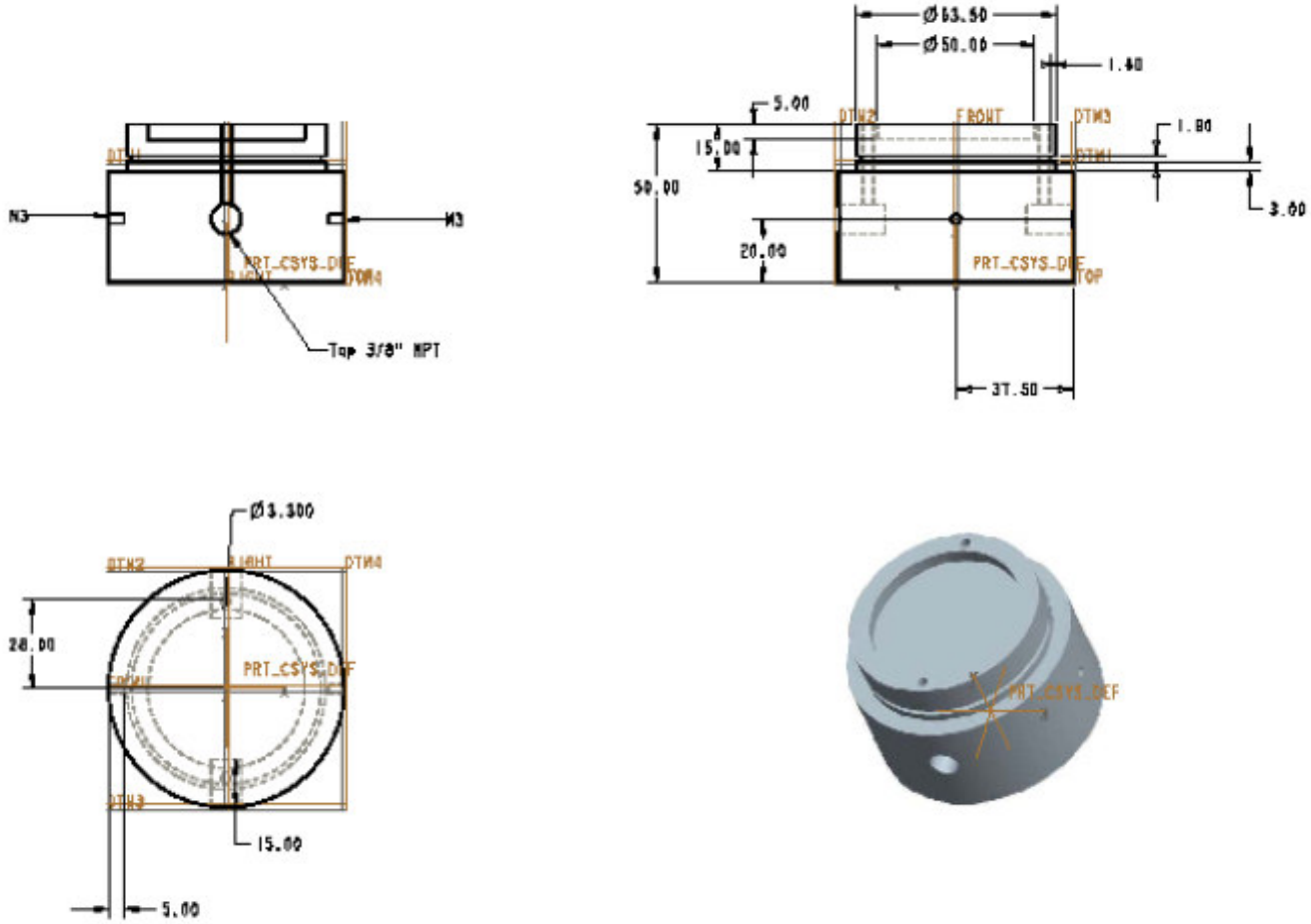

2

3

A6. Detailed Calculations to Determine Swelling Pressure of Silicone NP

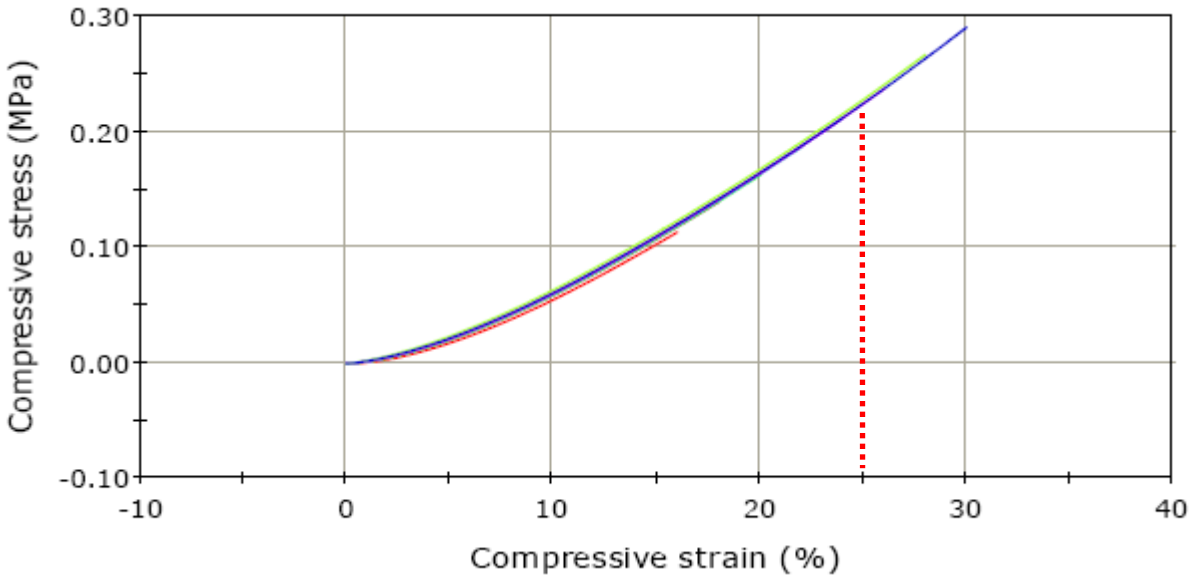

$$y = -1969411.29x^3 + 2329465.15x^2 + 225559.55x - 231.86$$

$$dy/dx = -5908233.87x^2 + 4658930.3x + 225559.55$$

Young's modulus at 25% compression = $dy/dx \,|_{0.25}$

$$\varepsilon_\theta = \frac{1}{E}[\sigma_\theta - \nu\,(\sigma_r + \sigma_a)]$$

Since $\sigma_r = 0$

$$\varepsilon_\theta = \frac{1}{E}(\sigma_\theta - \nu\,\sigma_a)$$

$$\sigma_\theta = E\,\varepsilon_\theta + \nu\,\sigma_a$$

where $\nu = -(\varepsilon_\theta / \varepsilon_a)$

1 Calculations of Hoop Stress at different Axial Compressions

ε (axial)	Hoop Strain	Axial Stress (Mpa)	Axial Strain	Young's Modulus (Mpa)	Poisson's Ratio	Hoop Stress (Mpa)
16%	0.069602273	-0.11988868	-0.1600403	1.077	0.434904663	0.022821502
18%	0.088068182	-0.141620492	-0.1800577	1.13	0.48911089	0.030248921
20%	0.103693182	-0.164293971	-0.2000915	1.174	0.518228819	0.036593925
22%	0.119318182	-0.187558003	-0.2200102	1.211	0.542330227	0.042775944
24%	0.132102273	-0.211880857	-0.2400276	1.239	0.550362845	0.047063365
26%	0.147727273	-0.237096041	-0.2600779	1.259	0.568011633	0.051315327
28%	0.164772727	-0.263304439	-0.2800952	1.272	0.588274013	0.05469575
30%	0.177556818	-0.290302777	-0.3000468	1.276	0.591763745	0.054771841

2

25%	0.140625	-0.224763793	-0.2500317	1.248	0.562428684	0.049086396

3

4 Calculation of Hoop Stress of Batch A at 25% Compression

Sample	Hoop Strain	Axial Stress (MPa)	Axial Strain	Young's Modulus	Poisson's Ratio	Hoop Stress (MPa)
A1	0.15	-0.2500032	-0.24906909	1.307	0.59999232	0.04605
A2	0.140625	-0.22476379	-0.2500317	1.248	0.562428684	0.049086396
A3	0.14640884	-0.27278432	-0.2500356	1.346	0.536720132	0.050657459
A4	0.15	-0.27246495	-0.2500687	1.363	0.550529515	0.05445
A5	0.15	-0.25926296	-0.2500304	1.35	0.57856316	0.0525
					Average	0.050548771
					Standard Deviation	0.002317866

5

A7. Details of Young's Modulus for Batches A to F

	Young's Modulus of Pre-Sterilized and Sterilized Silicone Discs											
	Batch A		Batch B		Batch C		Batch D		Batch E		Batch F	
	Before	After	Before	After	Before	After	Before	After	Before	After	Before	After
Sample 1	1.307	1.295	1.048	1.052	1.219	1.079	1.135	1.182	1.294	1.342	1.265	1.247
Sample 2	1.248	1.284	1.159	1.041	1.026	1.003	1.143	1.128	1.151	1.301	1.245	1.264
Sample 3	1.346	1.334	1.004	1.031	0.948	1.031	1.086	1.038	1.263	1.252	1.287	1.248
Sample 4	1.363	1.319	0.965	1.096	1.143	1.05	1.141	1.125	1.210	1.244	1.212	1.199
Sample 5	1.35	1.347	1.014	1.026	0.997	1.061	1.111	1.200	1.250	1.259	1.274	1.228
Average	**1.3228**	**1.316**	**1.038**	**1.049**	**1.067**	**1.045**	**1.123**	**1.135**	**1.233**	**1.280**	**1.257**	**1.237**
Standard Deviation	0.0467	0.0235	0.0738	0.0281	0.111	0.0292	0.0243	0.0634	0.0552	0.0416	0.0293	0.0248
P value	p=0.6605>0.05		p=0.5938>0.05		p=0.4641>0.05		p=0.4993>0.05		p=0.1669>0.05		p=0.0533>0.05	

A8. Details of Cyclic Loading Testing

	Young's Modulus of Batch B						Young's Modulus of Batch D					
	Day 1		Day 2		Day 3		Day 1		Day 2		Day 3	
	Before	After	Before	After	Before	After	Before	After	Before	After	Before	After
Sample 1	1.011	0.938	1.065	1.016	1.144	1.097	1.224	1.262	1.299	1.166	1.254	1.250
Sample 2	0.969	1.055	1.012	1.122	1.054	1.059	1.143	1.113	1.174	1.147	1.168	1.142
Sample 3	0.977	0.945	0.937	0.968	0.982	1.020	1.065	1.155	1.100	1.144	1.141	1.119
Sample 4	0.979	0.966	1.089	1.073	0.993	1.046	1.152	1.243	1.184	1.100	1.178	1.171
Sample 5	1.100	1.066	0.987	1.021	1.074	1.042	1.215	1.198	1.191	1.198	1.152	1.222
Average	**1.007**	**0.994**	**1.018**	**1.040**	**1.050**	**1.053**	**1.160**	**1.194**	**1.190**	**1.151**	**1.179**	**1.181**
Standard Deviation	0.0543	0.0616	0.0608	0.589	0.0656	0.0286	0.0643	0.0614	0.0713	0.0357	0.0442	0.0545
P value	p=0.366>0.05		p=0.293>0.05		p=0.461>0.05		p=0.412>0.05		p=0.323>0.05		p=0.938>0.05	

A9. Details of Hoop Strain Standardization

	Batch A	Batch B		Batch C			Batch D		Batch E		Batch F	
	25%	20%	23%	20%	23%	24%	25%	23%	25%	24%	25%	24%
Sample 1	0.15	0.1056	0.1441	0.1201	0.1268	0.1538	0.1607	0.1527	0.1607	0.1538	0.1637	0.1386
Sample 2	0.1406	0.1071	0.1555	0.0887	0.1321	0.1483	0.1571	0.1442	0.1571	0.1404	0.1571	0.1553
Sample 3	0.1464	0.121	0.1489	0.0922	0.1238	0.1485	0.1667	0.1476	0.1555	0.1576	0.1549	0.1443
Sample 4	0.15	0.1075	0.1471	0.1263	0.0848	0.1522	0.1809	0.1408	0.1577	0.1505	0.1495	0.1579
Sample 5	0.15	0.1103	0.1404	0.1025	0.0583	0.1525	0.1625	0.1462	0.1702	0.1456	0.1596	0.1535
Average	**0.1474**	**0.1103**	**0.1472**	**0.106**	**0.1275**	**0.1511**	**0.1656**	**0.1463**	**0.1603**	**0.1496**	**0.157**	**0.1499**
Standard Deviation	0.0041	0.0062	0.0056	0.0167	0.0042	0.0025	0.0092	0.0044	0.0059	0.0068	0.0053	0.0081
P value wrt Batch A		0.001	**0.9485**	0.0007	0.0001	**0.1237**	0.0037	**0.6914**	0.0039	**0.5539**	0.0126	**0.5562**

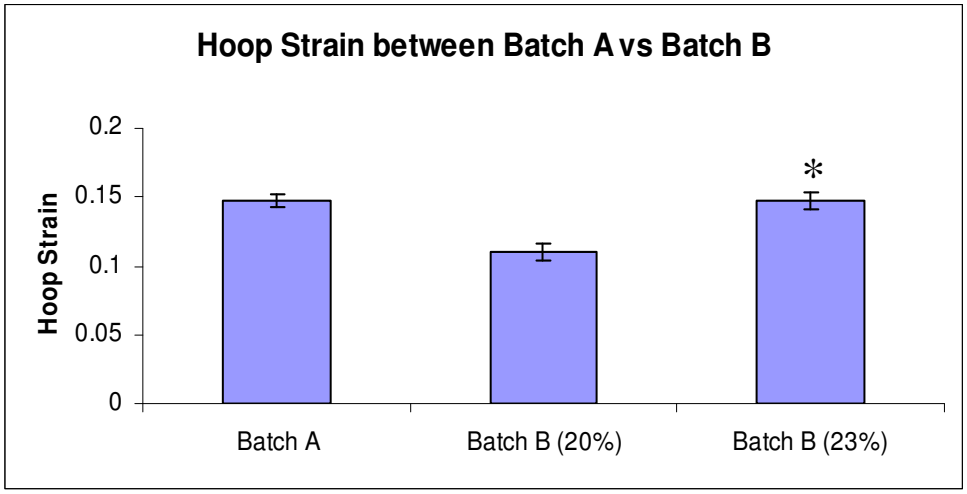
Hoop Strain between Batch A vs Batch B
Hoop Strain
0.2
0.15
0.1
0.05
0
*
Batch A
Batch B (20%)
Batch B (23%)

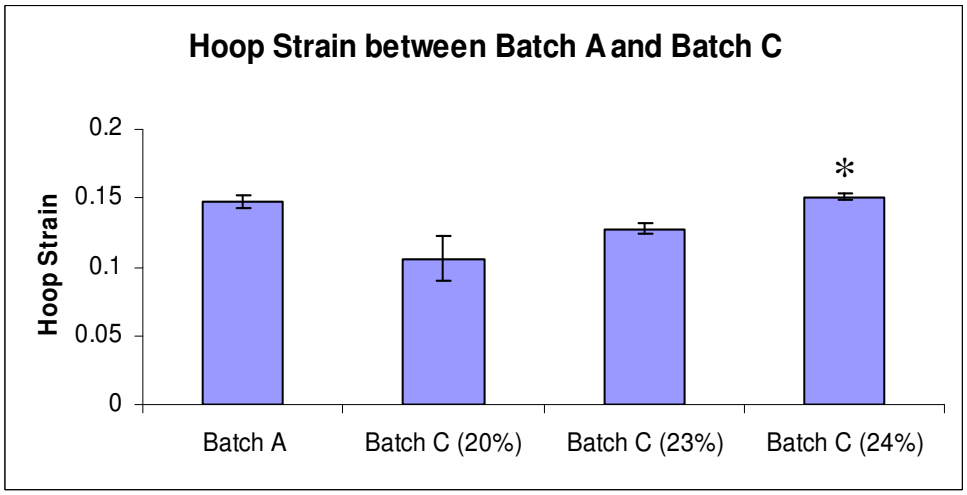
Hoop Strain between Batch A and Batch C
Hoop Strain
0.2
0.15
0.1
0.05
0
*
Batch A
Batch C (20%)
Batch C (23%)
Batch C (24%)

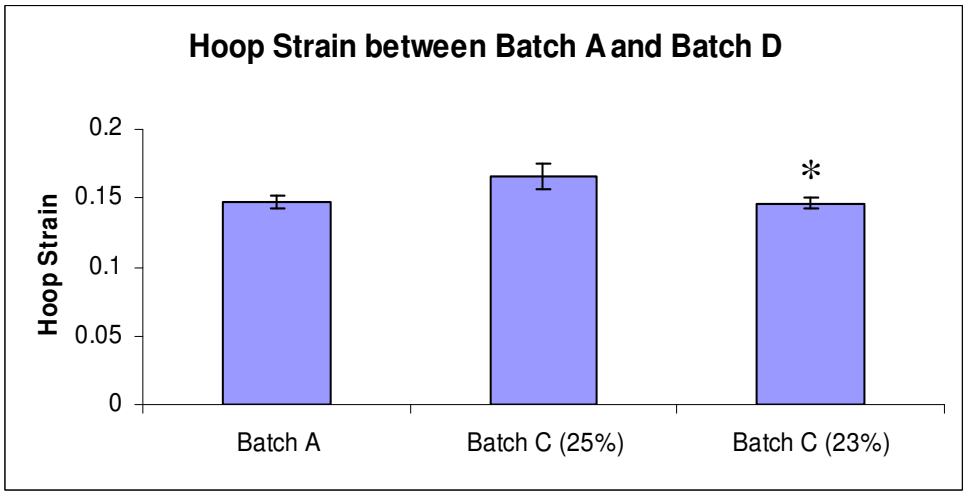
Hoop Strain between Batch A and Batch D
Hoop Strain
0.2
0.15
0.1
0.05
0
*
Batch A
Batch C (25%)
Batch C (23%)

*p>0.05

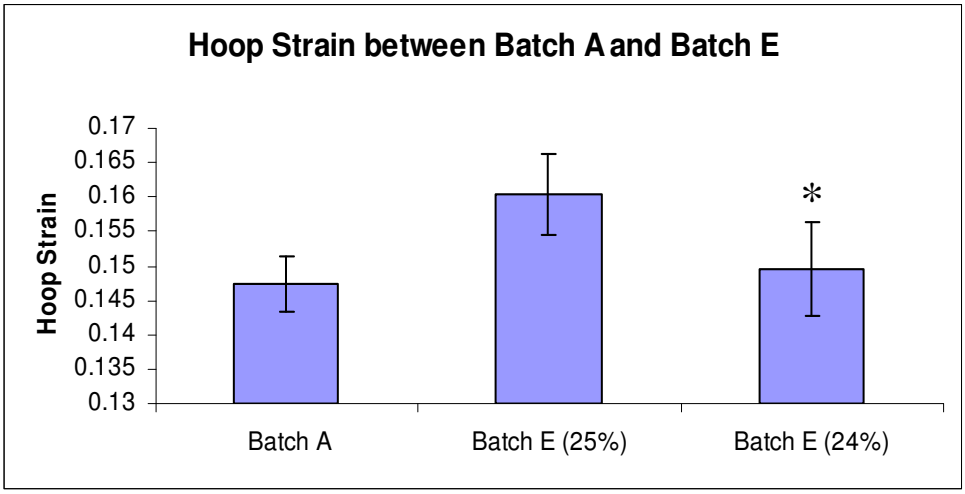
Hoop Strain between Batch A and Batch E
Hoop Strain
0.17
0.165
0.16
0.155
0.15
0.145
0.14
0.135
0.13
*
Batch A
Batch E (25%)
Batch E (24%)

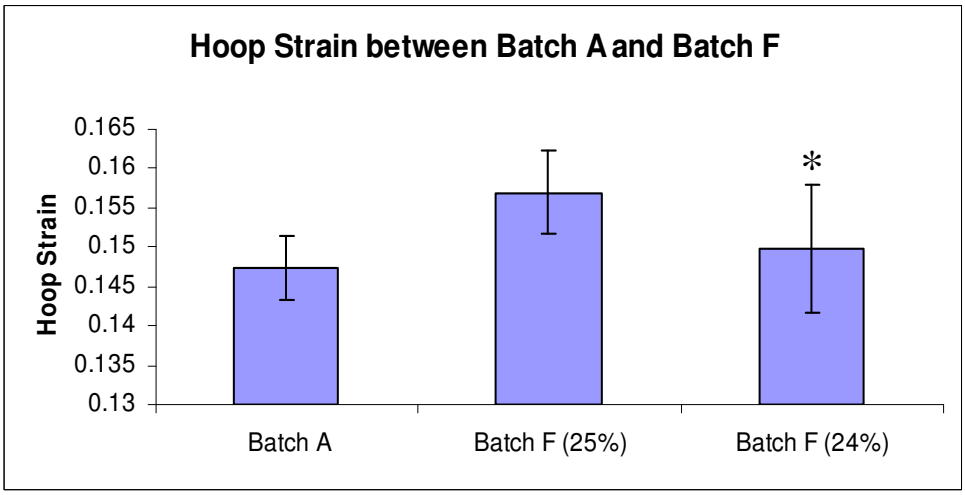
Hoop Strain between Batch A and Batch F
Hoop Strain
0.165
0.16
0.155
0.15
0.145
0.14
0.135
0.13
*
Batch A
Batch F (25%)
Batch F (24%)

1
2 *p>0.05

CHAPTER 11

PUBLICATION LIST

11. PUBLICATION LIST

Journals

1. See EY, Toh SL, Goh JC, Technique to accurately quantify collagen content in hyperconfluent cell culture. J Mol Histol. 2008 Dec;39(6):643-7.

2. See EY, Toh SL, Goh JC, Multilineage potential of bone-marrow-derived mesenchymal stem cell cell sheets: implications for tissue engineering. Tissue Eng Part A. 2010 Apr;16(4):1421-31.

3. See EY, Toh SL, Goh JC, Simulated intervertebral disc-like assembly using bone-marrow-derived mesenchymal stem cell cell-sheets and silk scaffolds for annulus fibrosus regeneration. (in preparation)

4. See EY, Toh SL, Goh JC, Novel bioreactor system for annulus fibrosus regeneration (in preparation)

Conferences

1. See EY, Toh SL, Goh JC, Novel Cell Sheet Technology for Ligament Tissue Engineering. 14th Nordic-Baltic Conference on Biomedical Engineering and Medical Physics (NBC-2008). June 16-20, 2008. Riga, Latvia.

2. See EY, Toh SL, Goh JC, BMSC sheets for ligament tissue engineering. 13th International Conference on Biomedical Engineering (ICBME-2008) December 6-10, 2008. Singapore

3. See EY, Toh SL, Goh JC, Bone Marrow Derived Mesenchymal Stem Cell Cell-Sheets Retain Multilineage Potential for Tissue Engineering. 2nd Tissue Engineering and Regenerative Medicine International Society (TERMIS*)* World Congress August 31-September 3, 2009. Korea, Seoul.

4. See EY, Toh SL, Goh JC, Bone Marrow Derived Mesenchymal Stem Cell Cell-Sheet Retain Multilineage Potential For Tissue Engineering. 3rd East-Asian Pacific Workshop on Nano-Biomedical Engineering. December 21-22, 2009. Singapore.

5. See EY, Toh SL, Goh JC, Cell-Sheets of Bone Marrow Derived Mesenchymal Stem Cell Maintains Multipotentiality. 6th World Congress on Biomechanics. August 1-6, 2010. Singapore